Alberta

MUNICIPAL AFFAIRS

Innovative Housing Grants Program

EVALUATION OF THE PERFORMANCE OF ATTIC RADIANT BARRIERS

June 1990

Prepared by:

Department of Mechanical Engineering
University of Alberta

The views and conclusions expressed and the recommendations made in this report are entirely those of the authors and should not be construed as expressing the opinions of Alberta Municipal Affairs.

With funding provided by
Alberta Municipal Affairs

ISBN: 0-88654-295-2

91-01250/

FOREWORD

The project documented in this report received funding under the Innovative Housing Grants Program of Alberta Municipal Affairs. The Innovative Housing Grants Program is intended to encourage and assist housing research and development which will reduce housing costs, improve the quality and performance of dwelling units and subdivisions, or increase the long term viability and competitiveness of Alberta's housing industry.

The Program offers assistance to builders, developers, consulting firms, professionals, industry groups, building products manufacturers, municipal governments, educational institutions, non-profit groups and individuals. At this time, priority areas for investigation include building design, construction technology, energy conservation, site and subdivision design, site servicing technology, residential building product development or improvement and information technology.

As the type of project and level of resources vary from applicant to applicant, the resulting documents are also varied. Comments and suggestions on this report are welcome. Please send comments or requests for further information to:

Innovative Housing Grants Program
Alberta Municipal Affairs
Housing Division
Research and Development Section
16th Floor, CityCentre
10155 - 102 Street
Edmonton, Alberta
T5J 4L4

Telephone: (403) 427-8150

ACKNOWLEDGEMENTS

The author wishes to gratefully acknowledge the assistance of the following people: Ian Buttar (technician) who helped with the field test set-up and data reduction; John Foy (technician) who assisted with the field test set-up; Mark Ackerman (AHHRF manager) for help with data acquisition programming; Brent Purnell (undergraduate student) who carried out the laboratory testing of moisture accumulation on radiant barriers.

TABLE OF CONTENTS

Page

LIST OF TABLES iii

LIST OF FIGURES iv

EXECUTIVE SUMMARY viii

1.0 INTRODUCTION 1

2.0 THERMAL PERFORMANCE OF ATTIC RADIANT BARRIERS 4

2.1 Laboratory Tests 4

2.1.1. Apparatus and procedure 4

2.1.2 Results of cold room tests 7

2.2 Field Tests 16

2.2.1 Test facility and procedure 16

2.2.2 Results of field tests 22

2.3 Discussion of Results 27

2.3.1. Energy Savings with Radiant Barriers 33

3.0 MOISTURE PERFORMANCE OF RADIANT BARRIERS 38

3.1 Laboratory Tests 38

3.1.1 Apparatus and procedure 38

3.1.2 Results of cold room tests 42

3.2 Field Tests 50

3.2.1 Test facility and procedure 50

3.2.2 Results of field tests 51

3.3 Discussion of Results 59

4.0 ROOF OVERHEATING 64

4.1 Field Tests 64

4.1.1 Test facility and procedure 64

4.1.2 Results of field tests 66
4.2 Discussion of Results 72

5.0 CONCLUSIONS 77
5.1 Thermal Performance and Cost Effectiveness 77
5.2 Moisture Performance 78
5.3 Roof Overheating 79

BIBLIOGRAPHY 80

LIST OF TABLES

		Page
Table 1.	Experimental Data for Thermal Performance of Radiant Barriers.	11
Table 2.	Details of House 5.	17

LIST OF FIGURES

		Page
Figure 1.	Schematic of the experimental apparatus.	5
Figure 2.	Percentage increase in the thermal resistance of a ceiling panel due to the presence of a radiant barrier as a function of the level of insulation.	8
Figure 3.	Percentage increase in the thermal resistance of a ceiling panel of fixed RSI 4.25 (R24) as a function of overall temperature difference, ΔT_{RA}.	9
Figure 4.	Heat flux versus box/cold room temperature difference, ΔT_{RA} for tests where the sheathing is at the same temperature as the cold room.	12
Figure 5.	Temperature difference ΔT measured by the thermocouple pair inside the fiberglass versus ΔT_{RA} for tests where the sheathing is at the same temperature as the cold room.	14
Figure 6.	Heat flux, q, versus sheathing/cold room temperature difference, ΔT_{SA}.	15
Figure 7.	Photograph of house 5 at AHHRF.	18
Figure 8.	Installation of the radiant barrier in the attic of house 5 at AHHRF.	20
Figure 9.	Thermocouple and heat flux gauge locations in attic of house 5.	21
Figure 10.	Average ceiling heat flux versus time for Oct. 17, 1989.	23

Figure 11a.	Average ceiling insulation temperature difference versus time for Dec. 18, 1989.	25
Figure 11b.	Average ceiling insulation temperature difference versus time for April 4, 1990.	26
Figure 12.	Scaled heat flux, $q/\Delta T_{RA}$ versus ΔT_{SA} for cold room experiments.	29
Figure 13.	Normalized temperature difference $\Delta T/\Delta T_{RA}$ versus ΔT_{SA} for cold room experiments.	30
Figure 14.	$\Delta T/\Delta T_{RA}$ versus ΔT_{SA} for field data from Oct. 13, 1989 to April 4, 1990.	32
Figure 15.	Effective ceiling thermal resistance versus ΔT_{SA}.	34
Figure 16.	Percentage change in daily energy loss through the ceiling due to radiant barrier for period October 14, 1989, to April 12, 1990.	36
Figure 17.	Schematic of laboratory apparatus, for moisture performance tests.	39
Figure 18.	Layout of insulation and radiant barrier coupons for laboratory tests of moisture performance	41
Figure 19.	Area-normalized moisture weight gain for insulation coupons versus time with no radiant barrier.	43
Figure 20	Area normalized moisture weight gains for insulation and radiant barrier (RB) coupons versus time.	44

Figure 21	Area normalized moisture weight gains for insulation and radiant barrier (RB) coupons versus time.	46
Figure 22	Temperature-time protocol and corresponding air leakage flowrates for laboratory tests of moisture accumulation on radiant barriers.	48
Figure 23	Area normalized moisture weight gains for insulation and radiant barrier (RB) coupons versus time for laboratory tests.	49
Figure 24	Attic temperature and air leakage flowrates for field tests over the period January 28, 1990 to February 16, 1990.	52
Figure 25	Area normalized moisture weight gains for insulation and radiant barrier (RB) coupons versus time over the field test period.	53
Figure 26A	Photos of frost accumulation on RB coupon and entire sheet at 8:45 a.m. January 30, 1990 for field tests.	55
Figure 26B	Photos of frost accumulation on RB coupon and entire sheet at 5:00 p.m. January 31, 1990 for field tests.	56
Figure 26C	Photos of frost accumulation on RB coupon and entire sheet at 9:05 a.m. February 3, 1990 for field tests.	57
Figure 27	Wet spot on the inside of the ceiling test panel caused by water drainage from the radiant barrier (February 4, 1990 at 10:18 am.)	58
Figure 28	Frost accumulation on the upper and lower surfaces of the radiant barrier directly above a light fixture. (February 1, 1990 at 8:45 a.m.	60

Figure 29	Type T thermocouples installed underneath roof shingles.	65
Figure 30A	Radiant barrier stapled to the underside of the top chord of the roof trusses in house 5.	67
Figure 30B	Open end of radiant barrier at the roof peak.	68
Figure 31	Average daily peak temperature of shingles on the south face of the roof versus time.	69
Figure 32	Average daily peak temperature of shingles on the north face of the roof versus time.	70
Figure 33	Difference between the average daily peak radiant barrier and uncovered temperatures versus average peak temperature for shingles and sheathing on the north and south faces of the roof.	71
Figure 34	Average daily peak temperature of sheathing on the south face of the roof versus time.	73
Figure 35	Average daily peak temperature of sheathing on the north face of the roof versus time.	74
Figure 36	Difference between the average daily peak shingle and sheathing temperatures for the south face of the roof versus time.	75

EXECUTIVE SUMMARY

INTRODUCTION

Attic radiant barriers have been used in southern climates to reduce summer cooling loads on a house by reducing heat gain through the ceiling. This reduction is due to the low emissivity of radiant barriers which reduces undesirable radiant heat exchange between the roof sheathing and the ceiling. Recent suggestions for using attic radiant barriers in northern climates to reduce winter ceiling heat loss have led to considerable debate regarding the effectiveness of radiant barriers in this situation.

The objectives of this project were a) to evaluate the thermal performance of attic radiant barriers for a heat loss situation; b) to estimate the installation costs versus energy savings for attic radiant barriers; c) to determine any effect that radiant barriers may have on ceiling moisture accumulation; and d) to determine the increase in roofing material temperatures caused by radiant barriers installed under the top chord of roof trusses.

APPROACH

Laboratory investigations into the thermal and moisture performance of radiant barriers were carried out in a cold room. A simulated ceiling section, consisting of drywall, fiberglass insulation, and radiant barrier was attached to a heated box and placed in the cold room. Roof sheathing was simulated by a large plane panel, oriented parallel to the ceiling sample. The sheathing panel temperature was controlled independently of the cold room and heat loss through the ceiling panel was measured for various cold room and sheathing temperatures, with and without the radiant barrier in place. Moisture accumulation on the radiant barrier occurred when warm, humidified air was allowed to escape from the heated box through a small hole in the drywall. The leakage air flow and moisture accumulation on the radiant barrier were measured.

Field tests on the thermal and moisture performance of radiant barriers were carried out in an unoccupied test house where half the attic floor was covered by a radiant barrier and half left uncovered. Ceiling heat loss, roof sheathing and attic air temperatures were monitored in each half of the attic through a winter season. Moisture accumulation on the radiant barrier by air leakage through a small ceiling orifice was monitored over a 2 to 3 week period when attic temperatures were sub-freezing, and moisture accumulated as frost.

Roof overheating tests were conducted during the summer months with a radiant barrier stapled to the underside of the top chord of the roof trusses. Shingle and roof sheathing temperatures were monitored through the summer test period.

RESULTS AND CONCLUSIONS

1. THERMAL AND ENERGY PERFORMANCE

The laboratory and field tests showed that the overall ceiling resistance, with and without a radiant barrier was dependent on the sheathing/attic temperature differences. When the sheathing was colder than the attic air (at night), radiant barriers reduced the ceiling heat loss by reducing the radiant exchange between the ceiling and the roof sheathing. When the sheathing was warmer than the attic air (during a winter day), the radiant barrier actually increased the ceiling heat loss by blocking the beneficial radiant exchange between the sheathing and ceiling. The results are summarized as an effective ceiling resistance. Radiant barriers increase the resistance up to 15% over that of uncovered insulation when sheathing is colder than the attic air, but decrease the resistance up to 43% when sheathing is warmer than the attic air. Over a winter period, there was a net reduction in ceiling energy loss of approximately 5%. However, this represented less than 1% of total energy usage, including air infiltration. For winter climates, attic radiant barriers result in a minor reduction in total house energy usage, but are not a cost effective method of enhancing ceiling insulation.

2. MOISTURE PERFORMANCE

Significant moisture accumulation on radiant barriers occurred at sub-freezing temperatures. Air leakage deposited frost at the radiant barrier/insulation interface resulting in significant localized accumulations over the test period. Under field conditions, enough frost was deposited on the radiant barrier over a brief cold period, that, when melting occurred, water drained through the insulation to the drywall. Evaporation of moisture through the small perforations in the radiant barrier was not large enough to prevent liquid drainage. Use of radiant barriers directly over ceiling insulation increases the amount of frost accumulation at the radiant barrier/insulation interface under sub-freezing temperatures and can lead to melt water draining to the ceiling drywall, causing localized damage.

3. ROOF OVERHEATING

The radiant barrier reflected radiant energy back to the roof resulting in peak roof shingle temperatures that were up to 4° higher than that for the uncovered half of the attic; peak roof sheathing temperatures were up to 10° higher than the uncovered half of the attic. In summer, roof shingle overheating due to radiant barriers is relatively small and does not pose a problem.

1.0 INTRODUCTION

Attic radiant barriers have been proposed as a way to reduce ceiling heat gain during summer months and to reduce ceiling heat loss during winter months. Radiant barriers refer to thin reflective, aluminum foil sheets that have a low emissivity. When placed in an attic space, radiant barriers reduce the radiant heat flow between the floor of the attic and the roof sheathing. During periods when there is solar gain on the roof, the roof sheathing temperature can be several degrees higher than the floor of the attic. Alternatively, during night time cooling, the roof sheathing can be colder than the floor of the attic. In either case, there is a net radiant heat exchange between these two surfaces given by the familiar Stefan-Boltzmann law [1]. The net rate of radiant heat flux depends on the difference between the temperature (raised to the fourth power) of the two surfaces and the physical characteristics of the surfaces, given by their emissivities.

Attic radiant barriers were initially introduced in southern climates where the principal energy usage is for cooling the interior of a house during warm weather. Initial studies [2] showed a noticeable increase in the thermal resistance of attic spaces when radiant barriers were used together with conventional ceiling insulation. Although the improvement in thermal performance in attics with radiant barriers has been shown, the reduction in overall energy usage was less than that claimed by the manufacturers, and this led to some misconceptions by the public. Additionally, there have been recent initiatives by radiant barrier manufacturers to promote the use of attic radiant barriers in northern climates to reduce cold weather ceiling heat loss. The cold weather thermal performance of attic radiant barriers has proven to be fairly contentious, again with regard to the reduction in overall energy usage. Recent field tests [3] were carried out to assess the thermal performance of radiant barriers for ceiling heat loss situations. The results showed an increase in thermal resistance of the ceiling; however, these increases were less than the increases for warm weather conditions. This is to be expected, since the temperature differences between roof sheathing and attic floor would be greater during the summer months, as compared to the winter months. Unfortunately, the field tests were conducted in a southern U.S. region where winter conditions were relatively mild. The obvious question is - how do radiant barriers perform under more extreme winter conditions typical of a Canadian climate?

One of the concerns regarding the use of radiant barriers in winter climates, is the possibility of moisture accumulation. This is of particular concern when the radiant barrier is directly laid over the ceiling insulation, as moisture may be trapped between the insulation and the underside of the radiant barrier. Moisture deposition is most likely to occur during the night when attic temperatures are close to outdoor ambient conditions, while moisture removal (by evaporation) is most likely to occur during the day when solar heating raises attic temperature above ambient. To enhance the evaporation of moisture, radiant barrier manufacturers perforate the radiant barrier with tiny holes spaced on a regular grid. Evidence of such a wetting-drying cycle has been reported [4] in a field study carried out in unoccupied houses near Knoxville, TN during the winter period. However, moisture appeared on the underside of the radiant barrier as liquid condensate only. During the day, drying of the liquid water occurred through the perforation as evidenced by circular dry patches surrounding each perforation. It seems that under these conditions, radiant barriers over ceiling insulation do not pose any serious moisture problems. The authors do, however, state that these results may not be applicable to prolonged periods of subfreezing weather. It was also noted in the field study that the moisture deposition was not uniformly distributed on the radiant barrier but concentrated in areas where there were ceiling penetrations, such as light fixtures, fans, and vent pipes. Warm moist air from the inside of the house can escape into the attic through these penetrations and convect a large amount of moisture to the cold radiant barrier. Under these conditions, moisture was deposited directly above the penetration. The amount and direction of airflow and hence moisture flow was dependent on the indoor/outdoor temperature difference, wind speed and direction, and attic configuration.

To reduce potential condensation problems, the Building Standards Branch of Alberta Labour [5] requires that radiant barriers be applied under roof sheathing (for new construction) and under the top chord of roof trusses (for retro-fit applications). For this method of application, concerns were raised about possible overheating of roof materials during summer months. Although a product listing has been issued for radiant barriers in Alberta, no direct measure of roof overheating has been carried out.

The objectives of this study were:

1. to evaluate the cold weather, thermal performance of attic radiant barriers placed on top of attic insulation;
2. to estimate the cost effectiveness (costs versus energy savings) of attic radiant barriers;
3. to determine any effect that radiant barriers may have on ceiling moisture accumulation, and
4. to determine the increase in roofing material temperatures caused by radiant barriers installed under the top chord of roof trusses.

Thermal performance and moisture accumulation were examined in controlled laboratory cold room experiments and in field tests that were conducted in an unoccupied test house during winter conditions. Roof overheating field tests were also conducted in the test house during summer months. The focus of the laboratory and field tests was to provide credible empirical evidence on the performance of radiant barriers under the extremes of Alberta winter conditions.

This report is divided into three sections dealing with the cold weather thermal performance of attic radiant barriers (section 2), the moisture performance of radiant barriers (section 3), and roof overheating due to radiant barriers (section 4). Procedures and results are discussed within each section, and general project conclusions are presented in section 5.

2.0 THERMAL PERFORMANCE OF ATTIC RADIANT BARRIERS

Laboratory and field tests have been carried out on the cold weather thermal performance of attic radiant barriers. The methods and results of those tests are discussed in this section.

2.1 Laboratory Tests

2.1.1. Apparatus and procedure

An initial set of tests were carried out in a cold room. The ceiling test section consisted of 12.7 mm (1/2") drywall, overlaid by fiberglass batt insulation of varying thicknesses. The test section measured 60 cm x 60 cm (2' x 2') and was attached to the top of a heated box that was thermostatically controlled to a constant temperature of approximately 20°C, simulating the interior environment. The test section and heated box were placed inside a cold room where temperatures could be controlled at constant values between -35°C and -10°C, simulating the attic environment. Two large fans circulated air inside the cold room to provide uniform temperature. The arrangement of the apparatus inside the cold room is shown in Fig. 1. The first set of tests was carried out with no sheathing panel assembly above the test panel. The test panel, with varying thicknesses of fiberglass insulation, was exposed directly to the air currents created by the circulating fans. The heat flux through the test panel was measured in two separate ways. First, a pair of type T thermocouples, spaced at 5.1 cm (2") was inserted in the middle of the fiberglass insulation, parallel to the heat flux. The heat flux was then deduced from the measured temperature difference and the thermal resistance of 5.1 cm (2") of fiberglass insulation. Second, a heat flux gauge was bonded to the insulation side of the drywall, directly below the pair of thermocouples. In addition, the cold room and heated box temperatures were also recorded. In this first series of tests, the thickness of fiberglass insulation was varied for a fixed temperature difference and then the temperature difference was varied for a fixed insulation level. For each test, the steady state heat flux with and without a radiant barrier on top of the insulation was measured.

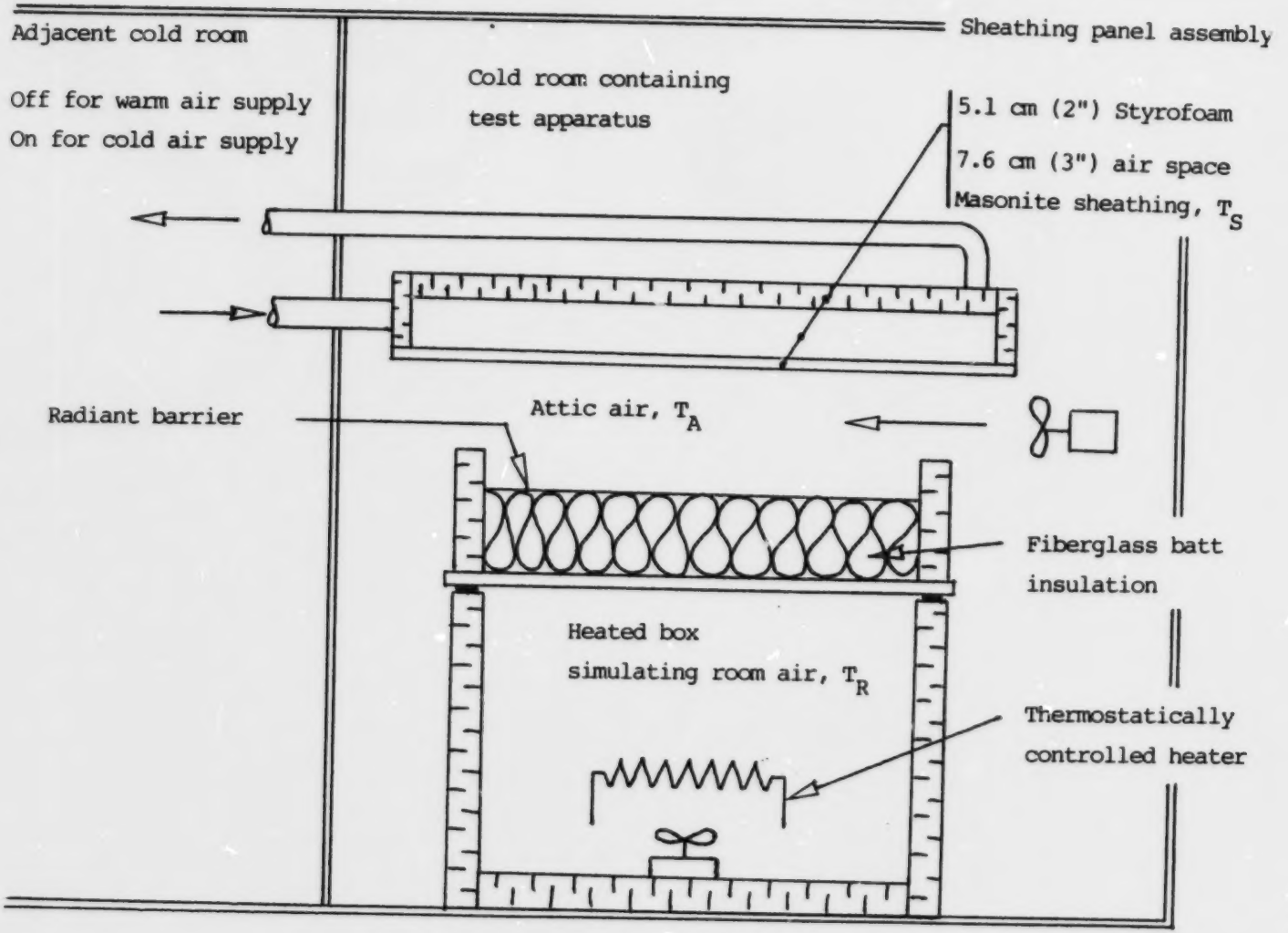

Figure 1. Schematic of the experimental apparatus.

A second series of tests were also carried out in the cold room. During the course of the field testing program, which commenced shortly after the cold room tests, it was noted that there were significant temperature differences between the roof sheathing and the attic air. This implied that there would have been a significant radiative heat exchange between the roof sheathing and the attic floor. In order to simulate the effects of roof sheathing, a large 1.3 m square panel was placed 40 cm (16") above the top surface of the fiberglass insulation. The underside of the panel (facing the fiberglass) was made of hardboard (Masonite) with the rough (high emissivity) surface facing downward. Behind the hardboard was an 8 cm (3") airspace, then 5 cm (2") of polystyrene foam. In order to control the temperature of the hardboard independently from the (attic) air temperature, air was circulated through the airspace by a small fan. The air supply for the panel was drawn from the adjacent cold room, which could be left off to circulate warm or cooled to provide cold air. To achieve panel temperatures warmer than the attic air, the flowrate of warm air from the adjacent cold room (left off) was adjusted to give the desired panel temperature; to cool the panel below attic air temperature, the adjacent cold room was brought down to a very cold temperature and again, the airflow through the panel was adjusted to give the desired undercooling. With this arrangement, panel temperatures could be varied by ±15° from the attic air temperature. The apparatus for this second series of tests is shown in Fig. 1.

For each test, the temperatures of the cold room (attic air temperature), heated box (room temperature), and surface of the sheathing panel were measured. In addition, thermocouples were placed on the insulation side of the drywall and on the radiant barrier to measure these selected temperatures. Heat flux was measured, as in the first set of tests with a pair of thermocouples and the heat flux gauge. The test protocol involved keeping the inside of the heated box at a fixed temperature of 20°C and independently varying both the air temperature and sheathing panel temperature. Tests were run at two nominal air temperatures of -20°C and -10°C. The panel sheathing temperature was varied from 12° above to 8° below the attic air temperature. Several tests were also conducted with no temperature difference between the air and sheathing. For each test, heat flux and

temperature measurements were taken with and without the radiant barrier in place.

2.1.2 Results of cold room tests

The results of the first set of cold room tests are shown in Fig. 2, where the percentage increase in the thermal resistance, $\Delta R/R_o$ of the test panel is plotted versus the overall resistance, R_o of the test panel. It can be shown that

$$\Delta R/R_o = (q/q_{RBT}-1) \quad (1)$$

where q_{RBT} and q are the heat flux through the test panel with and without the radiant barrier in place, respectively. The overall resistance, R_o includes the convective resistance as well as the conductive resistance of all components in the test panel. Fig. 2 includes all tests with varying levels of insulation and temperature differences. The effect of the latter is small as shown in Fig. 3 where $\Delta R/R_o$ is plotted versus the overall temperature difference between the heated box, T_R and the cold room, T_A or ΔT_{RA}. Under all test conditions the radiant barrier decreased the heat loss through the test panel, thereby effectively increasing the thermal resistance of the insulation. The change in thermal resistance decreased rapidly with an increase in the level of insulation and was only significant at RSI values below approximately 2.0; above RSI 2.0 the increase in thermal resistance was small (less than 5%). After obtaining these results, there was some concern that the increase in thermal resistance with the radiant barrier may not have been a true indication of its performance for two reasons. First, the test panel was directly exposed to the strong air circulation patterns in the cold room. This turbulence may have degraded the thermal performance of fiberglass insulation by scouring some of the air trapped within the insulation. Placing a radiant barrier on top of the insulation would have blocked the effect of cold room turbulence on the insulation, thereby increasing the thermal resistance of the fiberglass. Although this is a positive effect, any air resistant barrier placed over the insulation would have the same effect as the radiant barrier. Second, these tests were conducted in the cold room where the air and background wall temperatures were virtually the same (within 0.5° of each other). These test conditions do not adequately reflect the actual conditions

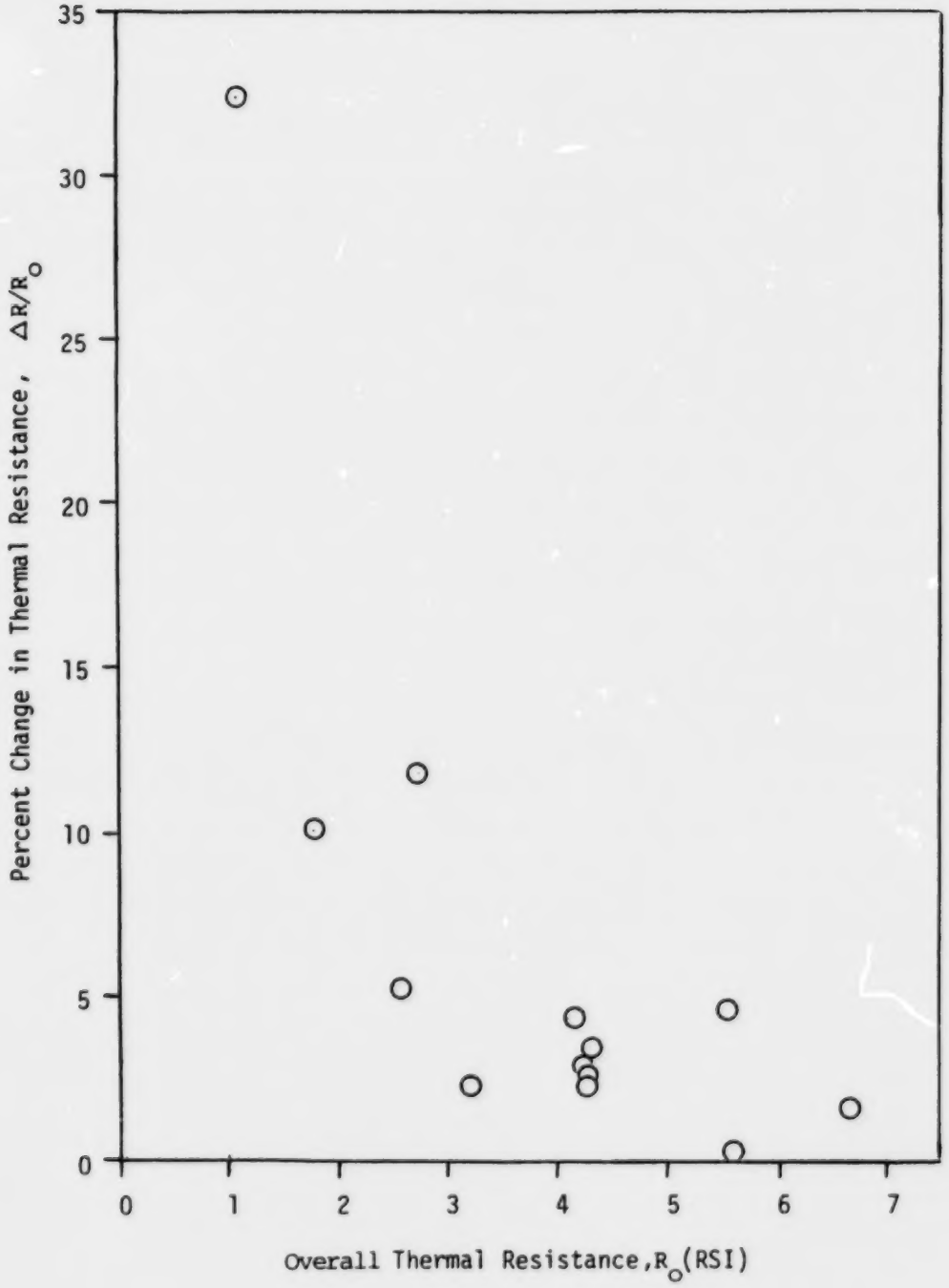

Figure 2. Percentage increase in the thermal resistance of a ceiling panel due to the presence of a radiant barrier as a function of the level of insulation.

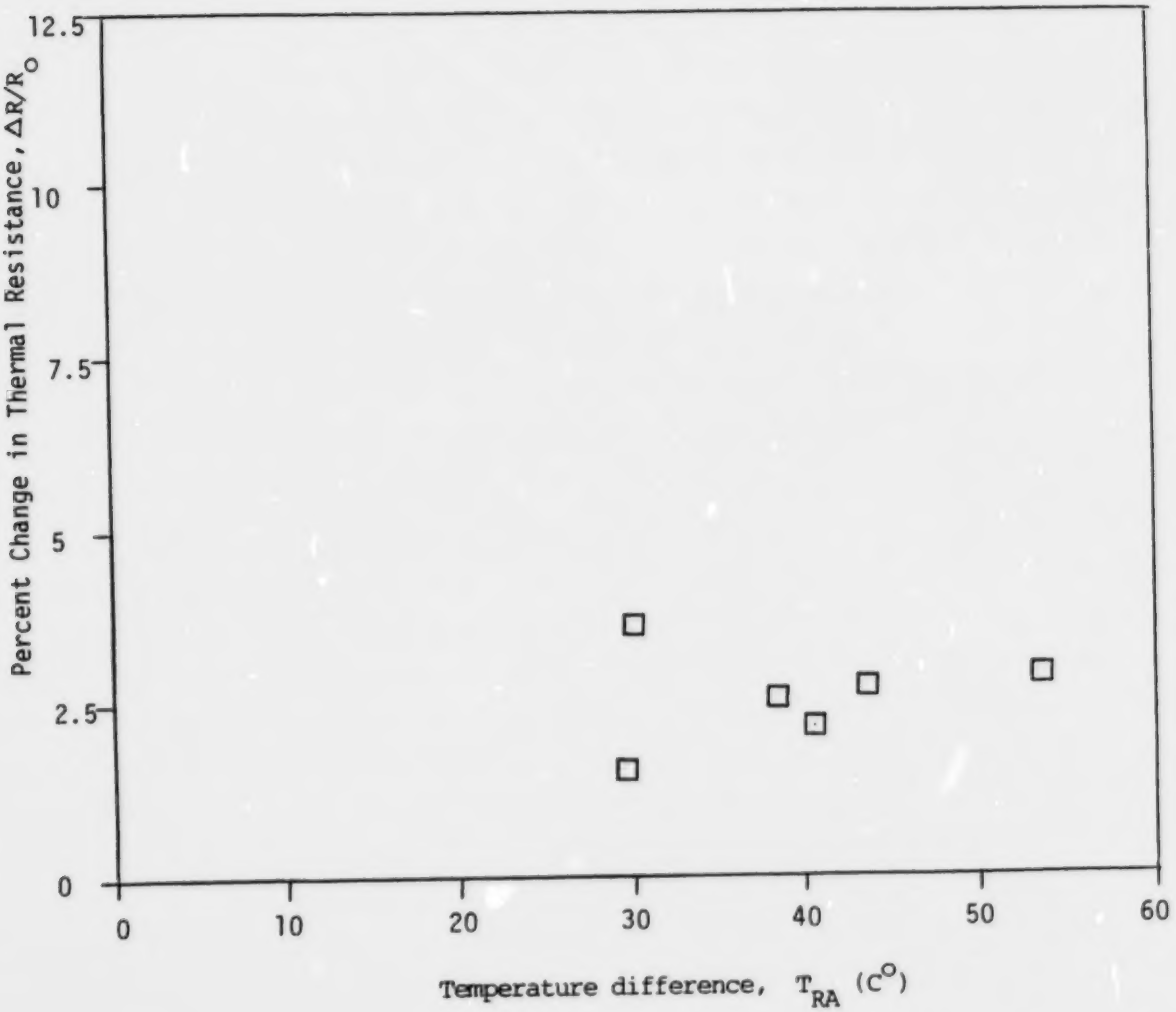

Figure 3. Percentage increase in the thermal resistance of a ceiling panel of fixed RSI 4.25 (R24) as a function of overall temperature difference, ΔT_{RA}.

existing in an attic space, where the roof sheathing can be at a different temperature from the attic floor. Thus, a true indication of the thermal performance of radiant barriers was not portrayed by the first set of tests.

The second series of cold room tests were carried out with a sheathing panel above the test panel to simulate the conditions in an attic space. The temperature difference between the heated box and the cold room was held approximately at three different values and at each temperature difference, the sheathing panel temperature was varied. The results of these tests are given in Table 1. The last entry in this table was a single test in which the heated box temperature, T_R was reduced to 6°C with the cold room temperature, T_A at -13°C and the sheathing at the same temperature (T_S=T_A). The object of this test was to measure the heat fluxes at a lower overall temperature difference. Since the cold room temperature could not be adequately controlled at temperatures above 0°C, the box temperature was lowered. In order to provide a partial check on the data, the heat fluxes with and without the radiant barrier are plotted versus the temperature difference between the cold air and the heated box for those data where the sheathing is at the same temperature as the air; this is shown in Fig. 4. To a first approximation, the heat fluxes should vary linearly with temperature difference with both curves passing through the origin. The solid lines in Fig. 4 are the least squares fit to each of the four data points. Neither line passes through the origin exactly; however, the zero ΔT_{RA} intercepts are -0.85 and -1.97 W/m^2, for the uncovered and the radiant barrier samples, respectively. For the uncovered sample, this magnitude of the intercept is within allowable experimental error for the heat flux measurements. For the radiant barrier curve, the magnitude of the intercept is slightly larger than allowable experimental error. However, this may be partially due to the relatively small sample size that was contained in this data set. A second method of checking the data for the uncovered sample is to calculate the overall resistance (RSI) of the sample from the slope of the straight line; the resistance is simply the inverse of the slope and yields a thermal resistance of 2.48 RSI. The bulk of the thermal resistance is from the fiberglass batt insulation. Based on the measured density of 10 kg/m^3, the thermal

TABLE 1

EXPERIMENTAL DATA FOR THERMAL PERFORMANCE OF RADIANT BARRIERS

T_{Air} (°C)	T_{Box} (°C)	$T_{Sheathing}$ (°C)	ΔT_{RA} (C°) (T_{Box}-T_{Air})	ΔT_{SA} (C°) ($T_{Sheathing}$-T_{Air})	Heat flux, q(W/m^2)	
					No RB	RB
-19.8	19.3	-23.0	39.1	-3.2	16.3	17.8
-20.0	20.0	-20.0	40.0	0.0	15.3	19.9
-20.0	20.0	-15.3	40.0	+4.7	17.3	23.1
-19.8	19.3	-14.2	39.1	+5.6	16.7	16.3
-20.0	20.0	-8.4	40.0	+11.6	13.9	22.9
-20.0	19.5	-7.7	39.5	+12.3	14.1	20.1
-9.9	19.4	-17.2	29.3	-7.3	13.4	14.0
-12.1	20.0	-16.1	32.1	-4.0	12.9	13.6
-10.4	18.5	-10.0	28.9	+0.4	10.5	14.8
-11.7	20.0	-11.3	31.7	+0.4	12.2	14.3
-11.3	20.0	-4.6	31.3	+6.7	10.9	14.5
-9.4	19.3	0.0	28.7	+9.4	11.5	13.8
-11.3	6.0	-11.0	17.3	+0.3	6.2	7.3

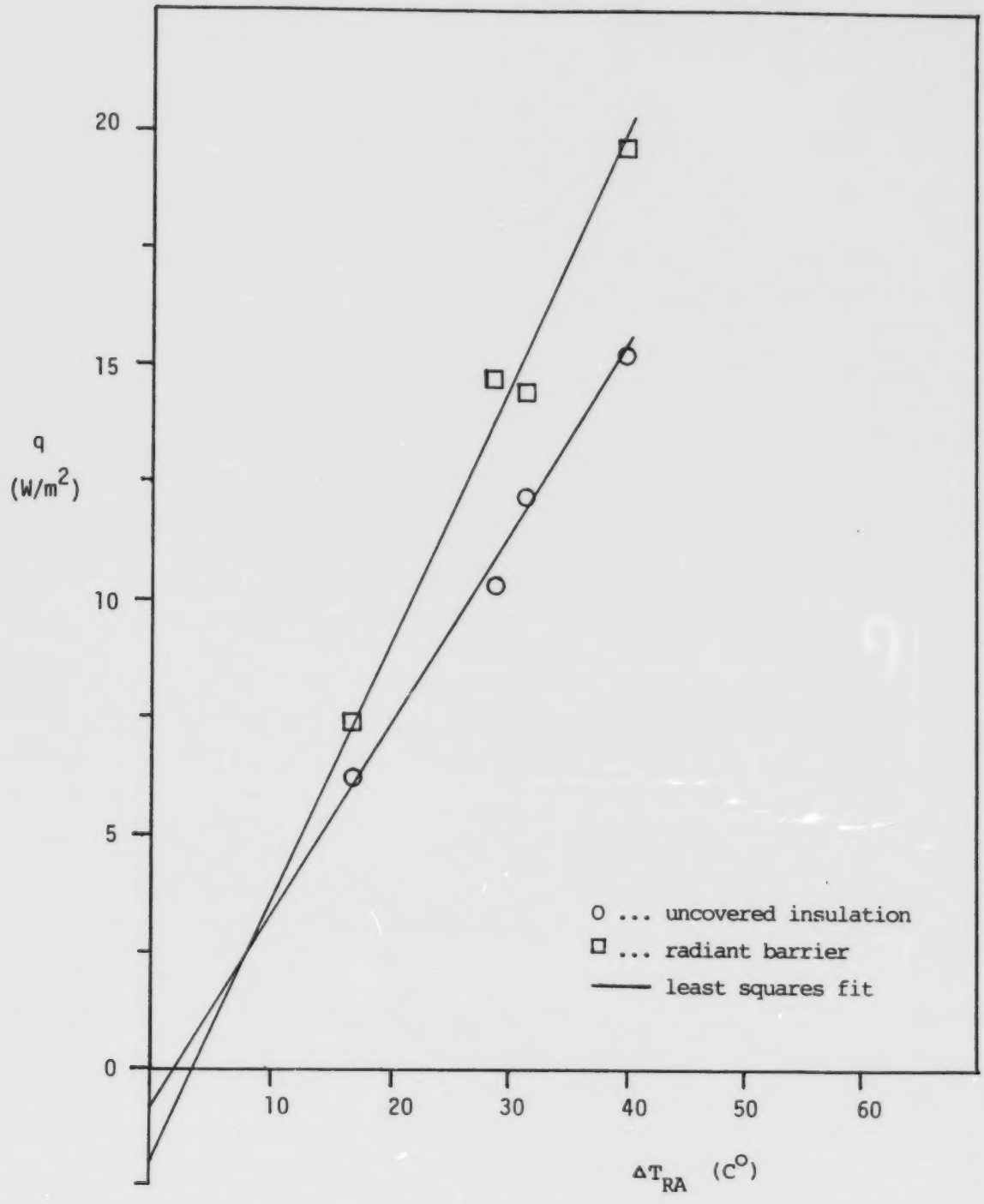

Figure 4. Heat flux versus box/cold room temperature difference, ΔT_{RA} for tests where the sheathing is at the same temperature as the cold room.

conductivity was estimated to be 0.045 W/m-C [6] and for the measured thickness of 0.108 m, the calculated resistance of the fiberglass was 2.40 RSI. There is a small additional resistance due to the convective resistance on the warm and cold sides of the sample which can easily increase the resistance to the estimated value of 2.48 RSI. Thus, the measurements for the uncovered sample were consistent with calculated values.

The interesting feature of Fig. 4 is the increase in heat flux when the radiant barrier was placed over the insulation. This same trend can also be seen in Fig. 5 where the temperature differences (as measured by the thermocouple pair inside the insulation) are plotted versus the overall temperature difference. The temperature differences measured with the radiant barrier in place were consistently larger than those for the uncovered sample implying that the heat fluxes with the radiant barrier were larger than the uncovered sample. Thus, the two independent sets of measurements shown in Figs. 4 and 5 were consistent with each other and showed that the radiant barrier increases the heat loss through the insulation as compared to the uncovered insulation.

The effect of varying sheathing temperatures on the heat fluxes is shown in Fig. 6. The heat fluxes through the insulation (with and without the radiant barrier) are plotted versus the temperature difference between the sheathing and the air. Positive values of the abscissa indicate that the sheathing temperature was higher than the air temperature, which simulates day-time conditions in the attic; negative values of the abscissa correspond to night-time conditions when the sheathing was colder than the air. For the latter situation, the sheathing undercooling was limited to a maximum of 7° since results from the initial field tests showed that sheathing undercooling never exceeded this value. Two different data sets are plotted corresponding to average room/attic air temperature differences of 39.8° and 30.4°, respectively. For both of these temperature differences, the heat fluxes for the uncovered insulation were less than those for

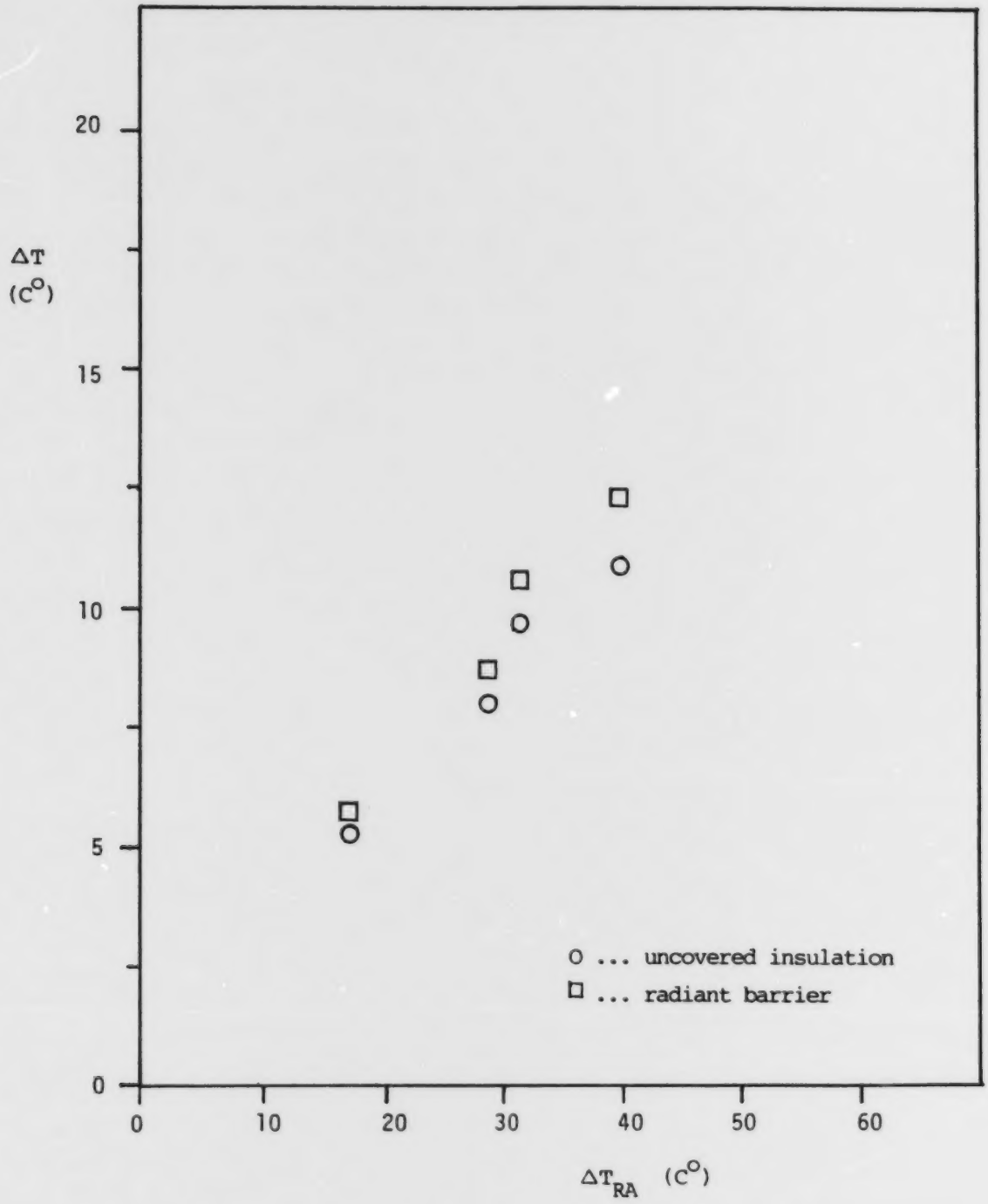

Figure 5. Temperature difference ΔT measured by the thermocouple pair inside the fiberglass versus ΔT_{RA} for tests where the sheathing is at the same temperature as the cold room.

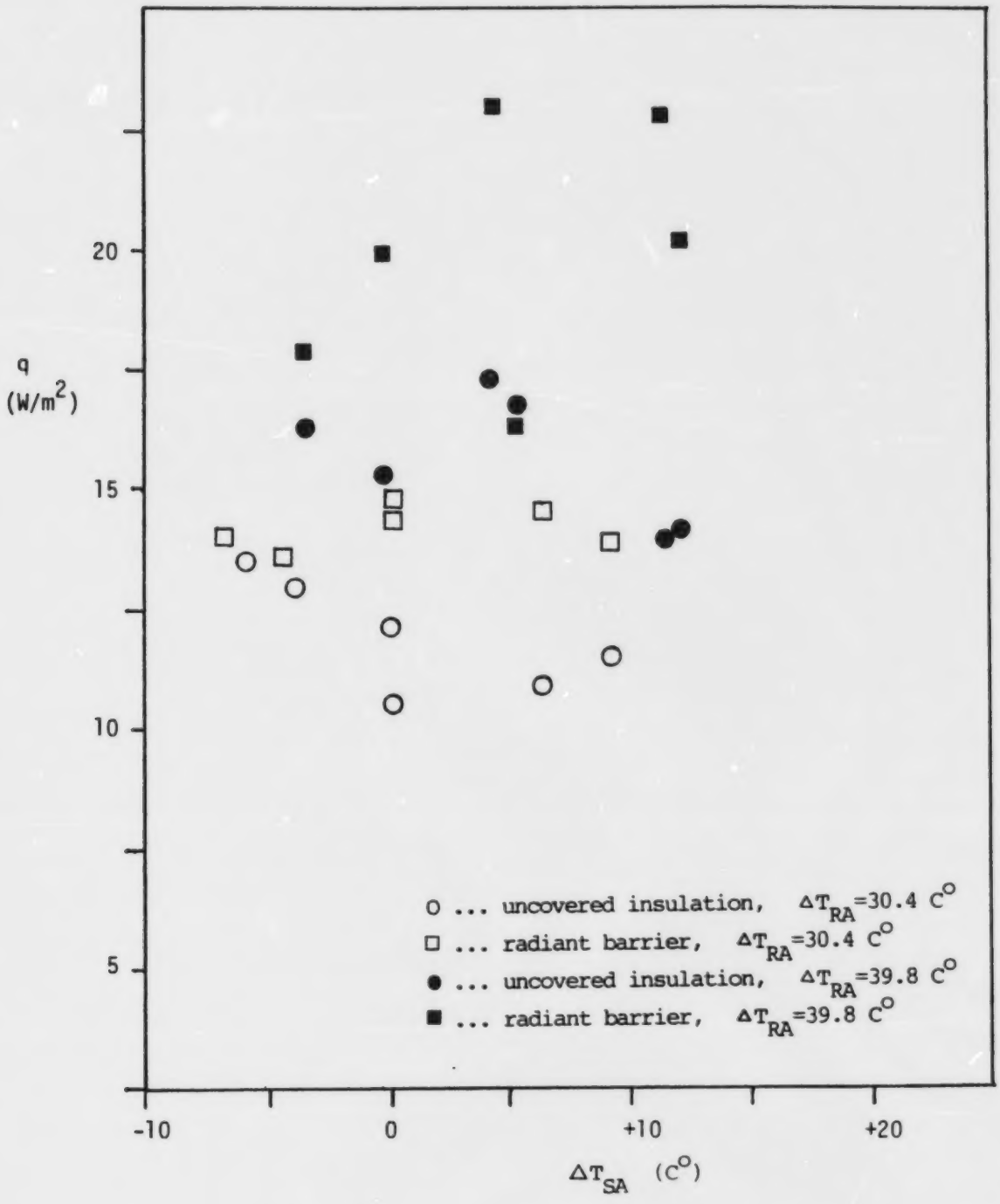

Figure 6. Heat flux, q, versus sheathing/cold room temperature difference, ΔT_{SA}.

the radiant barrier[1]. As the sheathing temperature increased, more radiant heat flowed from the sheathing to the insulation. For the uncovered insulation, this radiant heat opposed the heat being lost to the attic air. The net effect was a decrease in the heat loss through the uncovered insulation as the sheathing temperature increased. This trend can be seen in the circle data for both temperature differences of 39.8° and 30.4°. With a radiant barrier in place over top of the insulation, a large fraction of this radiant heat was reflected back to the attic. Thus, the heat loss through the insulation (with the radiant barrier) should remain relatively unchanged as the sheathing temperature increases. In Fig. 6, the data set corresponding to the 30.4° temperature difference shows that the heat flux with the radiant barrier in place was relatively constant at an average flux of 14 W/m^2. For the other data set shown in Fig. 6, the radiant barrier heat flux was not constant. However, the heat fluxes were greater than for the uncovered insulation.

2.2 Field Tests

2.2.1 Test facility and procedure

Field tests on the thermal performance of radiant barriers were carried out in house 5 at the Alberta Home Heating Research Facility (AHHRF), near Ellerslie, Alberta. House 5 is an unoccupied, single storey house with full basement and gable end roof. Construction details and a photograph of house 5 are given in Table 2 and Fig. 7, respectively. The attic trusses are made from 38x89 mm (2x4) lumber, spaced on 60 cm (2 ft) intervals. The ceiling insulation is fiberglass batts with a nominal insulation value of RSI 2.1 (R 12). Attic ventilation is provided by gable vents located near the peak of the roof which are sized according to building code requirements of 1:300 of attic floor area. The roof is covered with dark brown asphalt shingles. During winter, it is expected that dark shingles will provide slightly higher daytime sheathing temperatures than light colored shingles and will enhance the radiative exchange within the attic space. Installation of the radiant barrier was done by two technicians and half the attic space was covered

---

1 There was one pair of data points that show the opposite trend and it is not clear why this occurred.

TABLE 2

DETAILS OF HOUSE 5

Floor Area	6.7m x 7.3m (22' x 24')
Wall height	2.4m (8')
Basement Height	2.4m, 1.8m below grade (8',6' below grade)
Walls	9.5mm (3/8") Prestained Rough Tex Plywood 64mm (2-1/2") Fiberglass batts 51mm x 102mm (2" x 4") studs, 40cm (16") o/c 4 mil poly vapour barrier 12.7mm (1/2") drywall, painted
Wall area/Floor are	1.38/1
Windows	N 99cm x 193cm (39" x 76") double glazed sealed S none E 101cm x 193cm (40" x 76") double glazed opening W same as E
Window area/Floor area	11.9%
Ceiling	89mm (3-1/2") Fiberglass batts 4 mil poly vapour barrier 12.7mm (1/2") drywall, painted
Roof	CMHC approved trusses with 76cm (2-1/2") stub 95mm (3/8") Ext. GD plywood sheathing 210# asphalt shingles roof pitch 3.0:1
Basement	20cm (8") concrete wall 10cm (4") concrete slab on 6 mil poly
Electric Furnace Capacity	12 kW

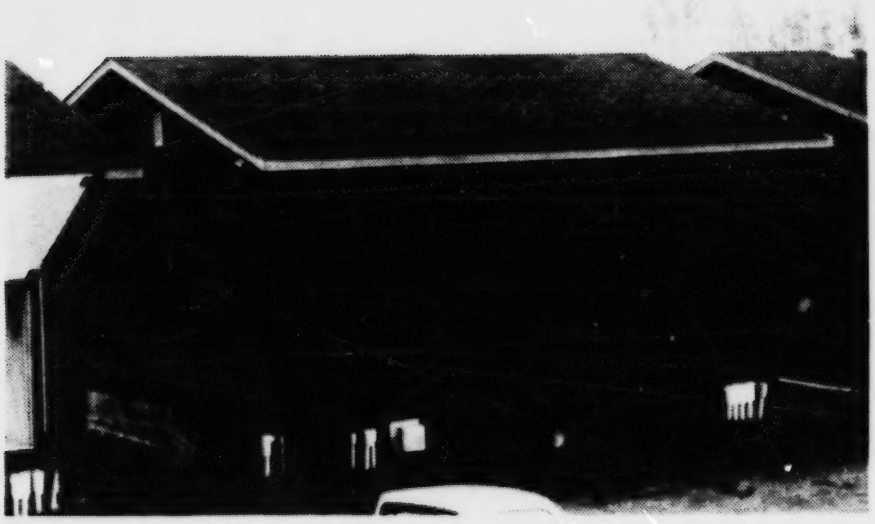

Figure 7. Photograph of house 5 at AHHRF.

in about one hour. As can be seen in Fig. 8, the radiant barrier was simply laid on top of the existing insulation with a small overlap between each layer. Where the radiant barrier had to fit around roof truss supports, it was cut and pressed around the protrusions.

In order to determine the thermal performance of radiant barriers, the field test was designed as a comparative test where the east half of the attic floor was left uncovered and the west half was covered with a radiant barrier. The radiant barrier was a double-sided perforated aluminum foil with a nylon mesh sandwiched between the two layers. This was placed directly over the ceiling insulation with a 3-5 cm (1-2") overlap between layers. Although the required method of installing radiant barriers is under roof sheathing (for new construction) or directly underneath the top chord of the roof truss (for retrofit applications) [5,7], the radiant barrier was tested in the above configuration since laying radiant barriers directly over attic insulation is the easiest method of retrofit application.

Temperature and heat flux measurements at several points in the attic were continuously recorded using a data acquisition system. Ten minute averages for each reading were recorded on a floppy disk. This time interval was chosen because at certain times of the day, for instance, at sunrise, temperatures can change quickly. Ceiling heat fluxes were measured in two separate ways. First, a pair of thermocouples, spaced at 5.1 cm (2") and oriented parallel to the heat flux was placed within the fiberglass insulation. The temperature difference was then related to the heat flux by the thermal resistance corresponding to 5.1 cm (2") of fiberglass insulation. Second, a heat flux gauge was bonded to the attic side of the ceiling drywall, directly below the pair of thermocouples. Thermocouple pairs and heat flux gauges were placed midway between the ceiling joists at three locations on each half of the attic. Roof sheathing temperatures were measured in the middle of each half of the attic, with two thermocouples on the north and south faces of the roof, respectively. In addition, attic and indoor temperatures were recorded. Figure 9 gives the locations of the various thermocouples and heat flux gauges. The indoor temperature was held constant

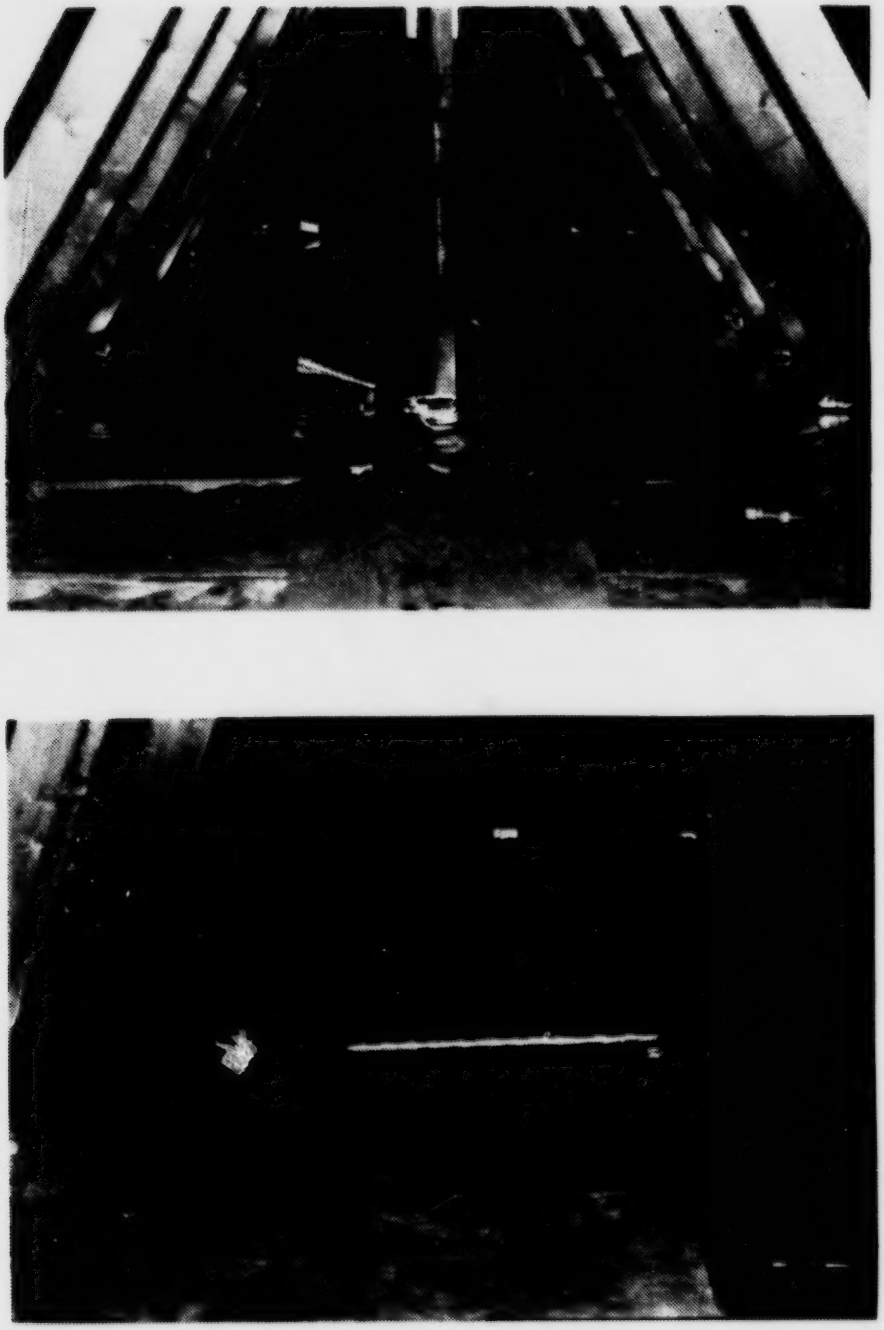

Figure 8. Installation of the radiant barrier in the attic of house 5 at AHHRF.

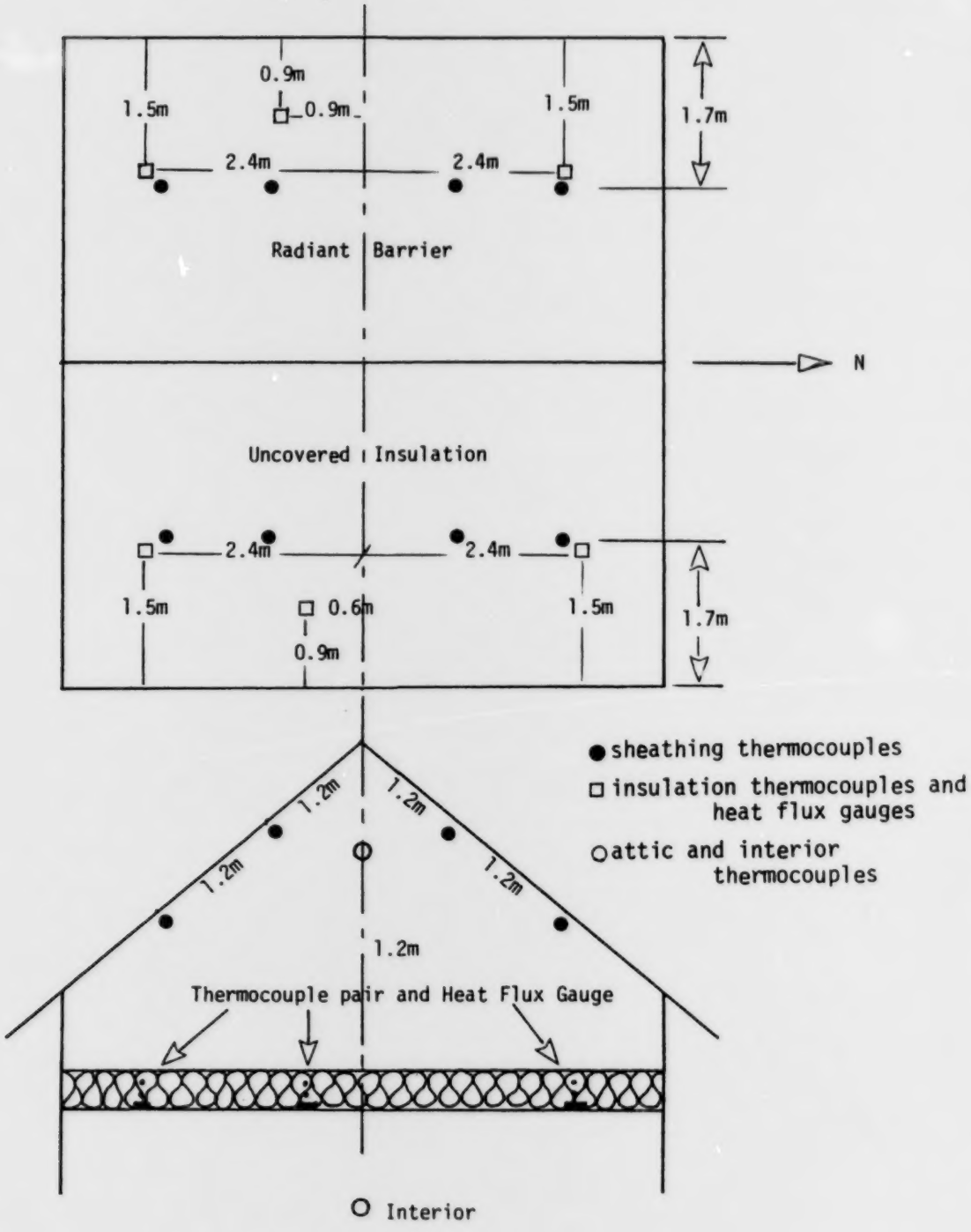

Figure 9. Thermocouple and heat flux gauge locations in attic of house 5.

at 20 ± 2°C. The data acquisition system resolution for temperature measurements was estimated to be ± 0.05°.

The heat flux gauges were bonded to the attic side of the ceiling drywall in order to minimize the effect of temperature fluctuations on the gauge output. Indoor temperature fluctuations occurred when the furnace cycled on and off. However, the heat flux gauges that were used were sensitive enough to record noticeable transient responses corresponding to furnace cycling. An example of this response is shown in Fig. 10 where the average heat flux gauge outputs for the radiant barrier and uncovered sides are plotted over a 24 hour period. When the furnace came on, gauge output showed a rapid increase in output followed by a slower decay back towards the correct value of heat flux, corresponding to the furnace-off condition. With the furnace cycling frequently (as is expected during cold nights), it was difficult to determine the true value of heat loss through the ceiling. Unfortunately, this was the case for much of the winter heat flux data and, consequently, these data were not useful for determining the thermal performance of radiant barriers. However, this figure does qualitatively demonstrate the effect of radiant barriers on thermal performance of the insulation. During the night, when sheathing temperatures were lower than attic air temperatures, heat loss through the insulation in the radiant barrier half of the attic was less than the uncovered half; during the day, when sheathing temperatures were higher than attic air temperatures, the opposite was true. This reversal in thermal performance of attic insulation with radiant barriers will be discussed further in the following section.

2.2.2 Results of field tests

The thermal performance of radiant barriers was determined from the temperature difference that was measured by the thermocouple pairs in the fiberglass insulation. Typical daily variations in this temperature difference are shown in Fig. 11 where the temperature difference has been averaged over the three ceiling locations for the radiant barrier and uncovered sides, respectively. Also shown is the difference between the sheathing and attic temperatures, where the sheathing temperature has been averaged over all eight roof locations. This

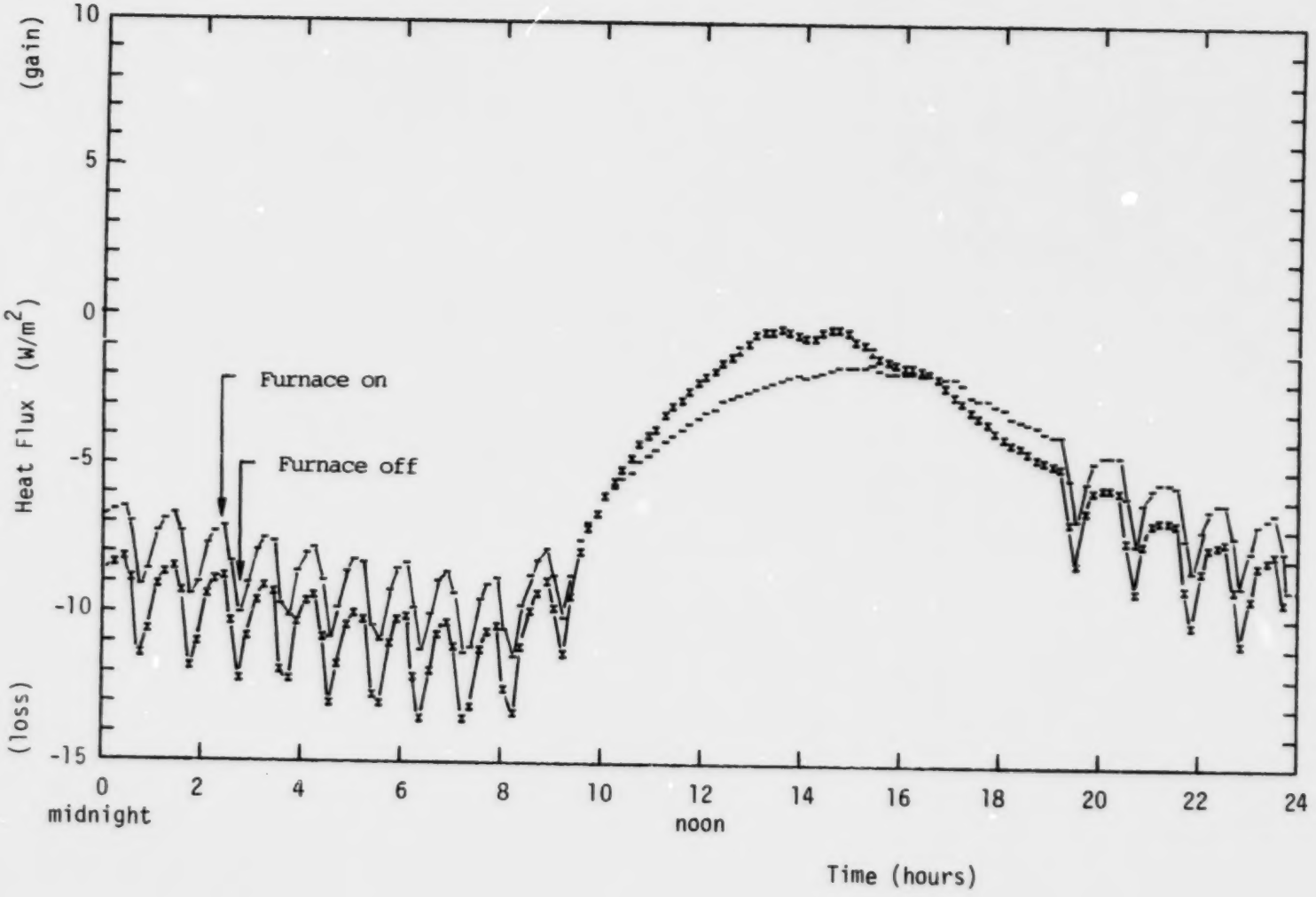

Figure 10. Average ceiling heat flux versus time for Oct. 17, 1989. x data for uncovered insulation; – data for radiant barrier.

averaging was done only for this figure in order to minimize the number of curves and thus, highlight the performance of radiant barriers. Subsequent thermal analysis uses sheathing temperatures that are averaged separately for the radiant barrier and uncovered halves of the attic. Figs. 11a and 11b show temperature variations that occurred on December 18, 1989 and April 10, 1990, respectively. These two days were selected to give an example of a winter day with little solar gain and a spring day where solar gain raised the sheathing temperature above the attic air temperature. Several points are noteworthy regarding the data in Fig. 11. First, unlike the heat flux data shown in Fig. 10, the fiberglass temperature differences showed little or no transient response to interior temperature fluctuations from furnace cycling. These temperature differences were used in the subsequent thermal analysis. Second, the temperature differences were relatively steady during the early morning and mid-day periods and these periods were chosen to evaluate the "steady" state thermal performance of the ceiling insulation. Third, Figs. 11a and 11b contrast the effect of radiant barriers on ceiling heat loss during cold periods. In Fig. 11a the average sheathing temperature was less than the attic air temperature over the entire 24 hour period. For this situation, there was a net radiative exchange from the floor of the attic to the sheathing and placing a radiant barrier between these two surfaces reduced the ceiling heat loss compared to the uncovered insulation. This resulted in smaller insulation temperature differences for the radiant barrier side, as shown in Fig. 11a. In Fig. 11b the sheathing temperatures were less than the attic temperatures during the night, resulting in smaller heat losses for the radiant barrier side compared to the uncovered side; however, around mid-day, solar gain was able to raise the sheathing temperature above the attic air temperature. This led to a net radiative exchange from the sheathing to the attic floor. This radiative heat flux counteracted the conductive heat loss through the ceiling and produced a beneficial reduction in ceiling heat loss through the uncovered insulation. The presence of a radiant barrier blocked this radiative gain and resulted in a larger ceiling heat loss compared to the uncovered side. Thus, in cold weather, a radiant barrier had a detrimental effect when sheathing temperatures were greater than attic air temperatures.

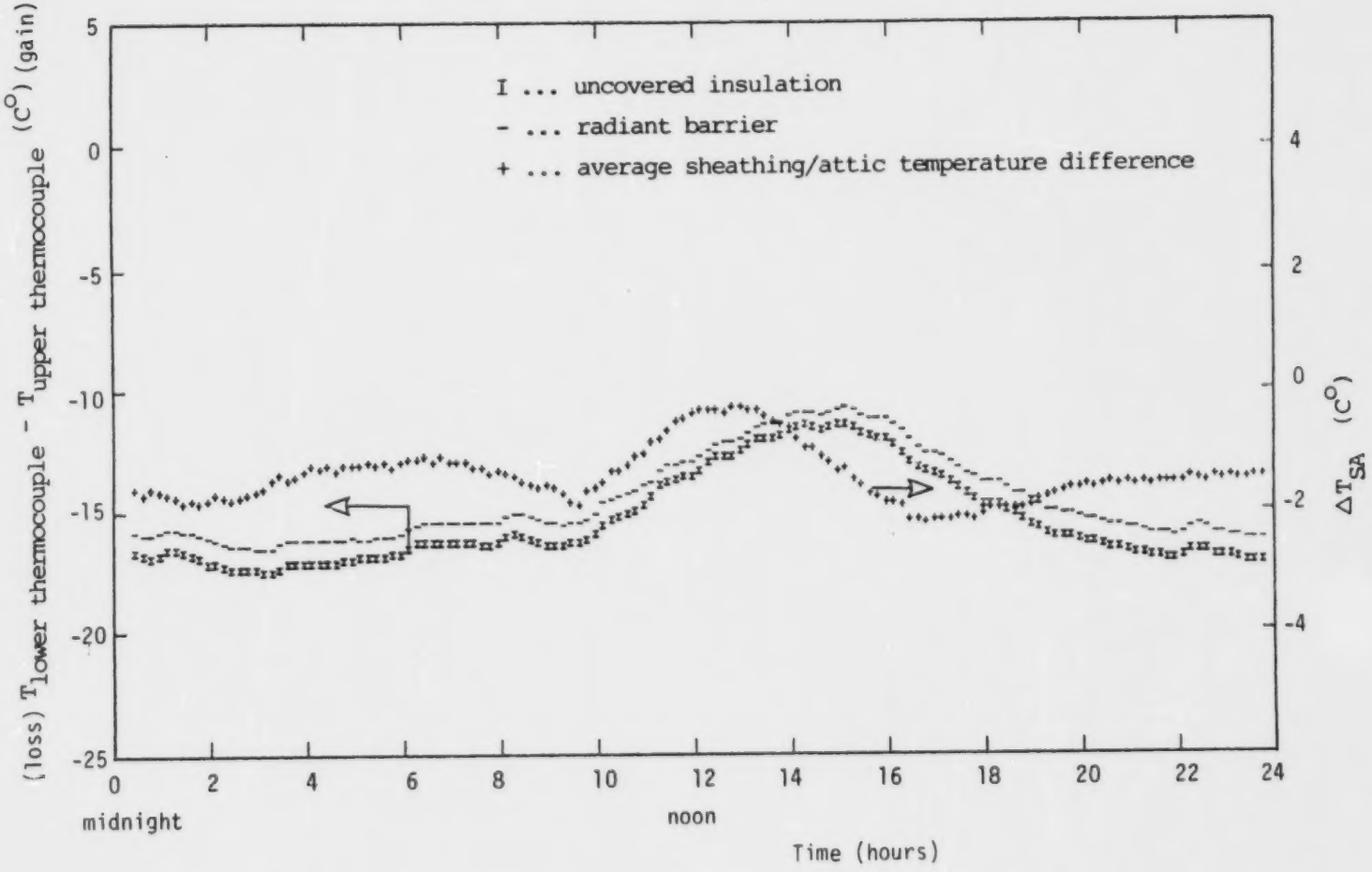

Figure 11a. Average ceiling insulation temperature difference versus time for Dec. 18, 1989.

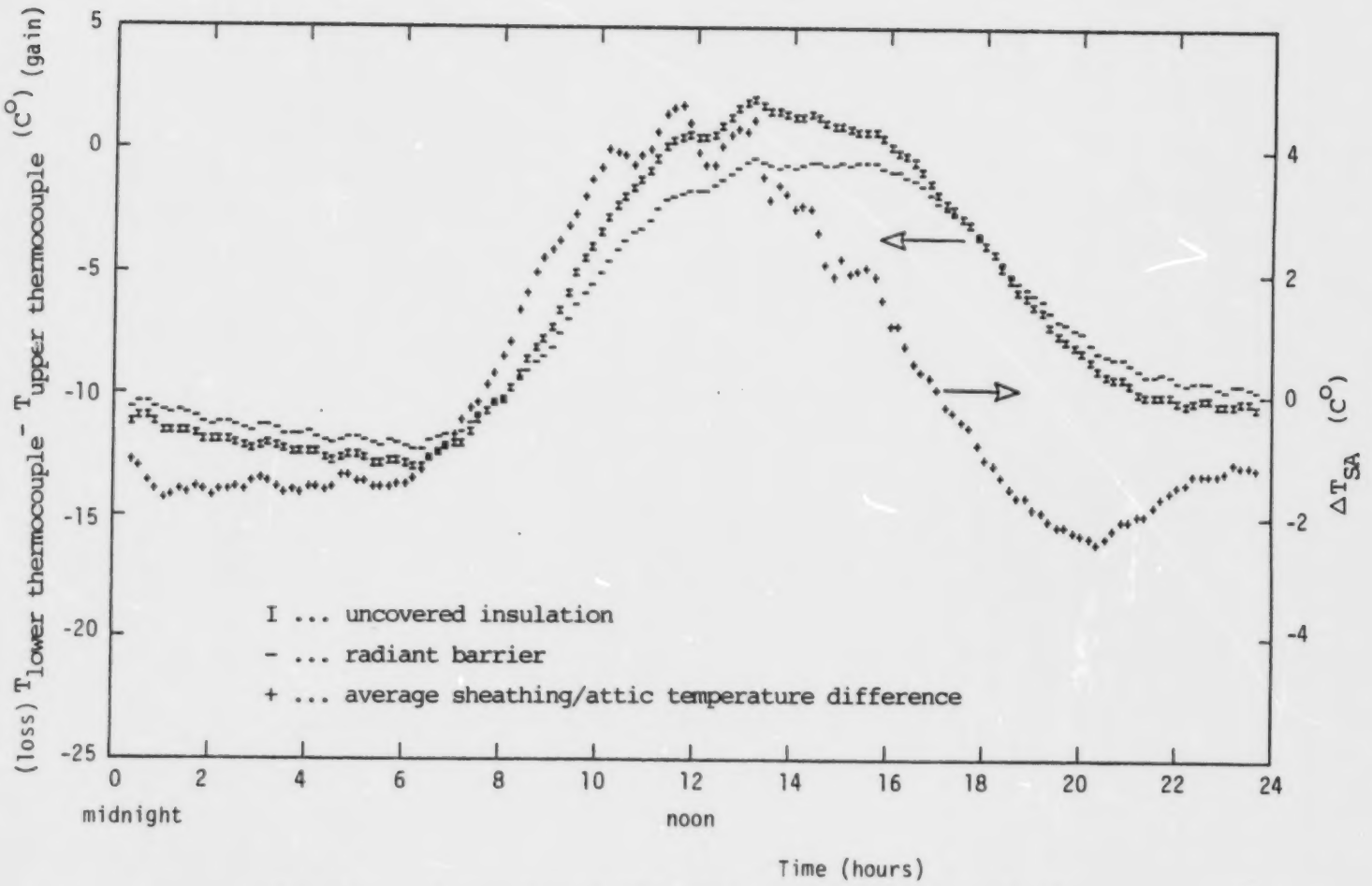

Figure 11b. **Average ceiling insulation temperature difference versus time for April 4, 1990.**

2.3 Discussion of Results

The laboratory and field tests of the thermal performance of attic radiant barriers show similar trends when the data are analyzed to determine effective ceiling resistance. In order to quantify the change in ceiling heat loss due to radiant barriers, the "effective" ceiling resistance was calculated from the measured temperature differences. The heat flux, q through the ceiling insulation is

$$q = \frac{\Delta T}{R_1} \tag{2}$$

where ΔT is the measured temperature difference in the fiberglass and R_1 is the resistance corresponding to 0.051 m (2") of fiberglass insulation. The same heat flux, q can be written in terms of the difference between the interior temperature, T_R and the attic air temperature, T_A

$$\Delta T_{RA} = T_R - T_A; \tag{3}$$

the ceiling heat flux is then

$$q = \frac{\Delta T_{RA}}{R_c} \tag{4}$$

where R_c is the "effective" ceiling resistance which includes the insulation resistance and the interior and attic side convective resistances. Combining Eqns. (2) and (4) yields

$$\frac{\Delta T}{\Delta T_{RA}} = \frac{R_1}{R_c} \tag{5}$$

The resistance R_1 is essentially constant, being weakly dependent on the mean temperature of the insulation [6]. The resistance R_c, however, depends on the radiative exchange within the attic space and this depends on the sheathing temperature, T_S relative to the attic air temperature. Thus,

$$\frac{\Delta T}{\Delta T_{RA}} = f(\Delta T_{SA}, T_A) \tag{6}$$

where $\Delta T_{SA} = T_S - T_A$ and f is a function determined from the measured data. The function, f, is mainly dependent on ΔT_{SA} and to a lesser extent on T_A. Thus, the measured data ΔT, ΔT_{SA}, and ΔT_{RA} were used in determining the correlation function, f.

For the second series of laboratory tests in which the roof sheathing was simulated, the data for the measured heat fluxes were divided by ΔT_{RA} and the results plotted versus ΔT_{SA} in Fig. 12. The two straight lines plotted in Fig. 12 are the least squares fit to the data for the uncovered insulation and the radiant barrier. In the absence of other information, any curve fit other than a straight line would not be justified. The least squares lines simply highlight the trends that are observed in the two data sets. A similar set of curves is shown in Fig. 13 where the temperature differences measured by the pair of thermocouples inside the fibreglass are normalized with ΔT_{RA}, according to Eqn 5. These two data sets show the same trends with the radiant barrier having higher ratios of $q/\Delta T_{RA}$ and $\Delta T/\Delta T_{RA}$ than those of the uncovered insulation. These results imply that the effective resistance of the fiberglass insulation with a radiant barrier is less than that of the uncovered fiberglass, particularly when ΔT_{SA} is positive. An interesting feature of both Figs. 12 and 13 is that the two data sets suggest that there is a "cross over" point. At low (negative) values of sheathing-attic temperature differences, the heat loss through the uncovered insulation is greater than that with the radiant barrier in place. In this case, there is a net radiant heat transfer from the insulation to the sheathing which the radiant barrier would significantly reduce. This implies that the radiant barrier increases the effective thermal resistance. However, from this data it is difficult to determine exactly at what sheathing-attic temperature difference the crossover point takes place. From a simple heat transfer point of view, the radiation exchange between the insulation and the roof sheathing should be very small when the attic and sheathing are at the same temperature and, thus the cross over should occur at ΔT_{SA} equal to zero. This does not seem to be the case for the laboratory measurements; however, the field data do seem to support the heat transfer viewpoint as discussed below.

The field data on heat loss through the ceiling of house 5 were analyzed in the same way as the laboratory data, using Eqn. 5. Data were chosen at two times during the day, at 4:00 a.m. and 12:00 noon, when conditions were near steady state (as noted previously). The data for ΔT were averaged over the three readings for each half of the attic and

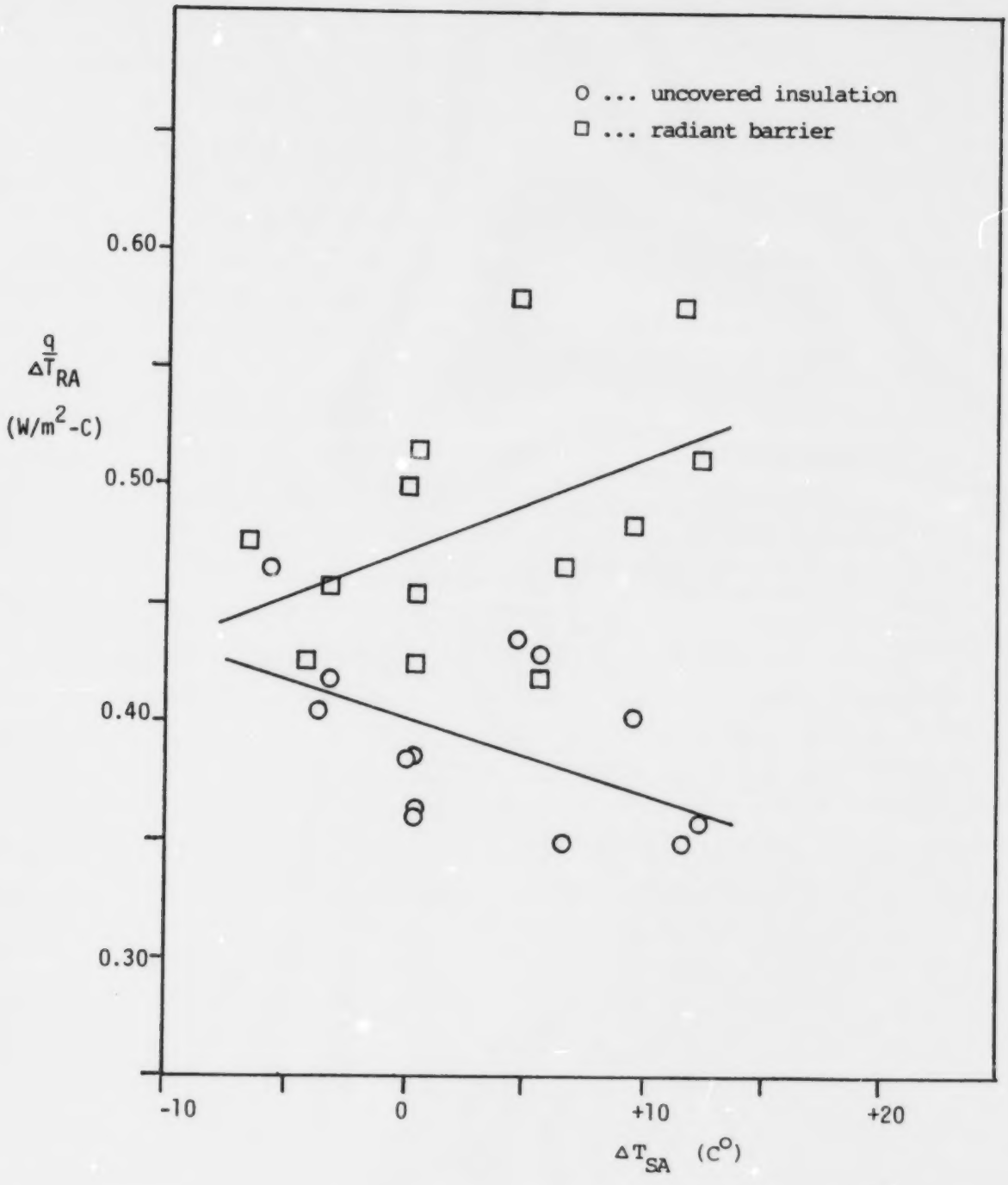

Figure 12. Scaled heat flux, $q/\Delta T_{RA}$ versus ΔT_{SA} for cold room experiments.

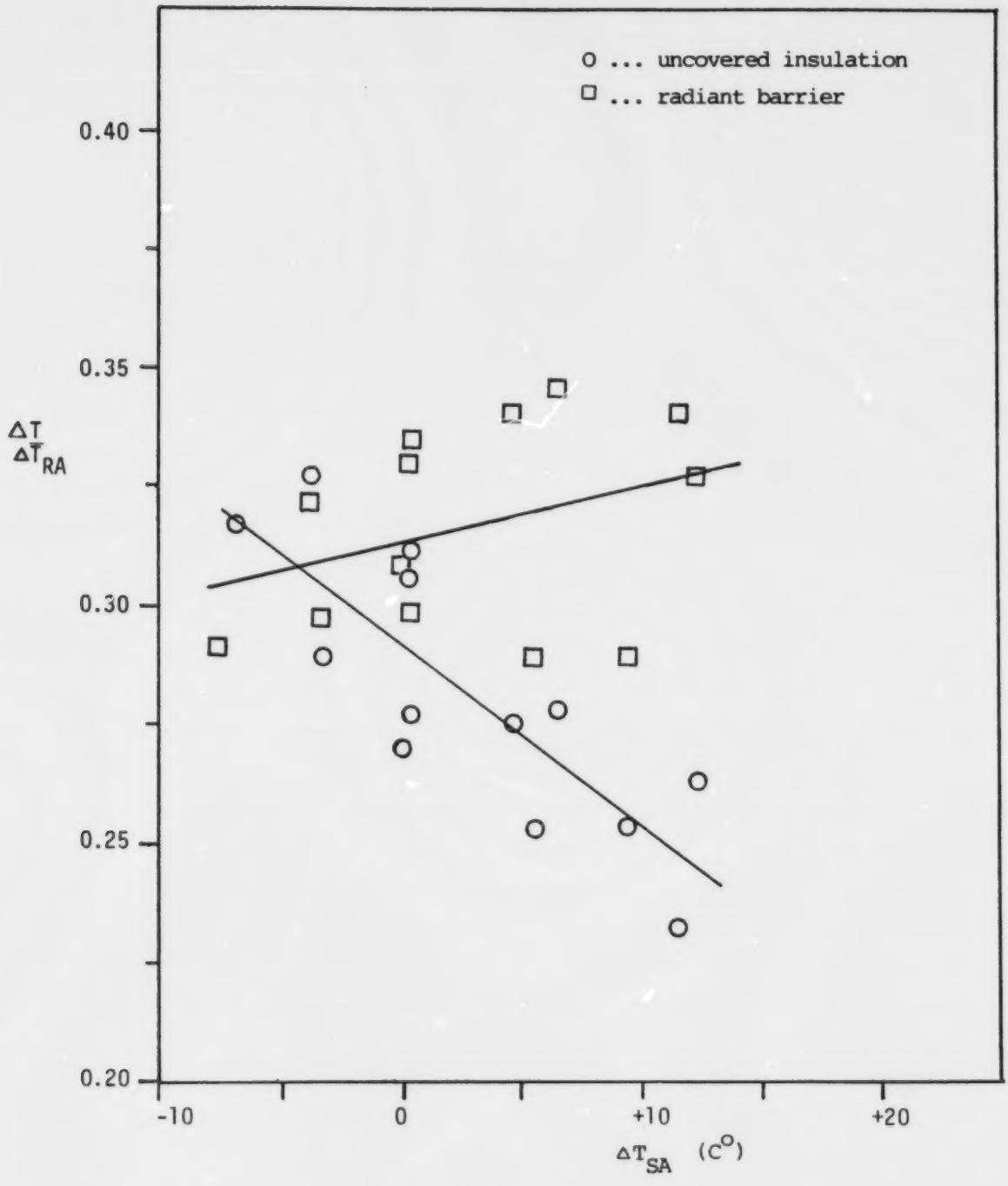

Figure 13. Normalized temperature difference $\Delta T/\Delta T_{RA}$ versus ΔT_{SA} for cold room experiments.

ΔT_{SA} was obtained by averaging over the four sheathing temperatures for each half of the attic. The correlation function was determined for a heating situation in which T_A was less than T_R; only data when ΔT_{RA} was greater than or equal to 3^o were used in the correlation. The 3^o threshold was selected arbitrarily to avoid division by small numbers that would have introduced large errors into the ratio $\Delta T/\Delta T_{RA}$. The above data reduction was carried out for the radiant barrier and uncovered halves of the attic. The results are shown in Fig. 14 where $\Delta T/\Delta T_{RA}$ is plotted against ΔT_{SA} with data selected from the period, October 13, 1989 to April 4, 1990. The two data sets show two separate correlations with ΔT_{SA}, although there is some scatter in the data, particularly for the radiant barrier when the sheathing was warmer than the attic air. For these conditions, part of the scatter is due to the averaging of the sheathing temperatures over the north and south faces of the roof. During the day, the south sheathing temperatures were as much as 2 to 3^o greater than those on the north side resulting in variability in ΔT_{SA}. In addition, large positive ΔT_{SA} usually corresponded to daytime conditions where ΔT_{RA} was small. With the error in $\Delta T/\Delta T_{RA}$ estimated to be $0.3/\Delta T_{RA}$, the error in $\Delta T/\Delta T_{RA}$ was 10% for the smallest value of ΔT_{RA}. On the other hand, when the sheathing was colder than the attic air, ΔT_{RA} was much larger and the two data sets show much less scatter. For the radiant barrier side, $\Delta T/\Delta T_{RA}$ increases monotonically with increasing ΔT_{SA}. From Eqn.5, the temperature difference ratio is inversely proportional to the "effective" ceiling resistance, R_c. Thus, increasing T_{SA} results in a decrease in R_c for the radiant barrier side. This is in contrast with the uncovered side, where $\Delta T/\Delta T_{RA}$ decreases slightly; hence, R_c increases with increasing ΔT_{SA}. Unlike the laboratory data of Figs. 12 and 13, the two data sets "cross over" when the sheathing is approximately equal to the attic air temperature. This is consistent with simple heat transfer theory; when ΔT_{SA} is zero, the attic floor and sheathing temperatures are very nearly equal and there is little net radiative heat exchange between the attic floor and the sheathing. Under these conditions, a radiant barrier will have little or no influence on the effective ceiling resistance. The correlation functions for the radiant barrier and uncovered insulation were obtained by fitting quadratic and linear least squares lines to the two respective data sets. For the radiant barrier, the correlation is

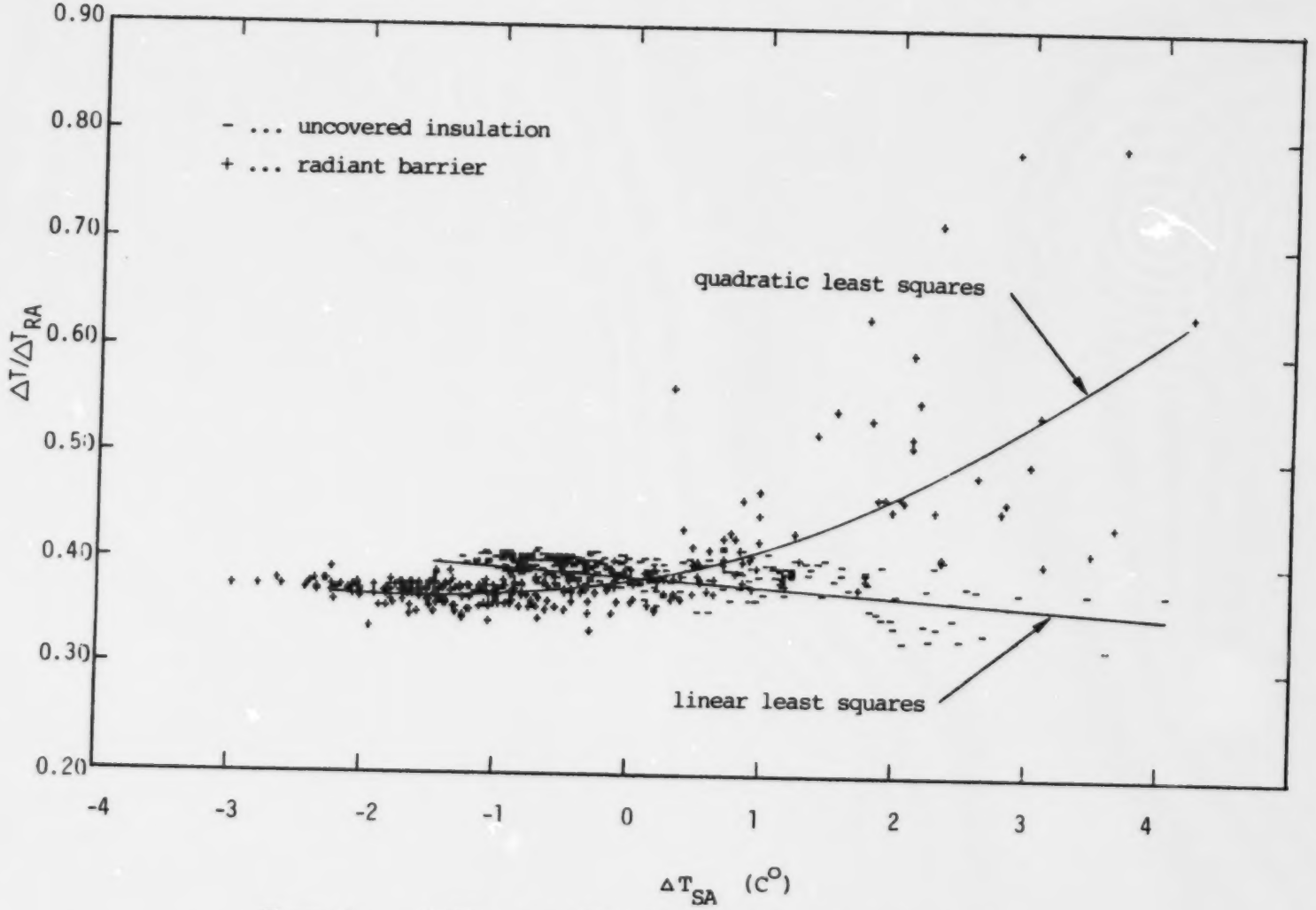

Figure 14. $\Delta T/\Delta T_{RA}$ versus ΔT_{SA} for field data from Oct. 13, 1989 to April 4, 1990.

$$\Delta T/\Delta T_{RA} = 0.379 + 0.0238\ \Delta T_{SA} + 0.0086\ \Delta T_{SA}^2 \quad (7)$$

valid for $-3^{o} \leq \Delta T_{SA} \leq 4^{o}$. For the uncovered insulation,

$$\Delta T/\Delta T_{RA} = 0.385 - 0.0086\ \Delta T_{SA} \quad (8)$$

valid for $-1.3^{o} \leq \Delta T_{SA} \leq 4^{o}$. The correlations given by Eqns. (7) and (8) are shown in Fig. 14 as the two solid lines. It should be emphasized that these correlations are specific to the attic of house 5 with its particular level of ceiling insulation and attic geometry.

The "effective" ceiling resistance, R_c was calculated using the correlations and a fiberglass resistance, R_1 of 1.09 RSI (R 6.16). The results are shown in Fig. 15. This figure highlights the thermal performance of radiant barriers. When the sheathing temperature is less than the attic air temperature, the radiant barrier increases R_c by a maximum of 15% over R_c for the uncovered insulation at the same conditions. However, when the sheathing temperature is greater than the attic air temperature, there can be up to a 43% decrease in R_c below that of the uncovered insulation. The results in Fig. 15 clearly show that the ceiling does not have a "single" effective resistance value for either the uncovered insulation or the radiant barrier covered insulation. The resistance of attic insulation depends strongly on the sheathing/attic air temperature difference. This temperature difference in turn depends on the thermal balance in the attic as dictated by the ambient temperature, sol-air temperature [8], wind speed, wind direction, and the particular attic configuration and leakage distribution. Predictive modelling of attic thermal balances is part of on-going research in the building sciences.

2.3.1. Energy Savings with Radiant Barriers

The net seasonal energy savings attributable to attic radiant barriers was estimated from the measurements made in house 5; the correlations are shown in Fig. 14. Total daily energy loss through the ceiling was estimated by calculating the heat flux for the uncovered and the radiant barrier covered insulation. The measured sheathing temperatures were averaged over the north and south roof faces to yield

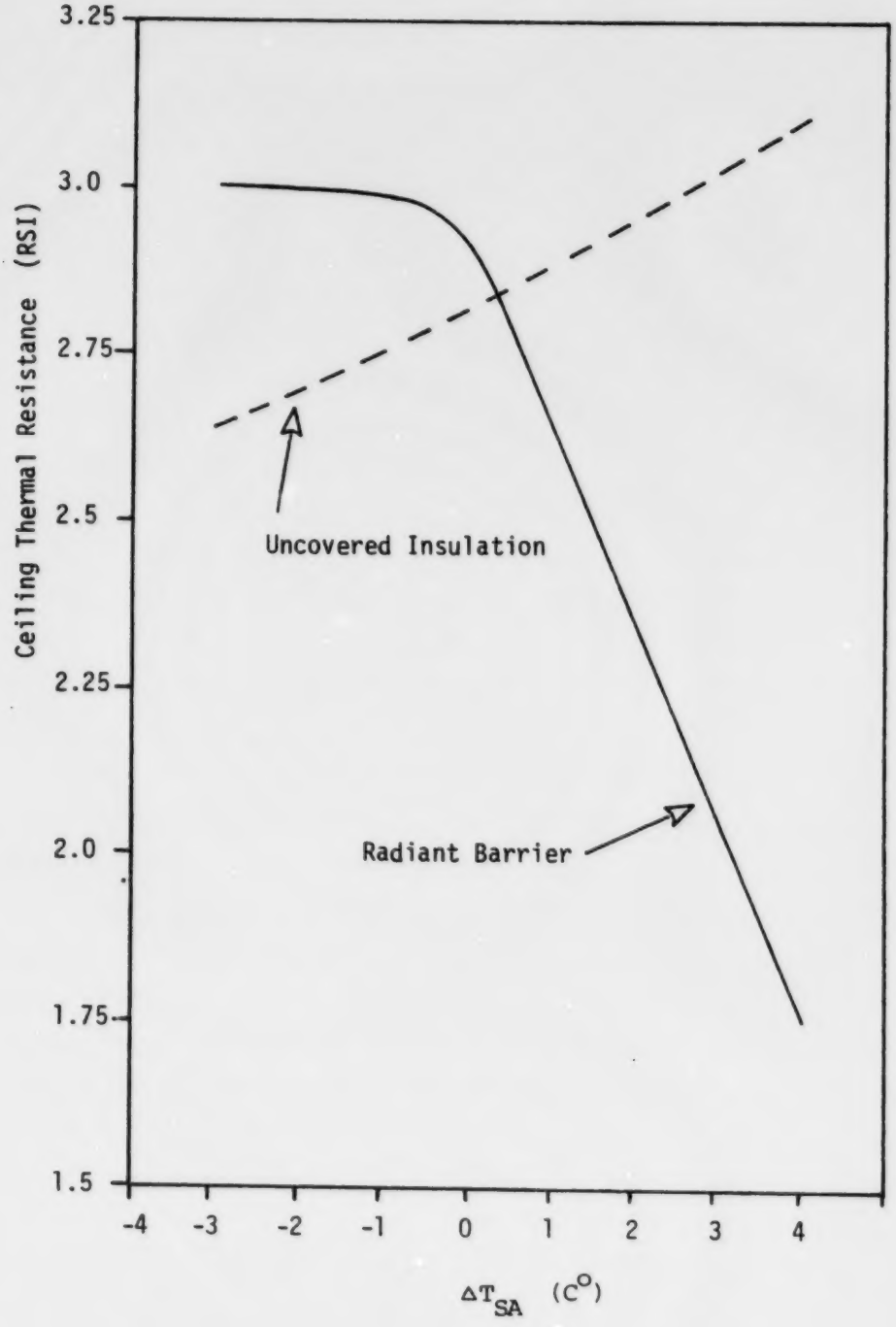

Figure 15. Effective ceiling thermal resistance versus ΔT_{SA}.

ΔT_{SA}. From the correlations in Eqns.6 and 7, the effective ceiling resistances were calculated and the total ceiling heat flux was obtained from

$$Q = A\ \Delta T_{RA}/R_c \qquad (9)$$

where A is the total ceiling area of 49 m^2. The daily energy loss was then obtained by integrating Q over each 24 hour period. In calculating ceiling heat loss, it was assumed that the entire ceiling area was covered with fiberglass insulation. The effect of the wood joists on total heat loss was not included because it is estimated that the joists enhanced the total heat flux by 15% for both cases and only the difference in energy loss was of interest. For those periods when the attic air temperature was greater than the interior temperature (i.e. ceiling heat gain) Q was set to zero. The above calculations were carried out on a daily basis for the heating period from October 14, 1989 to April 4, 1990. The percentage daily energy savings are shown in Fig. 16 for the heating period. During the winter months when solar gain was at a minimum, the radiant barrier provided a consistent 5 to 6% reduction in ceiling energy loss. During these winter days, the radiant barrier would have provided energy savings throughout the day since sheathing temperatures would be less than attic air temperatures throughout the day (as shown in Fig. 11a). During the fall and spring "shoulder" periods, ΔT_{SA} was generally positive during the day and negative at night. Thus, the net daily energy savings were dependent on the amount of solar gain which varied considerably from day to day. Fig. 16 shows that there is increased scatter in the energy savings during the shoulder periods. In fact, on certain days, there is an increase in heat loss through the ceiling, that is, daily heat loss through the insulation with a radiant barrier is greater than that for the uncovered insulation.

If the ceiling heat loss is averaged over the entire period shown in Fig. 16, the seasonally averaged energy savings due to radiant barriers is 5%. For this heating season, the total ceiling energy loss for uncovered insulation was approximately 5.0 GJ (gigajoule), with only 0.25 GJ energy saved when a radiant barrier was used. From previous measurements on house 5, the ceiling heat losses accounted

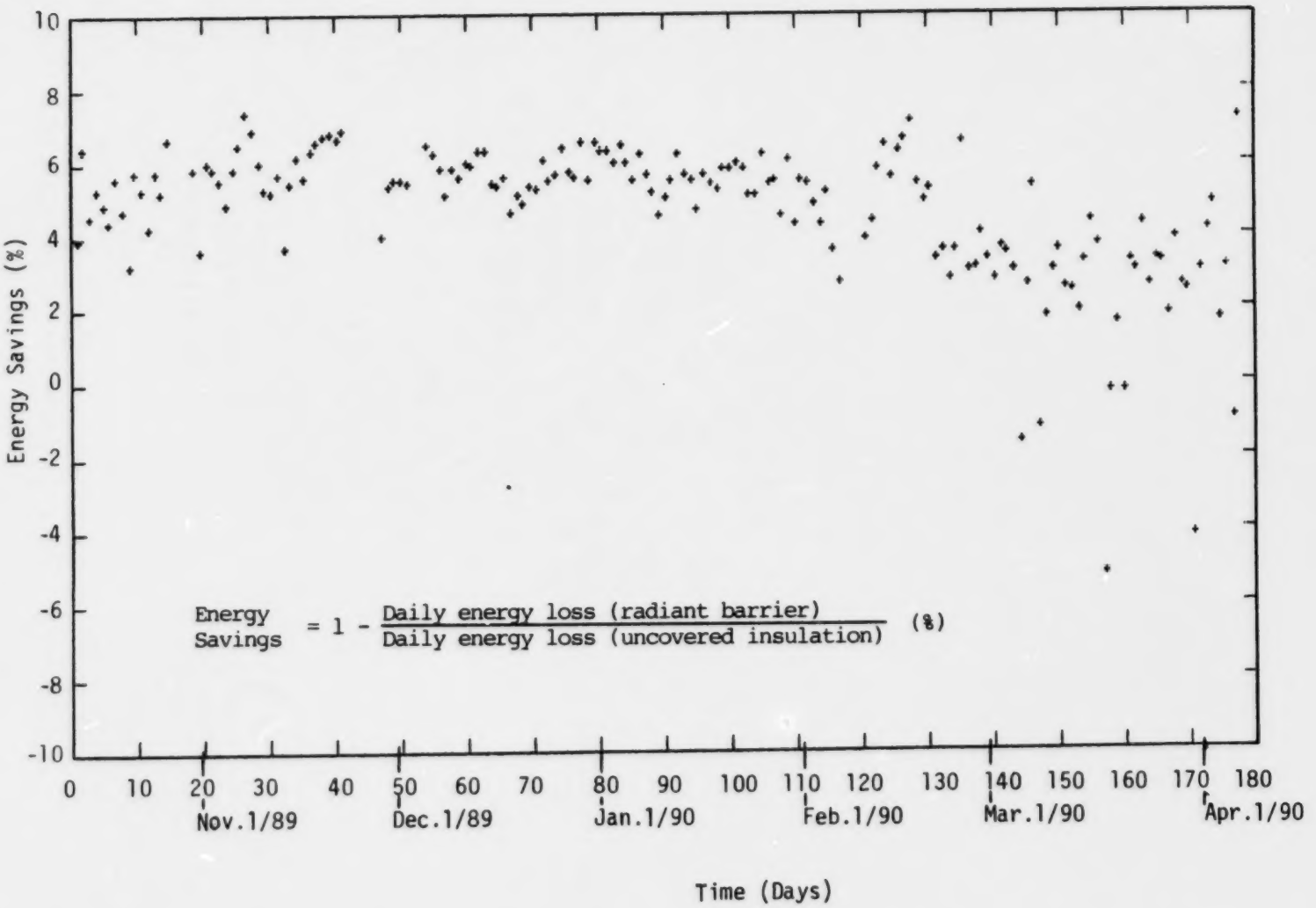

Figure 16. Percentage change in daily energy loss through the ceiling due to radiant barrier for period October 14, 1989, to April 12, 1990.

for approximately 15% of the total energy usage, including air infiltration losses [9]. Based on the seasonally estimated ceiling heat loss of 5.0 GJ and the 15% fraction, the total house energy usage was estimated to be 33 GJ which is close to the measured total energy usage. From an overall energy point of view, the use of radiant barriers in an attic can only be expected to save less than 1% of the total house energy usage. It is doubtful whether such a small change in energy usage would be noticeable given that energy usage can vary considerably from season to season. It should be emphasized that these estimated savings are based on the measured results in house 5. Houses with different attic configurations, leakage characteristics, and insulation levels will have different energy savings with the use of radiant barriers. For example, it is expected that energy savings for heat loss through ceilings with higher insulation levels (typical of more recent housing) will be less than the seasonally estimated 5%. A detailed estimate of energy savings when using radiant barriers in a given house requires a prediction of thermal conditions in the attic space as a function of ambient conditions.

Finally, a rough estimate was made of costs and potential savings from the use of attic radiant barriers for winter periods. The costs involve the purchase and installation of radiant barriers. After tracing several leads, one Alberta-based radiant barrier supplier estimated an installed cost of approximately, \$16/m^2 (\$1.50/ft^2). This is close to the estimate made by the original US-based supplier of the radiant barrier that was used in this study. Their estimate in February, 1989 was \$10.70 US/m^2 (\$1.00 US/ft^2). For house 5, radiant barrier costs would amount to \$784. This contrasts with the cost savings associated with energy savings of 0.25 GJ. For natural gas heating, this energy saving translates into a cost saving of only 60 cents per heating season based on current natural gas prices of \$2.30/GJ; for electric heating, the cost savings are estimated to be \$4.70 based on 6.75 cents/kWhr. A full cost benefit or payback analysis was not warranted because the capital and installation costs far outweigh any energy savings.

3.0 MOISTURE PERFORMANCE OF RADIANT BARRIERS

In this section, moisture accumulation due to attic radiant barriers is investigated. Both laboratory and field tests were carried out for cold weather periods, with sub-freezing temperatures and frost accumulations monitored throughout the test periods.

3.1 Laboratory Tests

3.1.1 Apparatus and procedure

The laboratory tests were designed to simulate moisture deposition on radiant barriers during sub-freezing temperatures. A sample of 90 mm (3.5") thick fiberglass insulation was placed on top of a 12.5 mm (1/2") piece of drywall to simulate a section of ceiling assembly. The test section measured 57 x 57 cm (23" x 23") and was placed on top of a heated box, as shown in Fig. 17. The temperature in the box was thermostatically controlled and the humidity was controlled by circulating air, within the box, across an open pan of water. Water was supplied to the pan to maintain a constant depth. This arrangement produced a relative humidity in the range of 25 to 35% which is typical of indoor relative humidities during winter. Interior temperature and relative humidity were monitored continuously. The box and ceiling sample were placed in a cold room where the temperature was kept constant at approximately -20°C.

Previous observations had noted that significant moisture accumulation accompanied air leakage from indoors to the attic. To simulate this, a 0.95 cm (3/8") diameter hole was made in the drywall at the center of the ceiling sample. The hole became the opening for a calibrated orifice-plate flowmeter which was attached to the bottom of the drywall. The area of the orifice was approximately 0.7 cm^2 (0.1 in^2) which is typical of electrical outlets and switches [10]. For the laboratory tests, the airflow was from the box to the cold room and was driven by the pressure difference generated by the stack effect. A 2.5 cm (1") diameter hole was drilled near the bottom of the box to allow air to enter the box from the cold room. For the box configuration and a box-cold room temperature difference of 40°, the stack effect was estimated to be 2 Pa (~0.02" water). A low range (±25 Pa) pressure transducer continuously monitored the pressure drop across the orifice flowmeter. During the tests, the airflow was virtually constant as long as

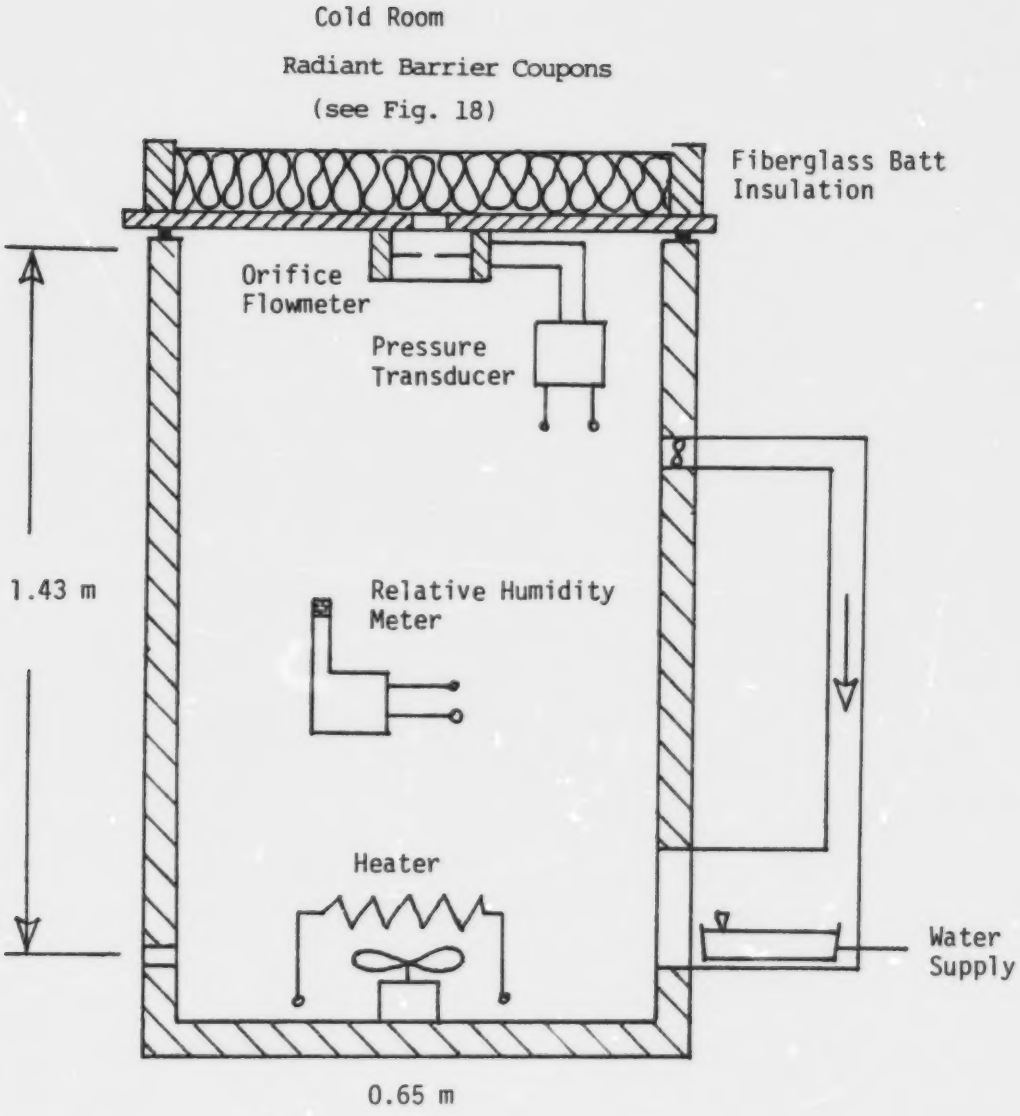

Figure 17. Schematic of laboratory apparatus, for moisture performance tests.

there was no external interference, such as opening the cold room door or changing the air circulation pattern in the cold room.

In order to quantify frost accumulation, the weight gain of three radiant barrier coupons was manually recorded throughout the test period. Coupon A (12 cm x 12 cm) was placed directly above the orifice, on top of the fiberglass insulation, while coupons B (18 cm x 9 cm) and C (18 cm x 9 cm) were located near the outer edge of the ceiling sample (see Fig. 18). In addition, moisture accumulation in the fiberglass insulation directly below each radiant barrier coupon was measured. Thin sections of insulation (approximately 2 cm thick), shown in Fig. 18 were used which measured 12 cm x 12 cm (coupon A), 12 cm x 5.5 cm (coupon B), and 12 cm x 5.5 cm (coupon C). This would indicate whether frost accumulation was concentrated at the radiant barrier/insulation interface or distributed within the insulation. The radiant barrier itself was a double-sided aluminum foil with a nylon mesh sandwiched between the two sheets. The tiny perforations in the foil averaged 0.097 mm (0.0038") in diameter and the perforation density was estimated at 10 holes/cm^2 giving an open hole area of 0.074%. It is not known whether this is typical of radiant barriers produced by other manufacturers. Two series of tests were carried out. The first was a long term (approximately 6 days) frost accumulation test under constant conditions. To establish a basis for comparison of results, the first test was with no radiant barrier over the insulation, followed by a test under identical conditions with a radiant barrier in place. In one of these tests, the weight changes of the radiant barrier and the fiberglass coupons were measured beyond the 6 day accumulation period when the air temperature in the cold room was increased to room temperature. This was done to determine the drying time. The second test was a short term test, which simulated a daily cycle of attic temperatures during moderately cold periods. During the night (approximately 18 hours) the cold room temperature was held at approximately -20° and during the day, the cold room temperature was allowed to increase above freezing for a 2 to 3 hour period. With temperatures above freezing, frost on the radiant barrier will melt and evaporation will occur through the perforations. The intent of these short

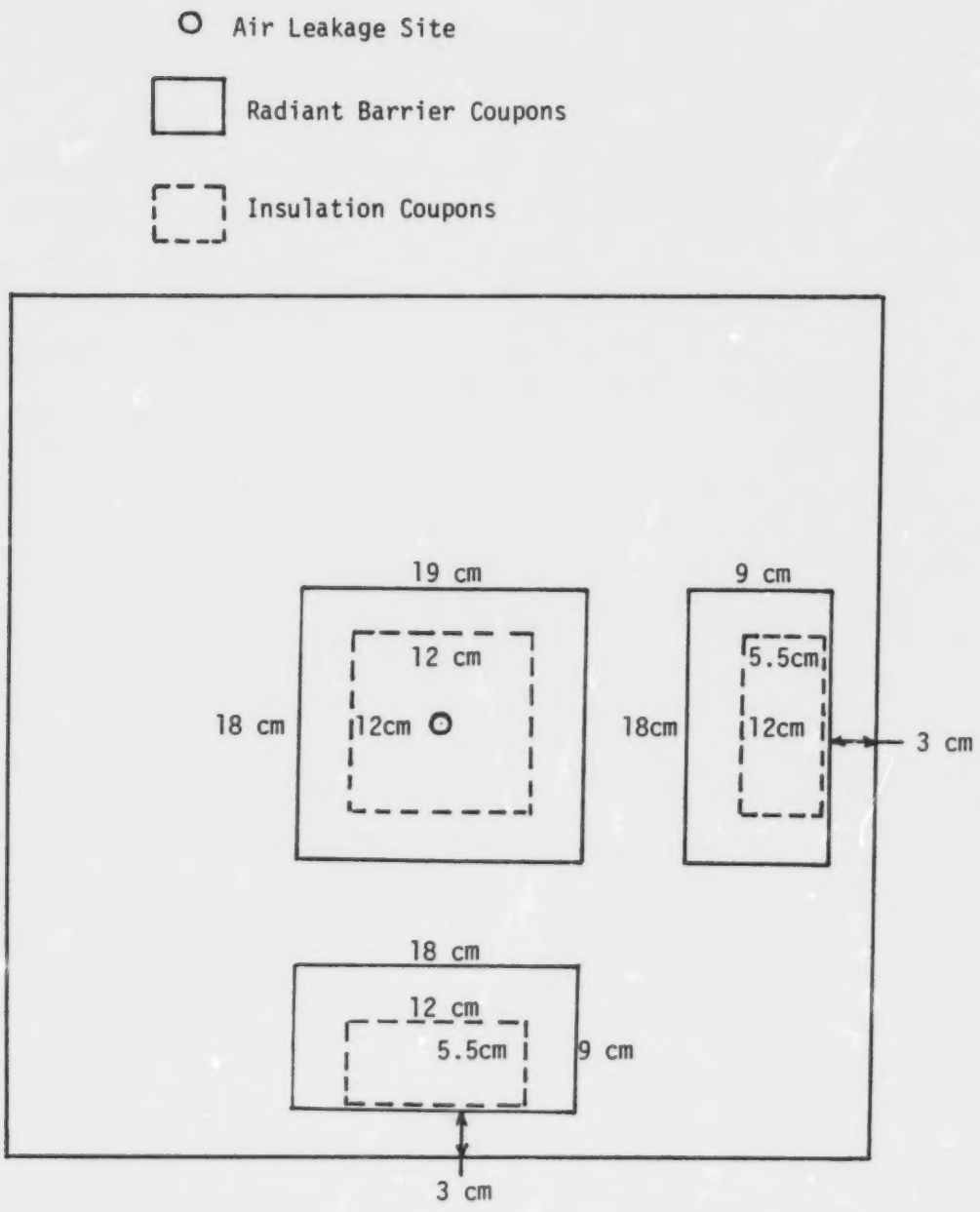

Figure 18. Layout of insulation and radiant barrier coupons for laboratory tests of moisture performance.

term tests was to determine if there was a significant amount of evaporation during the warm part of the daily cycle.

3.1.2 Results of cold room tests

The first test was a control to determine the amount of frost accumulation in the fiberglass with no radiant barrier. The box conditions were 23°C and 34% RH while the cold room temperature was -21°C. Under these conditions the airflow through the opening was constant at 0.17 m^3/hr over the test period of 6 days. The results are shown in Fig. 19 as mass of frost accumulating in the three fiberglass coupons normalized by the coupon area versus time. It should be noted that frost accumulation occurred at the upper surface of the fiberglass with little penetration into the insulation. Coupon A shows the largest weight gain over the test period since it was located directly over the orifice. Both coupons B and C showed very little moisture accumulation. Most of the air leakage flowed directly upward through the insulation and thus, it is expected coupon A would show the largest weight gain of the three. During the cold period, the moisture accumulation was roughly linear with time, although the weight gain measurement for coupon A at 68 hours was much larger than expected. This may be due to the small changes in weight that occur; over the entire 6 day period the total weight gain for coupon A was only 2.5 gms and small errors in measurement may explain part of this anomaly. At the end of the accumulation phase, the cold room was allowed to warm up to room temperature (approximately 20°C). This led to a rapid drying of the insulation which was complete after 6 hours. At the end there was no discernible damage to the fiberglass.

The second test followed the same protocol except that a radiant barrier was placed over the fiberglass. The results of this test are shown in Fig. 20 where the area normalized weight gains are plotted versus time for the three radiant barrier coupons as well as the insulation coupon A. Insulation coupons B and C are not shown because they showed little or no weight change. Comparison of Figs. 19 and 20 shows that the amount of frost accumulation in the insulation coupon A was only 30% larger for the radiant barrier test compared to the uncovered test. However, a large amount of frost did accumulate on the radiant barrier coupons

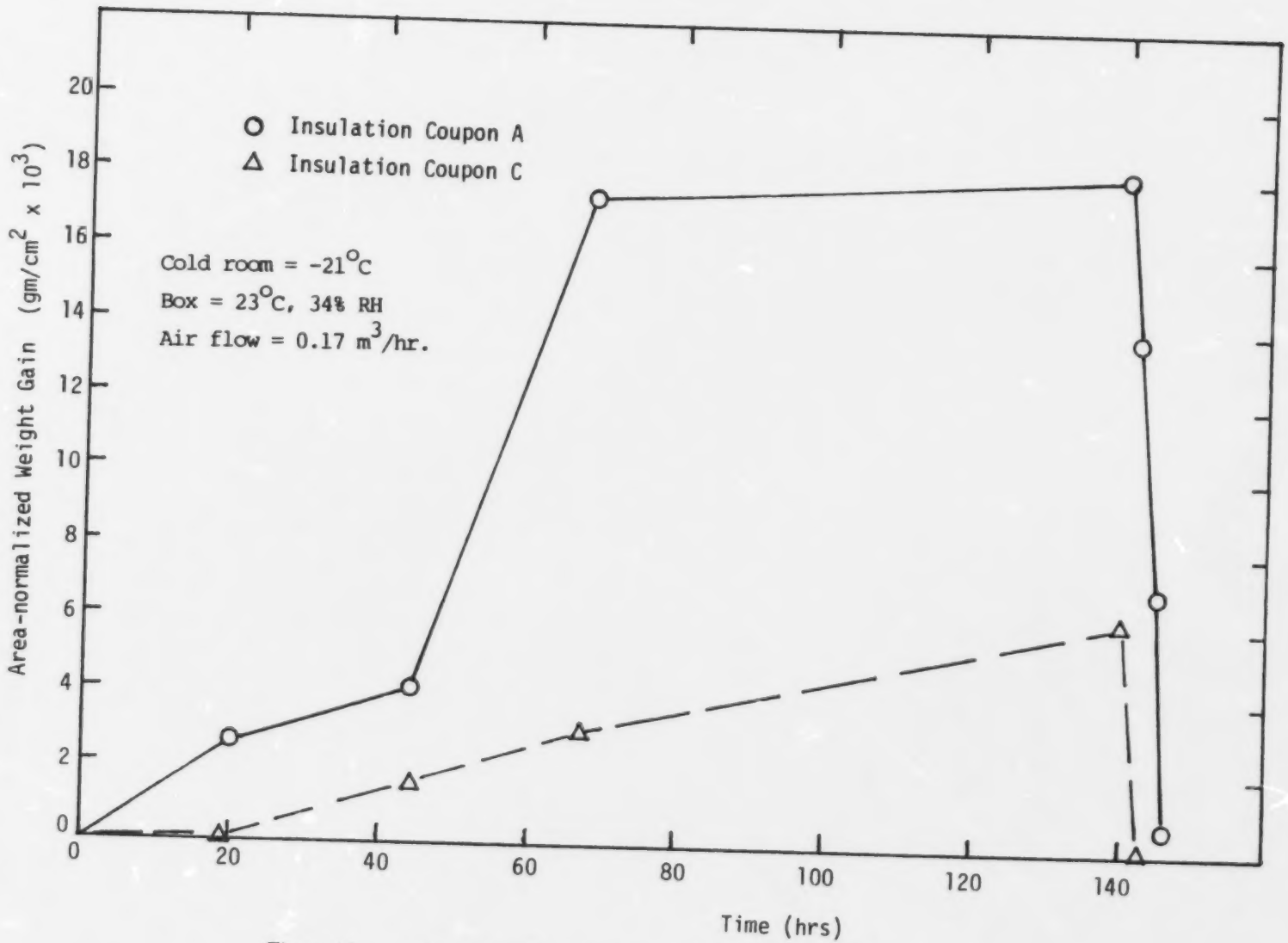

Figure 19. Area-normalized moisture weight gain for insulation coupons versus time with no radiant barrier.

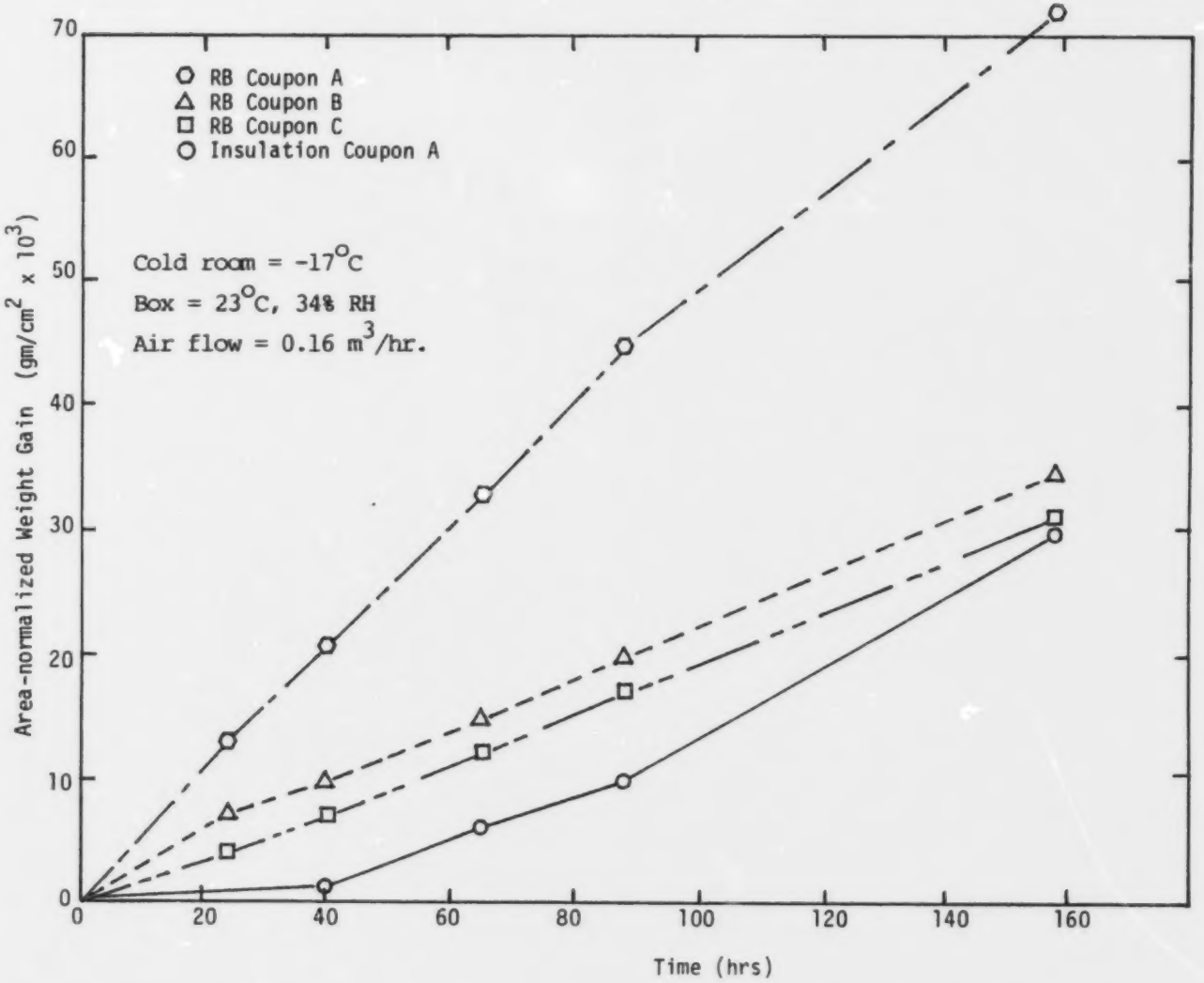

Figure 20 Area normalized moisture weight gains for insulation and radiant barrier (RB) coupons versus time.

with the highest concentrations located above the orifice. Radiant barrier coupons B and C showed identical amounts of frost accumulation which were about one half that of coupon A. Frost concentrations were highest above the orifice and decreased radially outward. The rate at which frost accumulated on the radiant barrier coupons was approximately constant. This reflects the fact that the airflow (and hence moisture flow) through the orifice was constant. Interestingly, if one calculated the moisture flowrate (based on the conditions inside the box) and distributed the moisture uniformly over the total area of the radiant barrier then the moisture deposition rate is 3.6×10^{-4} gm/cm^2-hr. This is reasonably close to the average measured deposition rate of 2.6×10^{-4} gm/cm^2-hr, and suggests that the other mechanism for transporting moisture to the radiant barrier, water vapour diffusion has a much smaller effect than moisture transport by air movement.

A third test was carried out to monitor the amount and distribution of moisture during the drying phase when the cold room temperature was raised above freezing. The results of this test are shown in Fig. 21. During the accumulation phase, the cold room temperature was -24°C and the box conditions were 24°C and 31% RH. For these conditions, the air leakage flowrate was 0.37 m^3/hr which was significantly larger than the flow in the first two tests. A new sample of fiberglass insulation was placed in the apparatus and it is possible that the new sample had a lower flow resistance than the previous sample. During the accumulation phase, the frost concentration on coupon A (above the orifice) was larger than coupon B and C which is similar to the distribution shown in Fig. 20. The only difference between the results of Fig. 20 and 21 is that the frost deposition rate was larger in the latter case and simply reflects the larger air leakage rate through the insulation sample. At 145 hours, the cold room temperature was raised to room temperature (approximately 20°C). The frost on the radiant barrier melted and evaporation of the liquid water occurred through the perforations in the radiant barrier. The results show that the radiant barrier coupons immediately began to lose moisture and were essentially dry within 40 hours. On the other hand, insulation coupon A (above the orifice) increased in weight shortly after melting took place. Clearly, some of the liquid on the radiant barrier drained down into the underlying insulation. In this test, there was no

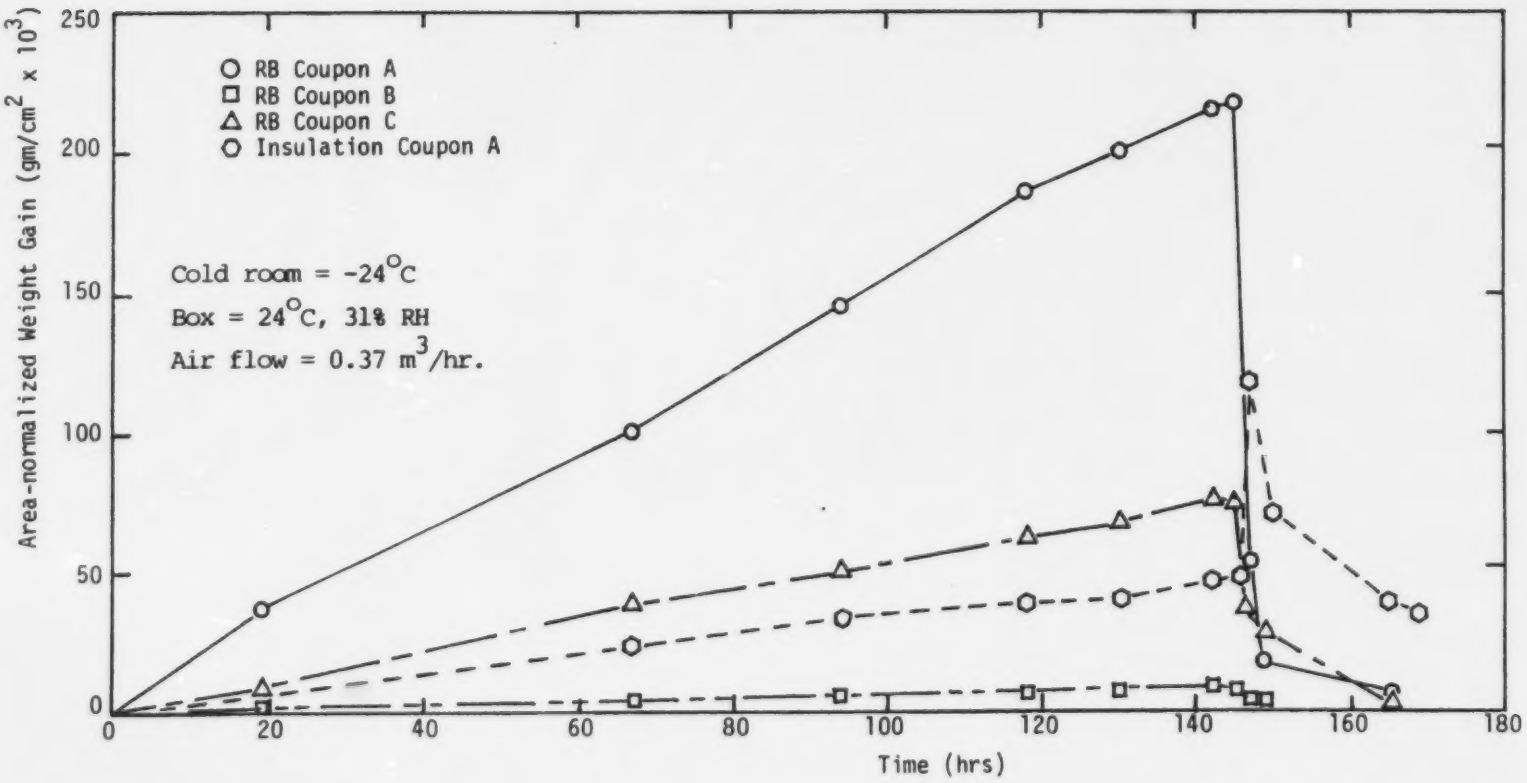

Figure 21 Area normalized moisture weight gains for insulation and radiant barrier (RB) coupons versus time.

evidence of liquid water actually percolating to the drywall, although this situation may occur, if sufficient frost is initially present and the evaporation rate is fairly low. It is estimated that another 40 hours would have been required to dry out the insulation. The last laboratory test was intended to simulate daily variations in attic temperatures and the resultant moisture accumulation on the radiant barrier. A 3 day test was chosen and the cold room temperature variation followed the protocol showed in Fig. 22. The peak temperatures were chosen to be a few degrees above freezing so that the frost would melt and some evaporation would take place. The corresponding air leakage flowrates are also shown in Fig. 22. Since air flowrates are driven solely by the box-cold room temperature difference, the flowrate is highest at the lowest room temperature and is essentially zero at the warmest temperature. Moisture accumulation in the insulation and the radiant barrier coupons is shown in Fig. 23. First, the results follow the general trends in the previous tests, with more moisture accumulation on radiant barrier coupon A (above the orifice) than coupons B and C. Furthermore, only insulation coupon A showed any moisture accumulation and the magnitudes are comparable to those in the control test described above. The results clearly show that moisture accumulation followed daily variations in temperature. For radiant barrier coupon A, frost accumulated during the cold temperature phase of the cycle and when the frost melted, some of the moisture did evaporate. However, the amount of moisture that evaporated was only about one third of the moisture that had been deposited during that particular cycle. (This was true at least for the first two cycles). Each succeeding frost accumulation was added to the moisture that had not evaporated in the previous cycle, resulting in a "ratchet" effect, that is, total moisture accumulation increased with time. Radiant barrier coupons B and C also showed a similar response in moisture accumulation; however, very little evaporation occurred during the warm phase and by the end of the test period, the moisture on these two coupons was close to that on coupon A. This is different from the long term tests in which the moisture accumulation on coupons B and C was about one half that on coupon A. Visual observations of the moisture on the coupons showed clear evidence of melting during the warm phase followed by re-freezing of the liquid water and subsequent frost accumulation.

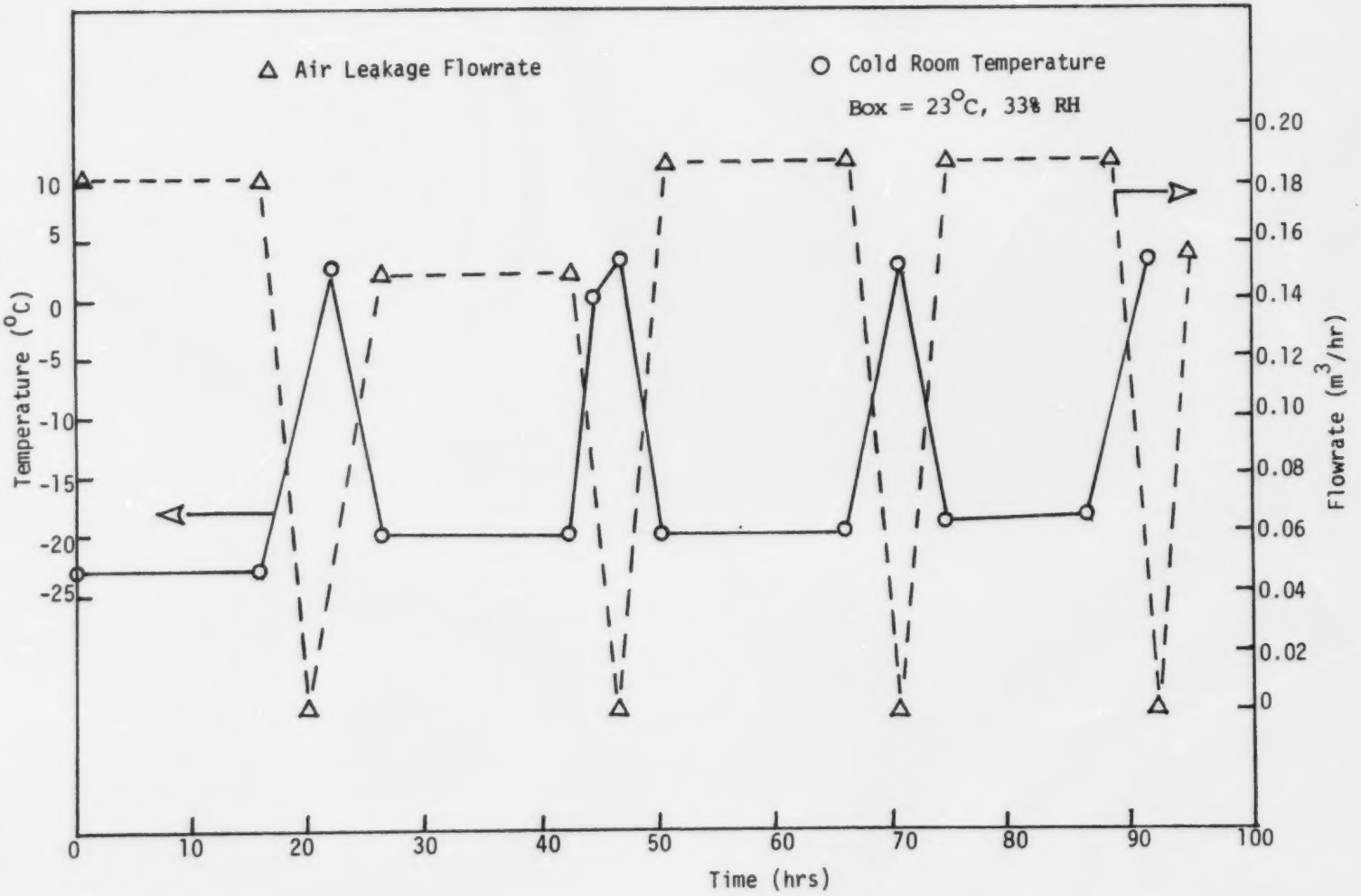

Figure 22 Temperature-time protocol and corresponding air leakage flowrates for laboratory tests of moisture accumulation on radiant barriers.

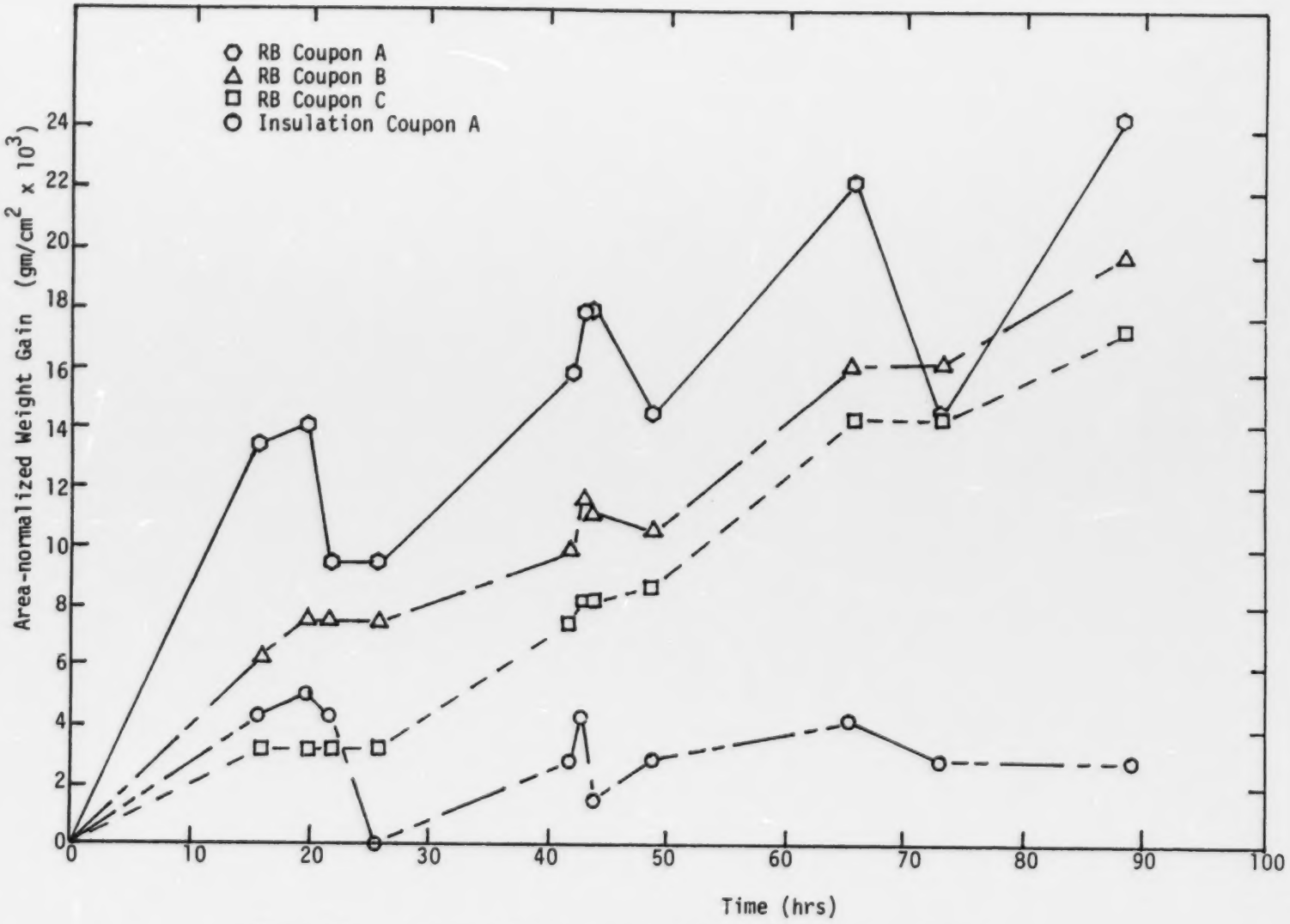

Figure 23 Area normalized moisture weight gains for insulation and radiant barrier (RB) coupons versus time for laboratory tests.

3.2 Field Tests

3.2.1 Test facility and procedure

Field tests on moisture accumulation were carried out in house 5 at AHHRF. One section of the attic radiant barrier covered a ceiling test panel that had a 0.95 cm (3/8") diameter orifice plate flowmeter located mid-way between adjacent ceiling joists, spaced at 60 cm (2 ft) intervals. The interior side (warm side) of the test panel was plexiglass to allow visual observation of any water that may have drained down from the radiant barrier. Ceiling insulation was 90 mm (3.5") thick fiberglass batt insulation, the same as was used for laboratory work. A low range pressure transducer was attached to the orifice plate and air leakage flowrates were monitored by the same data acquisition system used for thermal performance testing. The data acquisition system stored the flowrates as 10 minute averages. Unlike the laboratory tests, in which air flowrates were unidirectional, the air flow could be directed into the attic space or into the interior of the house. Thus, the data acquisition system stored not only the average flowrates in and out of the attic, but also the number of occurrences of in and out flow. Moisture accumulation on the radiant barrier was recorded manually by periodically weighing a radiant barrier and insulation coupon directly above the orifice. The radiant barrier and insulation coupons measured 19.5 cm x 22.4 cm and 15.5 cm x 14 cm, respectively.

Field tests on moisture accumulation lasted a total of 20 days and commenced January 29, 1990, at the start of a cold period. It was anticipated that the worst case would occur during the cold periods when air leakage flowrates would be the highest and be directed predominantly into the attic space by the stack effect. Prior to testing, the interior of house 5 had not been humidified, and the corresponding relative humidities were in the range of 20 to 25%. Air leakage flowrates were also measured prior to the start of moisture testing to collect data for use in subsequent air infiltration work. At the start of the test, interior relative humidity was raised to a constant value of 35% by a drum type humidifier. During testing, relative humidity fluctuated between 32% and 39%. Indoor temperature averaged about 20°C during the test. For these indoor conditions, the moisture content in the air ranged from 6.0 to 7.4 gm /m^3 (moist air).

3.2.2 Results of field tests

Attic temperatures are shown in Fig. 24. Data begin on January 28 and show that there was a noticeable drop in nighttime temperatures between January 28 and 29. The attic temperature followed a daily cycle; however, during the first four days of testing, peak attic temperatures were well below freezing. This was followed by an eleven day period when attic temperatures cycled above and below freezing during the day. Finally, at the end of the test period, there was another four day period when attic temperatures remained below freezing.

Corresponding air leakage flowrates are also plotted in Fig. 24. At each point in time, the 10 minute averaged flowrates into and out of the attic are plotted (negative flowrates are into the attic while positive flowrates are out of the attic). During the night when temperatures were lowest and wind was relatively light, air leakage was driven mainly by the stack effect. For these periods, for example, AB in Fig. 24, the flow was into the attic for 100% of the time. At other times, for example, CD in Fig. 24, when wind was present, the air flow fluctuated in direction. The relationship between air leakage flowrates and wind speed, wind direction, and other variables is the subject of on-going studies at AHHRF.

Daily-averaged moisture flow into the attic is shown in Fig. 25. Moisture flows are obtained by calculating total volumetric air flow into the attic on a daily basis and multiplying by water content of moist air, expressed as gms/m^3. For a portion of the test period (Feb. 8 to Feb. 12) the data acquisition system was not collecting data; however, this was not a serious problem as the attic temperatures were well above freezing during the day and very little moisture accumulated on the radiant barrier.

Specific moisture accumulation (gm/cm^2) on the radiant barrier is shown in Fig. 25 over the entire test period. During the initial cold phase, moisture accumulation increased with time and all moisture was deposited as frost. Figure 26 shows a sequence of photographs of the radiant barrier coupon and the entire radiant barrier on January 30, 8:45 a.m., January 31, 5:00 p.m., and February 3, 9:05 a.m. At each point in time, the photographs show that the highest

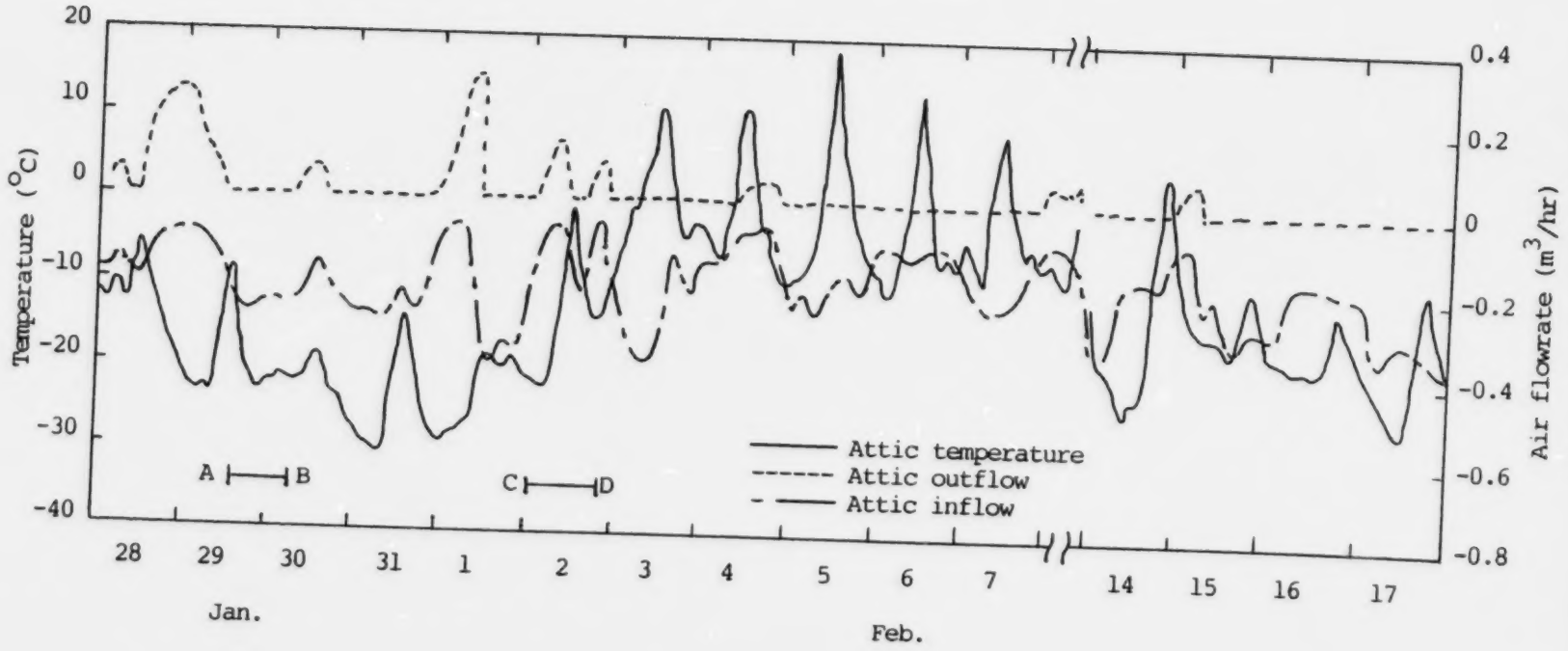

Figure 24 Attic temperature and air leakage flowrates for field tests over the period January 28, 1990 to February 16, 1990.

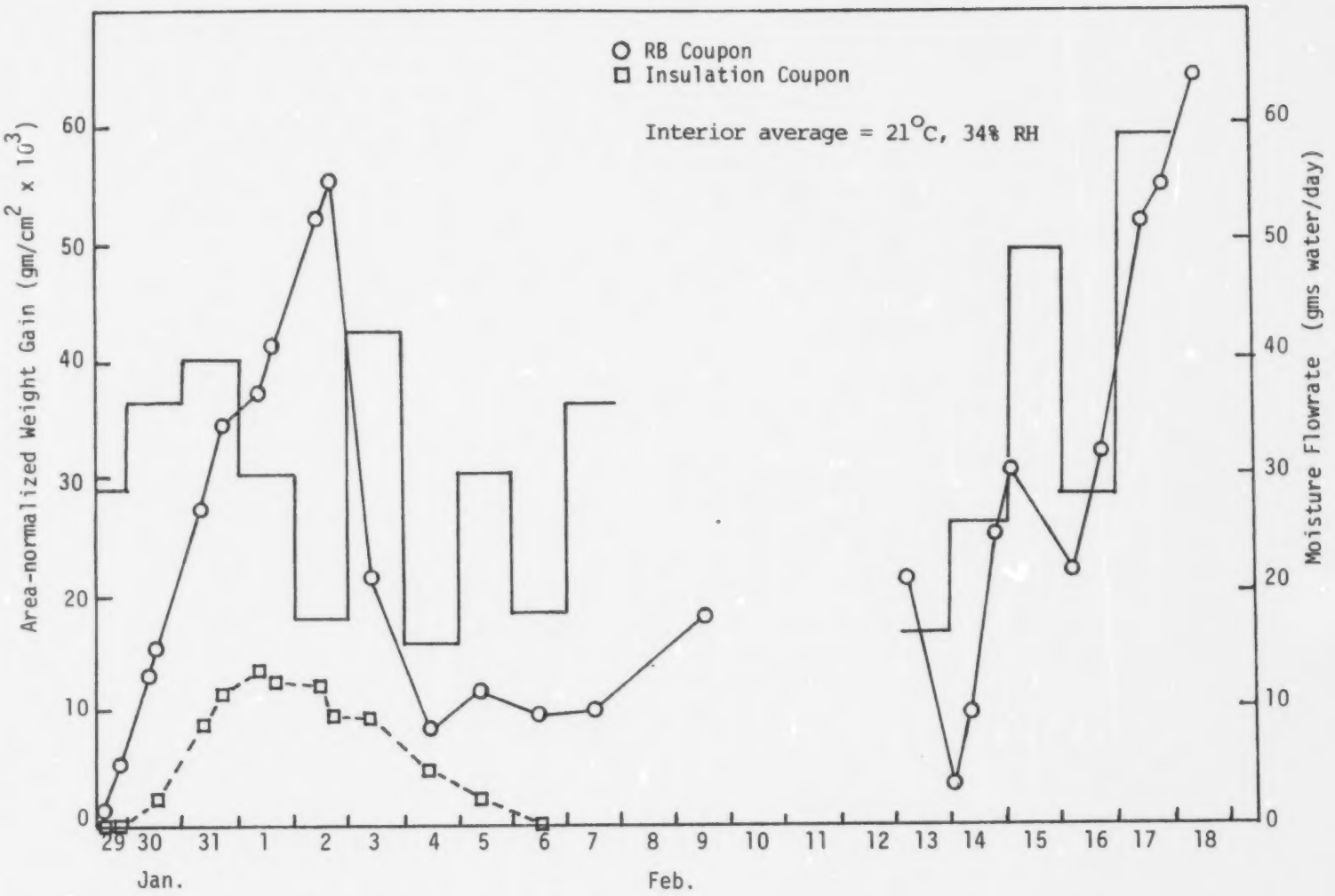

Figure 25 Area normalized moisture weight gains for insulation and radiant barrier (RB) coupons versus time over the field test period.

concentration of frost occurred directly above the orifice on the radiant barrier coupon and tapered off away from the orifice site. All frost accumulation during the test period was confined to one joist space. One interesting feature is that the perforations in the radiant barrier remained visible during the frost deposition which indicates that the air flowed out through the perforations after the moisture had been deposited. On February 3, the attic temperature rose above zero and the photographs in Fig. 26c show that all the frost had melted. Fig. 25 shows that there was a significant decrease in moisture on the underside of the radiant barrier starting February 3. Two separate mechanisms caused this reduction in moisture. First, some evaporation was taking place since the attic temperatures were above freezing and the resulting vapour pressure under the radiant barrier was larger than in the attic space. Second, some water had drained through the insulation to the plexiglass plate. Evidence of drainage was first noticed on February 4 and Fig. 27 is a close-up photograph of the "wet spot" as observed from the inside of the house through the plexiglass plate. The wet spot on the plexiglass eventually dried by February 6. It is difficult to assess whether the water that drained down would have caused any problems such as drywall staining. Had the cold period lasted longer, more frost would have accumulated and the resultant water drainage would have been greater. Thus, a potential problem exists with moisture accumulation on radiant barriers in cold climates.

During this initial frost deposition/melting cycle, the moisture accumulation in the insulation coupon directly below the radiant barrier coupon was measured. The results are shown by the dashed line in Fig. 25. For the initial cold period, the moisture accumulation increased steadily with time but at a rate that was considerably less than the radiant barrier coupon. This is essentially the same result that was observed in the laboratory tests. There was more scatter in these measurements compared to the radiant barrier because small tufts of fiberglass adhered to the frost layer on the radiant barrier as can be seen in Fig. 26 and this caused some variation in the dry weight of the insulation coupon. When the frost melted on February 3, there was no sudden rise in weight of the insulation coupon, as was observed in the laboratory tests of Fig. 21. In the laboratory test, however, no water drainage occurred and one would therefore, expect more water

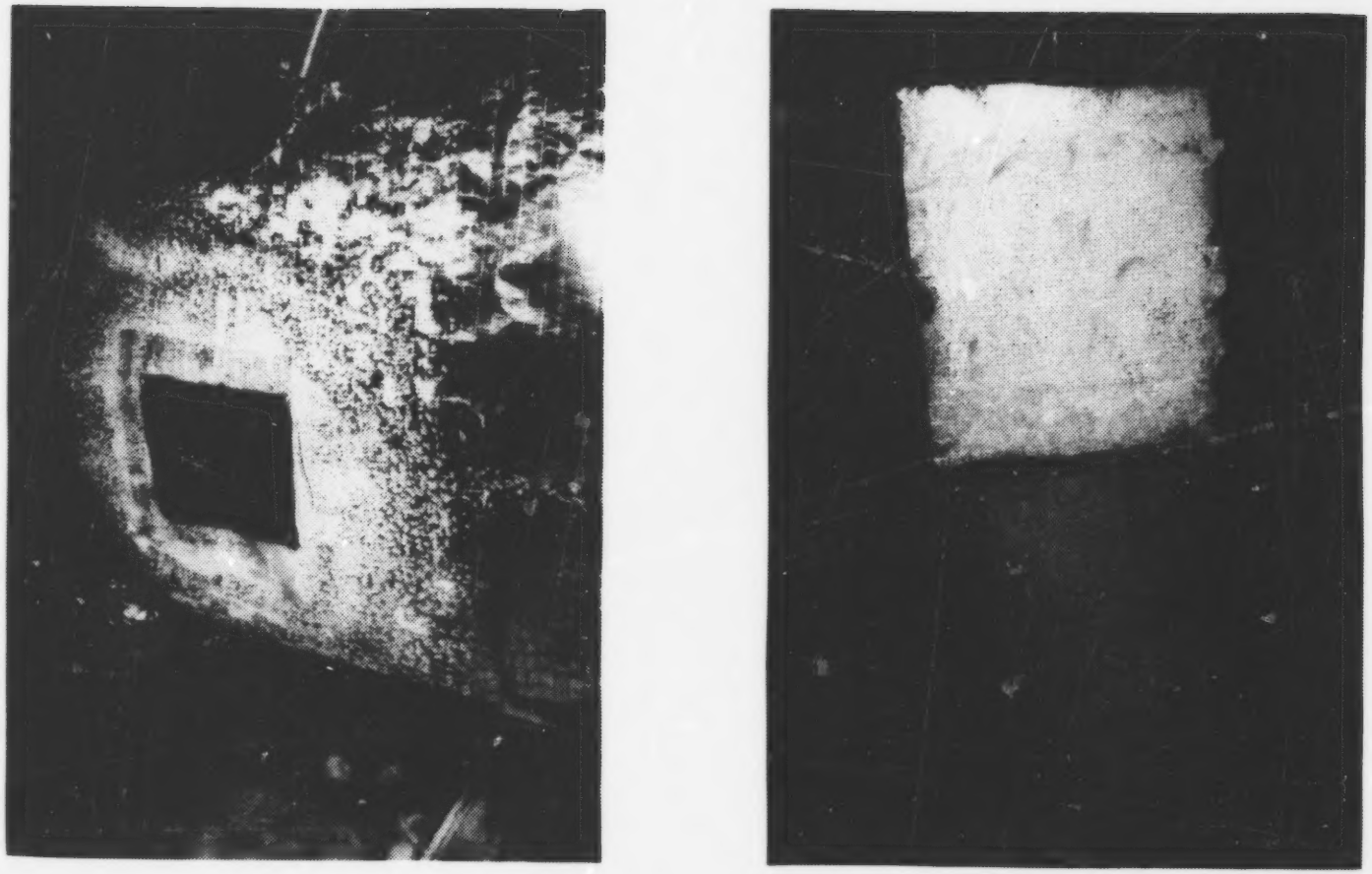

Figure 26A Photos of frost accumulation on RB coupon and entire sheet at 8:45 a.m. January 30, 1990 for field tests.

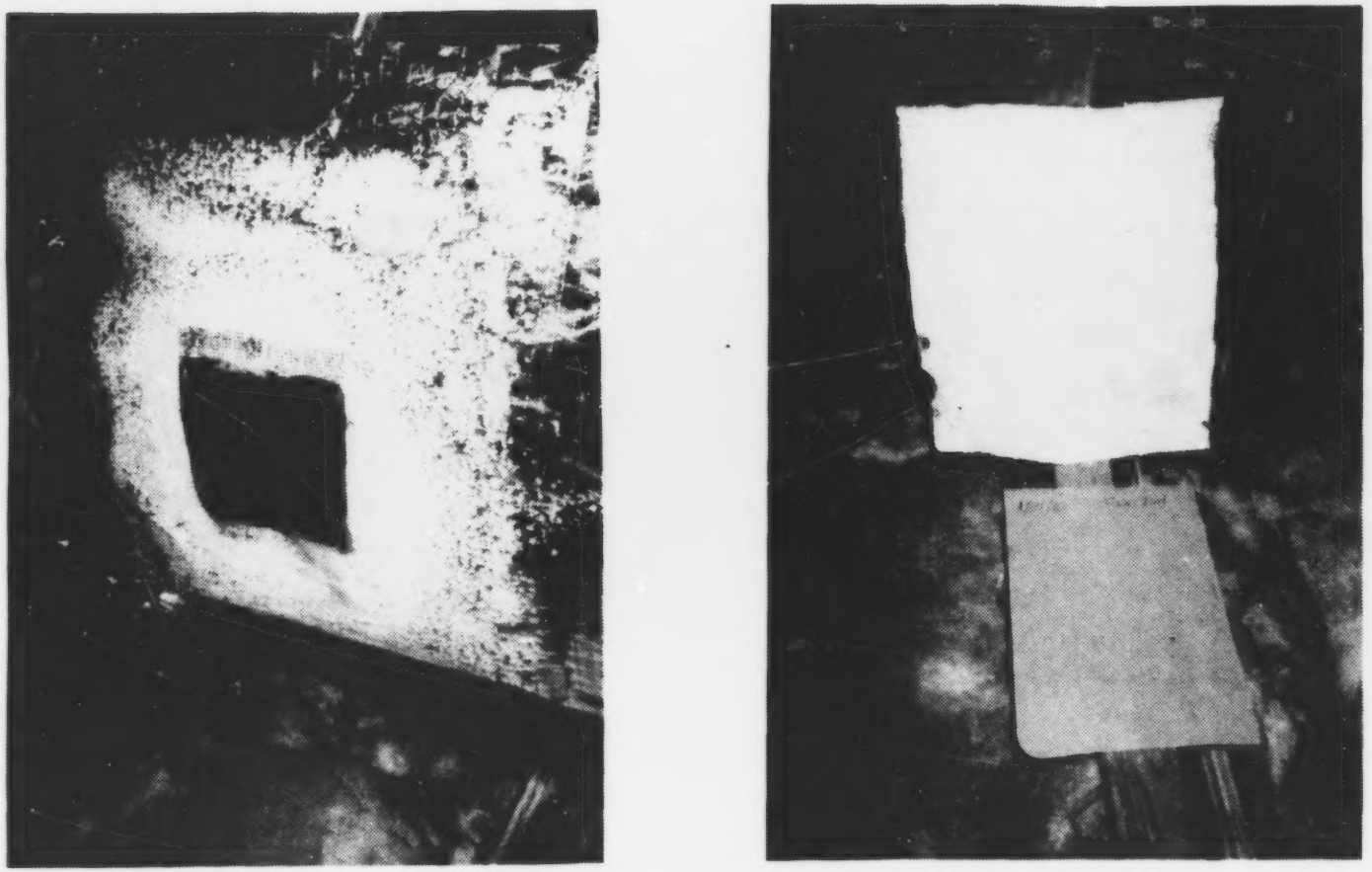

Figure 26B Photos of frost accumulation on RB coupon and entire sheet at 5:00 p.m. January 31, 1990 for field tests.

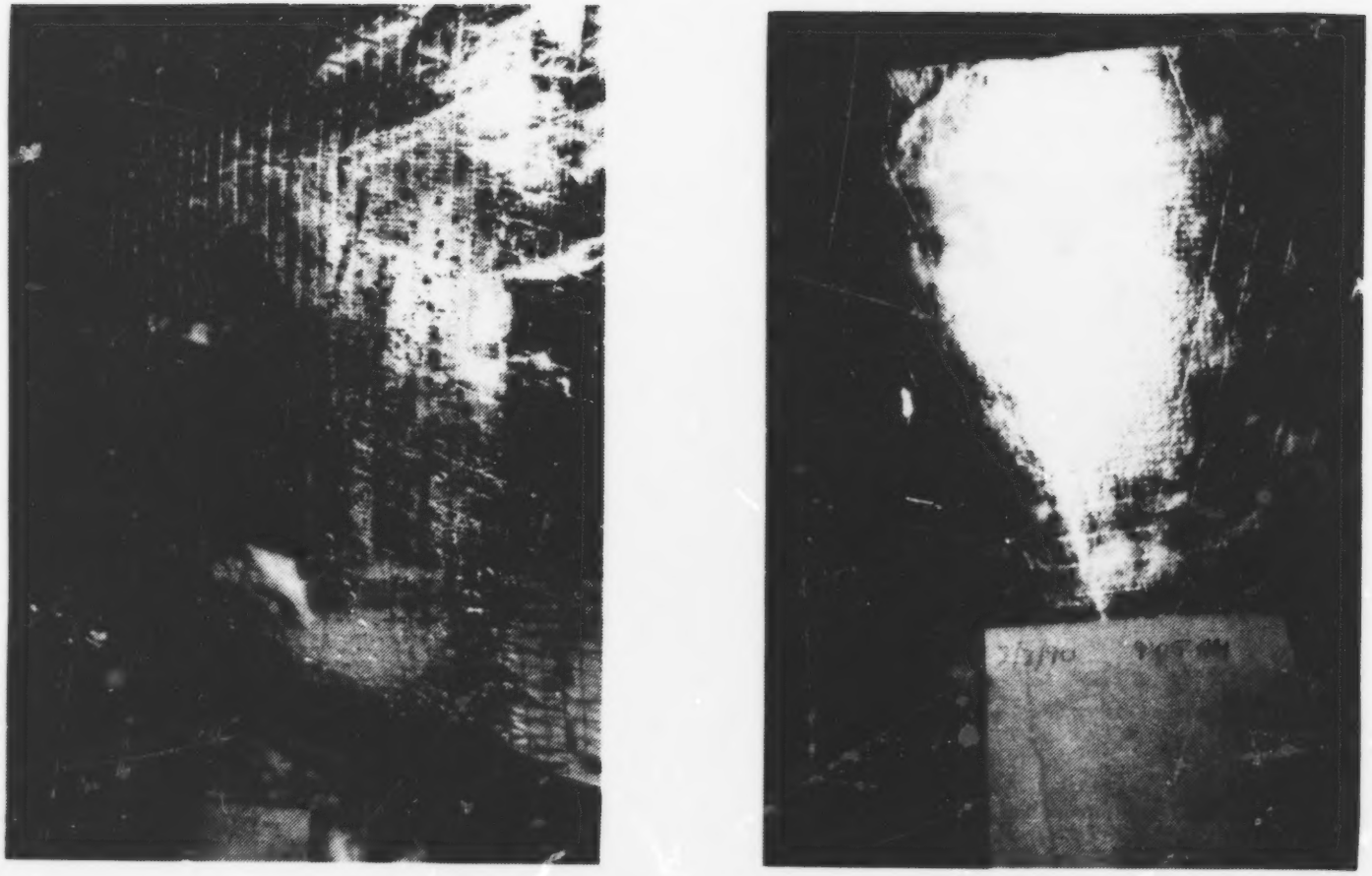

Figure 26C Photos of frost accumulation on RB coupon and entire sheet at 9:05 a.m. February 3, 1990 for field tests.

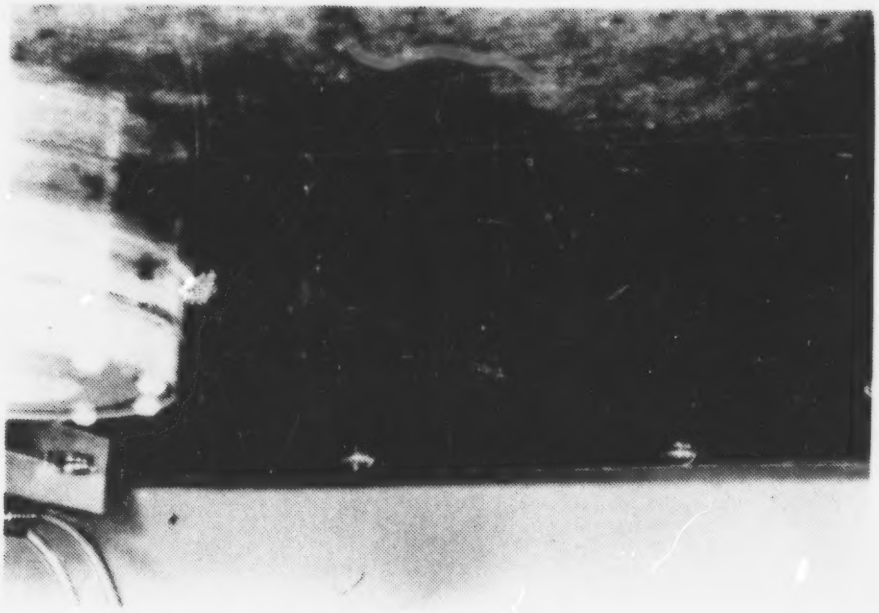

Figure 27 Wet spot on the inside of the ceiling test panel caused by water drainage from the radiant barrier (February 4, 1990 at 10:18 am.)

to be stored in the fiberglass insulation. The field tests did not indicate a threshold moisture accumulation level at which drainage would occur. On February 14, Fig. 25 shows there was a second cold phase which lasted approximately four days. A new layer of frost was deposited on the radiant barrier coupon which had essentially dried by February 13. The constant frost accumulation rate was interrupted by one day when attic temperatures went above freezing causing a small decrease in weight. It was not possible to make a visual observation of liquid water drainage after this second frosting cycle, so the data in Fig. 25 stops at February 18.

There is one final noteworthy observation from the field tests. House 5 has two fluorescent light fixtures mounted on the ceiling. One fixture is in the middle of the radiant barrier half of the attic and the other in the middle of the uncovered half. Electrical wiring is connected to each fixture through a hole in the ceiling. Thus, air can escape through these holes from the indoors to the attic space. A frost outgrowth was noticed over the radiant barrier light fixture on January 31. This frost outgrowth is shown in Fig. 28. Also note the frost growing on the upper side of the radiant barrier around the perforations. Fig. 28 shows a substantial amount of frost growth on the underside of the radiant barrier, directly above the ceiling opening for the light fixture. There was some frost on the insulation, but most of it was concentrated on the radiant barrier. The frost accumulation seemed to be denser and more concentrated than on the ceiling test panel site; however, there was no attempt to measure the frost accumulation. The light fixture undoubtedly has a leakage area that is larger than the test panel leakage site and this would allow more air (and hence, moisture) to be convected from indoors to the attic. The important point is that the same trends regarding frost accumulation were observed for this case as for the laboratory and field tests.

3.3 Discussion of Results

Laboratory tests of moisture accumulation on radiant barriers were carried out in a cold room where temperatures were maintained below freezing. These conditions would be expected to be the worst case for two reasons. First, at sub-freezing temperatures, any

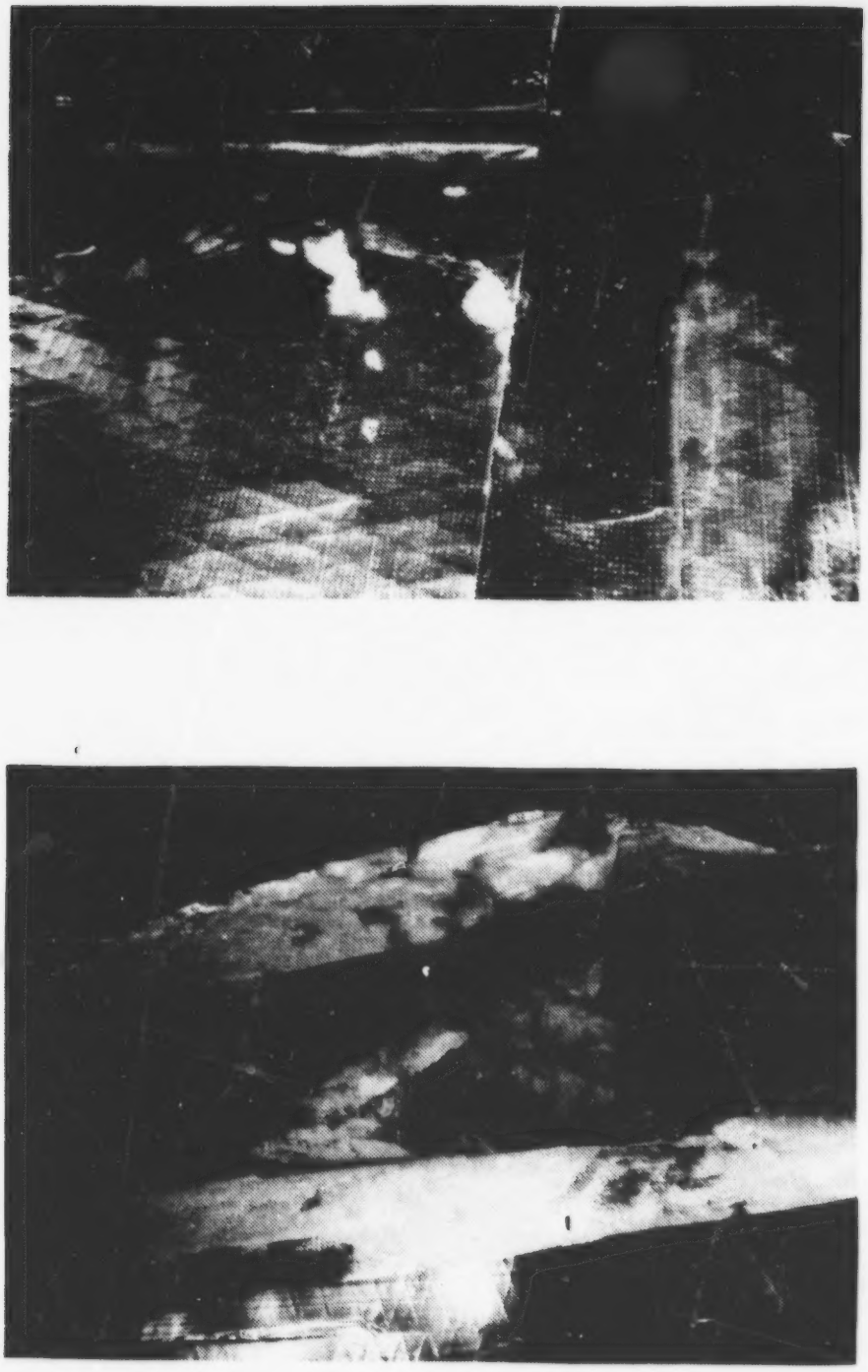

Figure 28 Frost accumulation on the upper and lower surfaces of the radiant barrier directly above a light fixture. (February 1, 1990 at 8:45 a.m.)

moisture on the radiant barrier would be in the form of frost which is basically immobile. Frost does not drain away from the radiant barrier as does water. Furthermore, the rate of evaporation of frost is much less than that of water since the vapour pressure of ice is less than that of water. Thus, moisture in the form of frost is trapped in place and subsequent moisture deposition simply adds to the mass of the frost layer. Second, at sub-freezing conditions there is a large temperature difference across the ceiling of a typical house. Due to the stack effect, there will be a relatively large pressure difference on the order of 1 or 2 Pa across the ceiling which will tend to drive warm moist air from indoors into the attic space. Thus, the leakage air flow will be relatively constant and over a long period will transport a great deal of moisture to the radiant barrier. From the laboratory results shown in Fig. 20, frost accumulation increased with time at a constant rate, that rate being dictated by the leakage air flow. The frost concentration was largest directly above the leakage site and decreased to about 1/2 the concentration at 30 cm (12") from the leakage site. Air leakage would tend to follow the path of least resistance which would mean that air would first come in contact with the radiant barrier directly above the leakage site and then migrate along the barrier as it escaped through the tiny perforations in the radiant barrier. Figs. 19 and 20, show that the amount of frost accumulation in the fiberglass insulation was approximately the same whether a radiant barrier was present or not. The large amounts of frost accumulation occurred at the interface between the radiant barrier and the insulation. Thus, a radiant barrier (or any other barrier that lies over the insulation) can be expected to increase frost accumulation by trapping moisture at the interface. Over a long period of time, this may present a situation where melting could release a great deal of water in a short period of time. Evidence of this scenario was shown in Fig. 21 where frost accumulated over a 150 hour period. When the cold room temperature was raised to room temperature, the frost melted, resulting in a sudden drop in weight of the radiant barrier coupons. However, the insulation directly above the leakage site increased in weight. Some of the frost that melted percolated into the insulation, although there was no evidence of water draining down to the drywall. Nonetheless, this situation may occur if enough frost has accumulated on the radiant barrier. When melting occurs, some of the water evaporates through the small perforations in the radiant barrier, but it was difficult to determine the evaporation rate from the weight change measurements.

The last set of laboratory tests simulated a typical winter cycle of temperature in the attic i.e. short, 1 to 2 hour periods during the day when attic temperatures are above freezing, followed by prolonged sub-freezing temperatures. The results of this test are shown in Fig. 23. Frost accumulated at the interface between the radiant barrier and the insulation; the rate of frost accumulation during the sub-freezing portion of the cycle averaged 6.8 x 10^{-4} gm/cm^2-hr. During the warm portion of the cycle, there was a noticeable decrease in weight of the moisture accumulation but not enough to completely remove all of the moisture. Subsequent sub-freezing conditions led to a further increase in frost accumulation. The average moisture accumulation over the entire duration of the test was 2.8 x 10^{-4} gm/cm^2-hr. The important point regarding this rate is that it is a positive value which implies that moisture gradually builds up on the radiant barrier during winter conditions even though there may be periods when attic temperatures are above freezing.

Field testing for moisture accumulation in radiant barrier installations parallelled laboratory tests. Air flow through a specific ceiling leakage site was monitored over a 2 to 3 week period. Unlike the laboratory tests in which air leakage flowrates were constant over the test period, the field measured air flowrates, shown in Fig. 24, sometimes fluctuated in direction, due to the turbulent motion of the wind creating a fluctuating pressure difference across the ceiling. Generally, wind increased in strength during the daytime, while the night air was relatively calm. It was during the night that sustained air flowrates into the attic occurred, carrying moisture to the radiant barrier. The rate of frost accumulation on the radiant barrier was relatively insensitive to the fluctuating air flowrate as long as the attic temperature was sub-freezing. This situation occurred over the first 4 to 5 days of the field test (Jan. 29 to Feb. 2).

The initial cold period was followed by a warmer period (Feb. 3 to Feb. 13) in which attic temperatures varied above and below freezing. The effect on moisture accumulation was much the same as was indicated by laboratory tests (Fig. 23). The amount of frost on the barrier decreased significantly but was never completely removed. When a subsequent cold period returned (Feb. 14 to Feb. 17), the frost accumulation increased at approximately 5.6 x 10^{-4} gm/cm^2-hr. Thus, field observations tended to confirm the idea of a "ratchet" effect in which moisture accumulated during a cold period, decreased

somewhat during a warm (above freezing) period, and increased again when a cold period returned. If such cold-warm cycles continued throughout the winter, there would be a possibility of water damage occurring to the ceiling. Such was the case in the field test in which water drained from the radiant barrier to the drywall layer after the initial sub-freezing period.

4.0 ROOF OVERHEATING

Field testing on the overheating of roof components due to attic radiant barriers is detailed in this section of the report. For a radiant barrier installed under the top chord of the roof trusses (required retrofit practice in Alberta), some concerns were raised about possible overheating of roofing materials, particularly roof shingles, during summer months.

4.1 Field Tests

4.1.1 Test facility and procedure

Overheating tests were conducted in house 5 at the AHHRF from June 28, 1989 to September 6. It was anticipated that data would be obtained over the summer solstice (when the sun is at its highest point above the horizon). However, during this period there was a large amount of cloud cover associated with frequent rain and it wasn't until this rainy period ended that the tests were started.

To provide a basis for comparison, the gable attic was divided in half, with one half having no radiant barrier. This served as the reference configuration. In the other half, the radiant barrier was stapled across three truss spaces underneath the top chord of the truss. The three truss spaces were located at the mid-point of this half of the attic and the radiant barrier covered both the north and south-facing slopes of the roof. Type T thermocouples for temperature measurement were placed under the asphalt roof shingles (see Fig. 29) and on the underside of the roof sheathing, along the center of the middle truss space at points 1/3 and 2/3 of the way up the roof slope. For the undercovered half of the attic, a similar set of thermocouples was located at the central truss space. In addition, temperatures in the air space between the radiant barrier and the roof sheathing, the radiant barrier, and the attic air were recorded.

The roof of house 5 is covered with medium dark brown asphalt shingles. Although the solar absorptivity of these shingles was not directly measured, it is estimated that the value lies in the range of 0.85 to 0.90 (compared to black shingles with absorptivities in the range 0.90 to 0.95). Thus, peak temperatures for these shingles will be slightly less than black shingles (worst case).

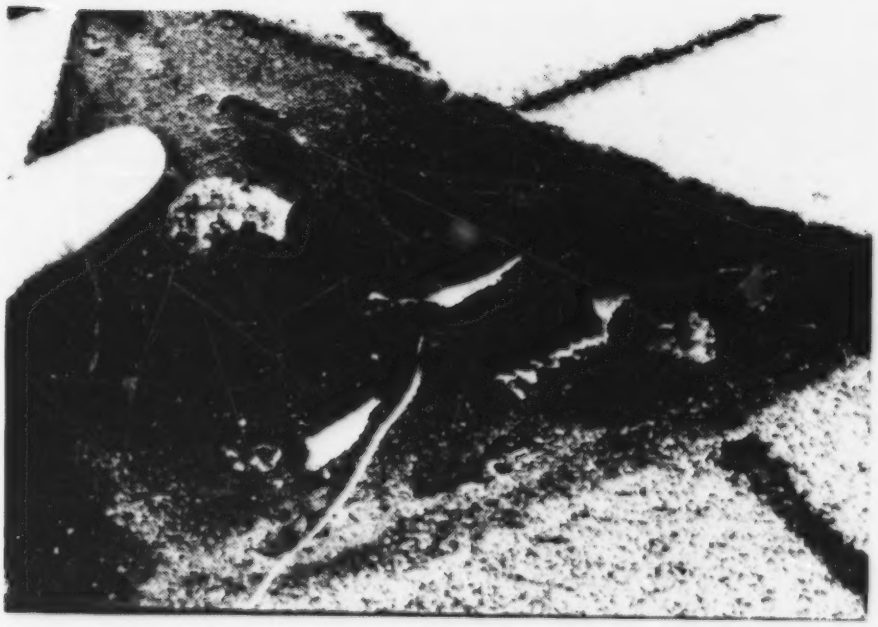

Figure 29 Type T thermocouples installed underneath roof shingles.

The installation of the radiant barrier underneath the top chord of the trusses was carried out by two technicians. Fig. 30 shows details of the installed radiant barrier. The installation was relatively straightforward but required a little more time than installing the radiant barrier directly on top of the ceiling insulation.

4.1.2 Results of field tests

Since the objective of this phase of field testing was to measure the overheating that may have occurred, each daily temperature record was scanned to determine the peak temperature that was measured for both the shingles and sheathing. Figs. 31 and 32 show the daily peak temperatures for the south and north shingles, respectively. The daily peak temperatures in most cases occurred around noon and generally lasted about two hours. In each figure, the temperatures for the radiant barrier side are compared with the corresponding temperatures on the uncovered side of the attic. Several observations can be made. First, the shingle temperatures on the south face of the roof were higher than the north face. The only exceptions were on cloudy days where both faces of the roof received equal diffuse radiation; in this case, the shingle temperatures were much lower. For example, on July 6, the shingle temperatures at all four locations had the same value of 18°C. Second, for the most part, the shingle temperatures on the radiant barrier side were larger than the uncovered side. However, the difference reached a maximum of only 4C° at the maximum recorded average shingle temperature of 75°C. This can be seen more clearly in Fig. 33, which shows the temperature difference between the radiant barrier side and the uncovered side as a function of the average peak temperature. A general trend can be seen, in which the difference increased as the peak temperature increased. This trend is to be expected since the radiant exchange between two surfaces varies with absolute temperature raised to the fourth power. With the radiant barrier underneath the trusses, the temperature of the roof sheathing and shingles will be greater than if no radiant barrier were present since a larger fraction of the radiant energy leaving the roof sheathing will be reflected back by the radiant barrier.

Figs. 34 and 35 show the daily peak temperatures for the south and north roof sheathing, respectively. In each figure, the radiant barrier and uncovered sides of

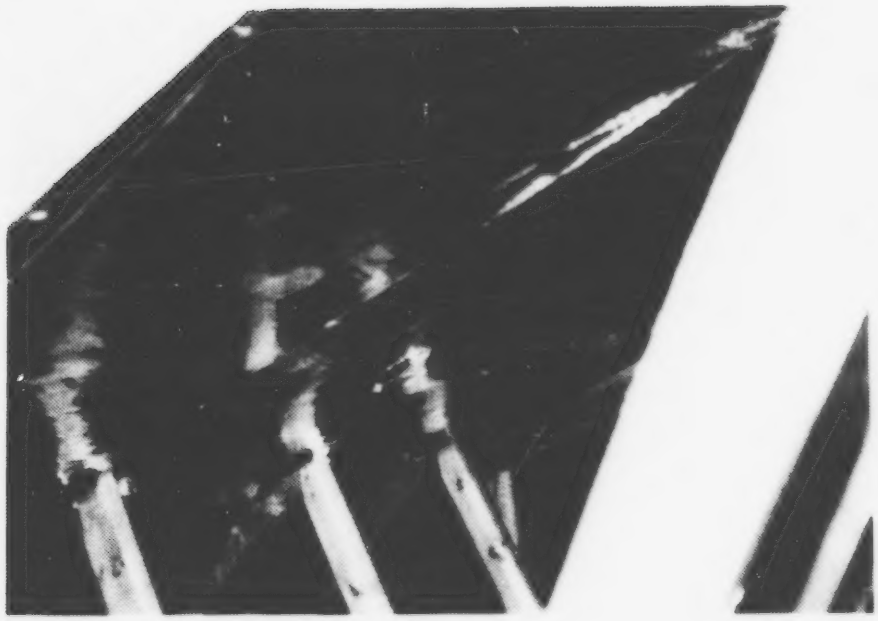

Figure 30A Radiant barrier stapled to the underside of the top chord of the roof trusses in house 5.

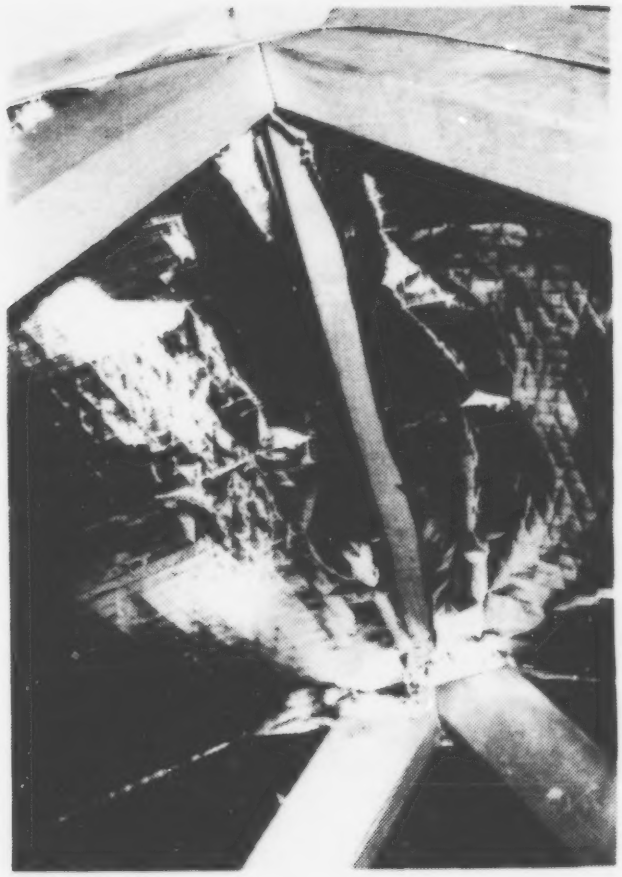

Figure 30B Open end of radiant barrier at the roof peak.

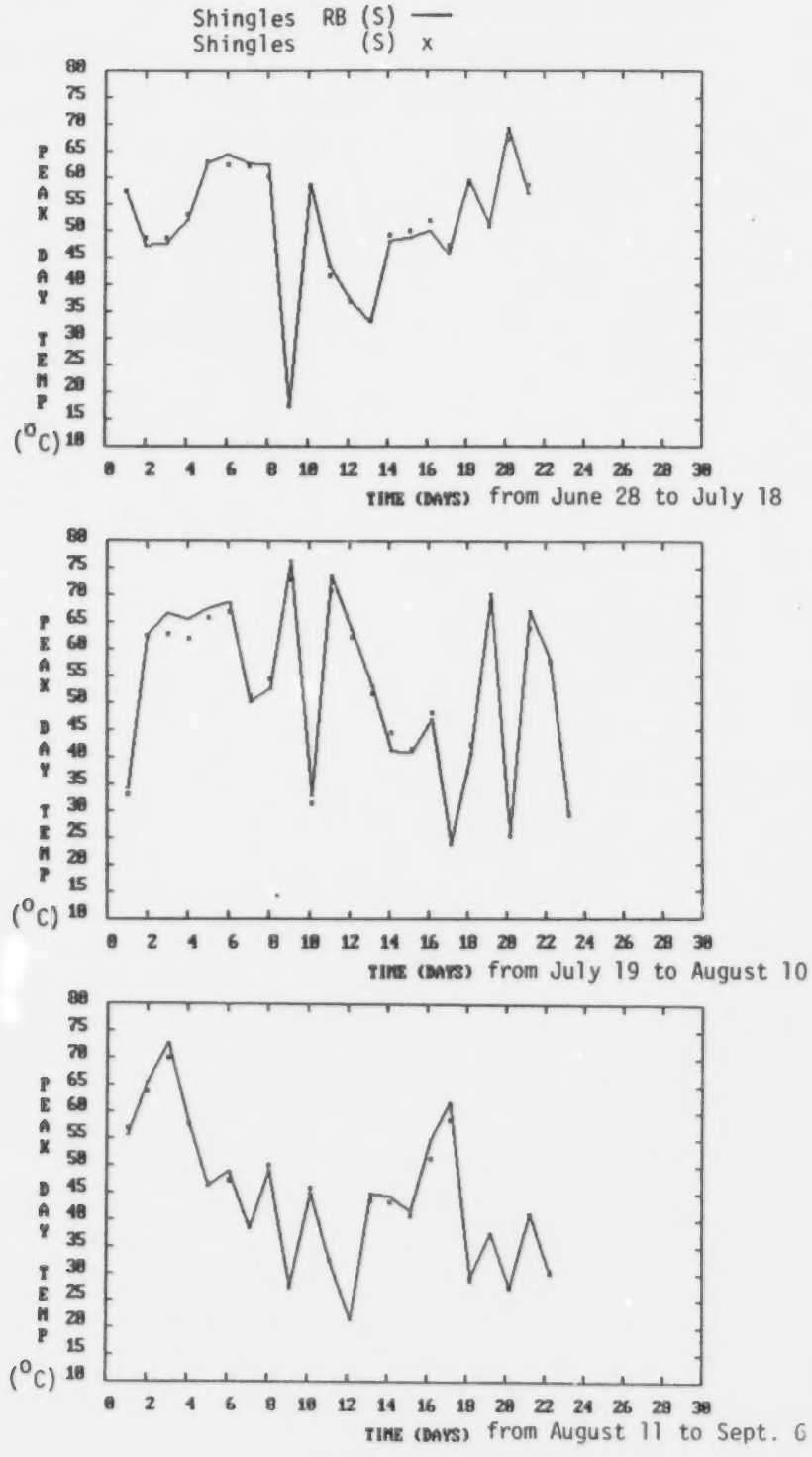
Shingles RB (S)
Shingles (S) x
PEAK DAY TEMP (°C)
TIME (DAYS) from June 28 to July 18
TIME (DAYS) from July 19 to August 10
TIME (DAYS) from August 11 to Sept. 6

Figure 31 Average daily peak temperature of shingles on the south face of the roof versus time.

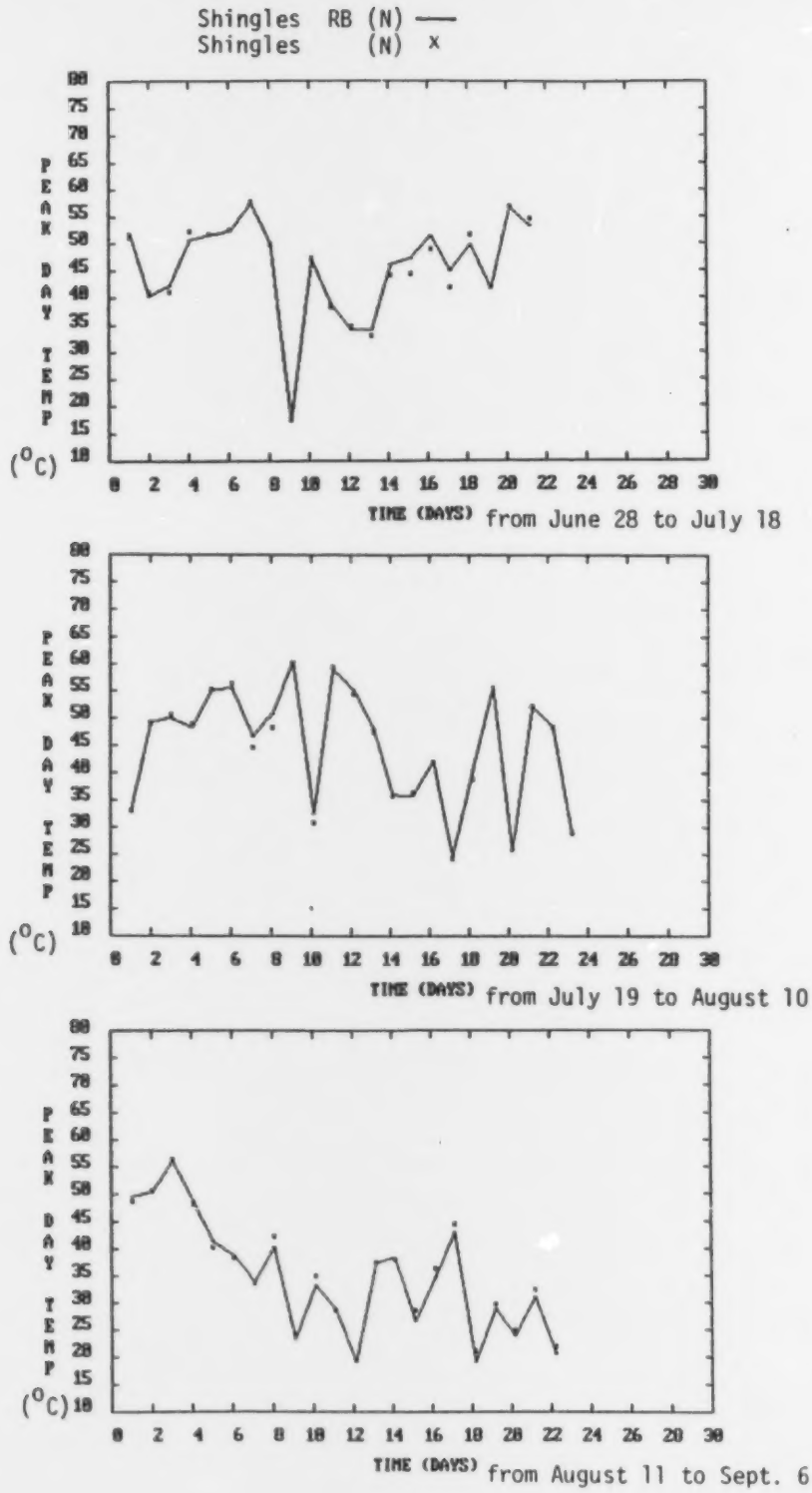
Shingles RB (N)
Shingles (N) x
PEAK DAY TEMP (°C)
TIME (DAYS) from June 28 to July 18
TIME (DAYS) from July 19 to August 10
TIME (DAYS) from August 11 to Sept. 6

Figure 32 Average daily peak temperature of shingles on the north face of the roof versus time.

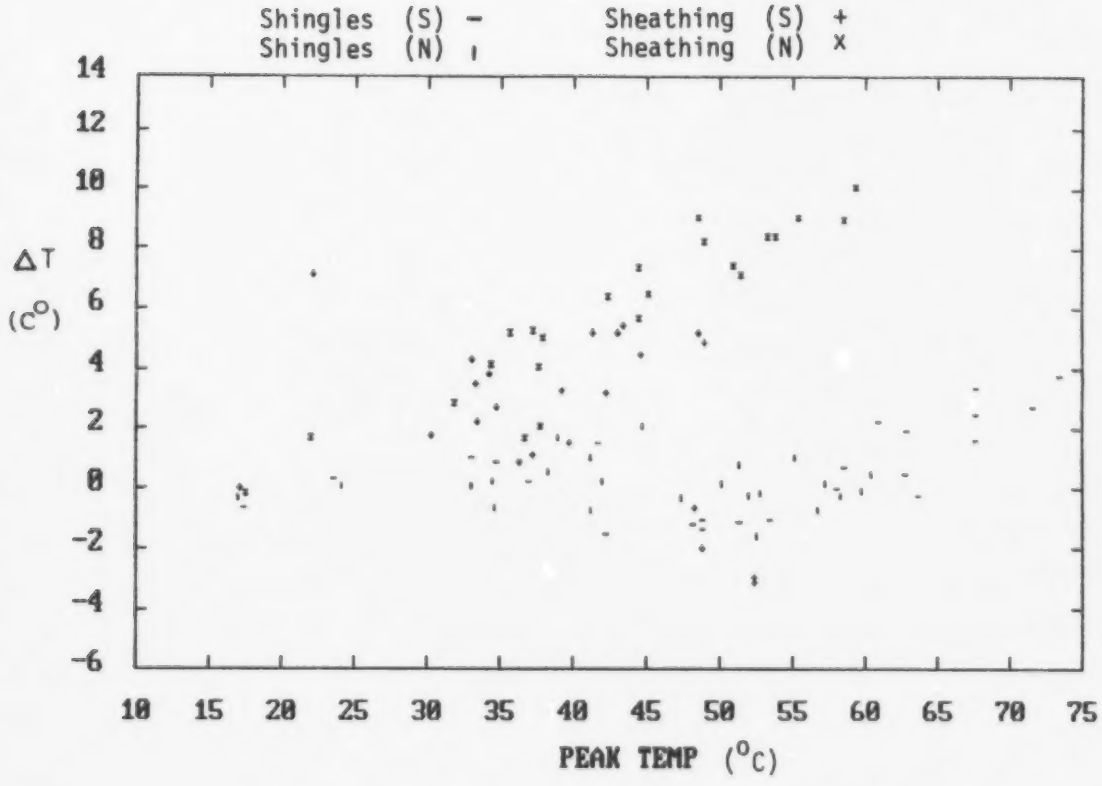

Figure 33 Difference between the average daily peak radiant barrier and uncovered temperatures versus average peak temperature for shingles and sheathing on the north and south faces of the roof.

the attic are compared. The same general trends are observed as with the shingle temperatures; the sheathing temperatures on the south face were generally higher than on the north face except on cloudy days. For the south face, the sheathing with the radiant barrier had a consistently higher temperature than the uncovered side; this temperature difference reached a maximum of 11C° at the maximum average sheathing temperature of 60°C. The sheathing temperature difference between the radiant barrier and uncovered side is also plotted in Fig. 33 as a function of the average peak temperature. The same trend noticed for the shingles is obtained for the sheathing, in that the temperature difference increased with an increase in peak temperature; however, this difference is much larger than that for the shingles. With the radiant barrier in place, the sheathing absorbs thermal radiation that is reflected by the radiant barrier resulting in a higher temperature as compared to the uncovered side.

4.2 Discussion of Results

The heat balance in an attic space is altered by the presence of a radiant barrier on the underside of the top chord of the roof trusses. By comparing the results for the shingles to those for sheathing on the south face of the roof, shown in Figs. 31 and 34, respectively, it is clear that the shingle temperature was always greater than the sheathing temperature. This implies that the attic was gaining heat due to solar radiation. When the difference between the peak shingle and sheathing temperatures[2] is plotted over the test period, the effect of a radiant barrier on this attic heat gain can be clearly seen. These temperature differences are plotted in Fig. 36 for the radiant barrier and uncovered sides of the attic. These temperature differences act across a purely conductive thermal resistance (9.5 mm (3/8") plywood sheathing and one layer of asphalt shingles) and give a direct measure of the heat flux through the roof. Fig. 36 clearly shows that the temperature difference for the radiant barrier side was consistently less than for the uncovered side; thus the radiant barrier reduced the heat flux through the roof. However, in order to achieve this reduced heat flow to the attic, the sheathing and shingle temperatures increased, so that the fraction of the incident solar energy that was not

---

2 The peak shingle and sheathing temperatures were in phase within the 10 minute averaging time period used for data collection.

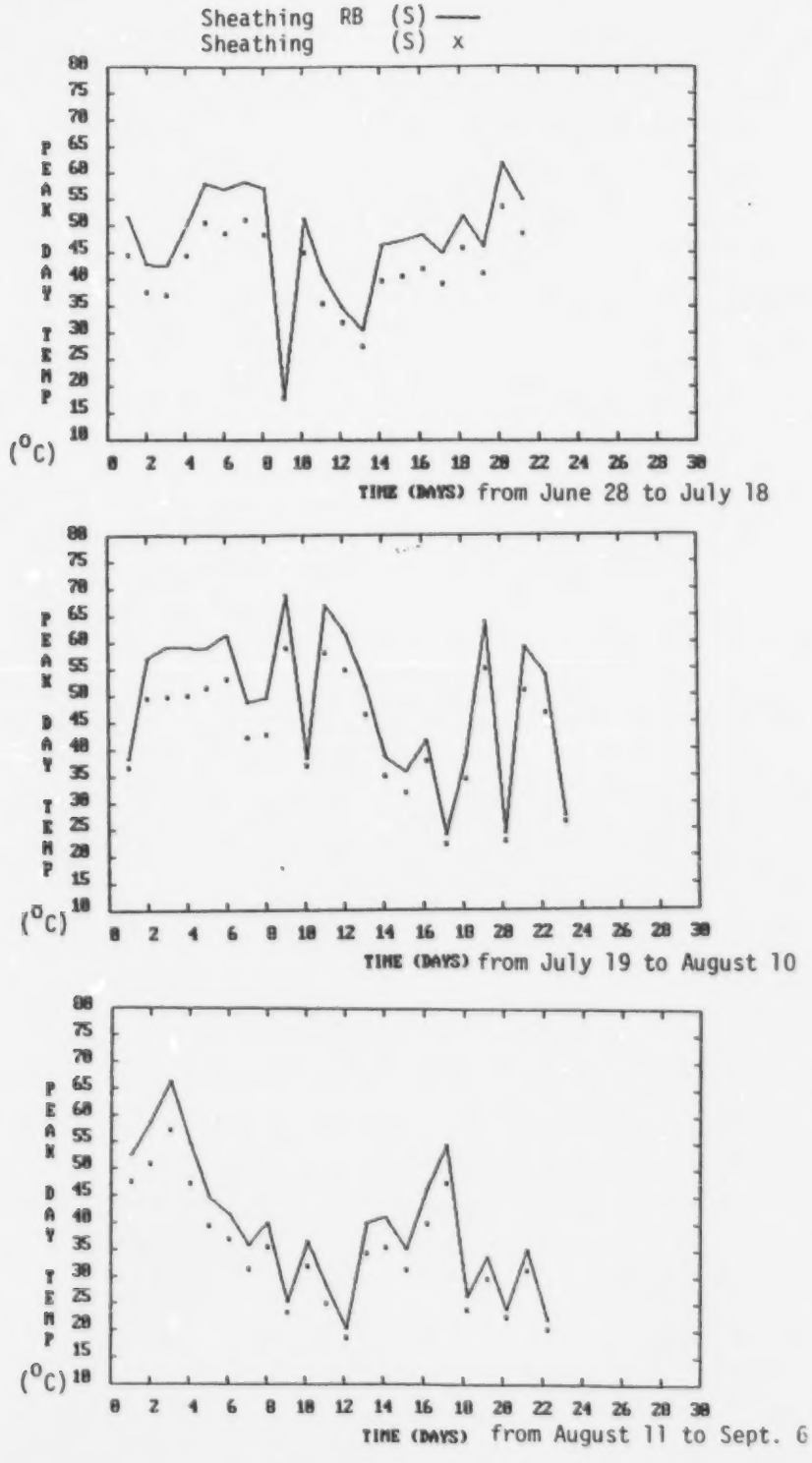
Sheathing RB (S)
Sheathing (S) x
PEAK DAY TEMP (°C)
TIME (DAYS) from June 28 to July 18
TIME (DAYS) from July 19 to August 10
TIME (DAYS) from August 11 to Sept. 6

Figure 34 Average daily peak temperature of sheathing on the south face of the roof versus time.

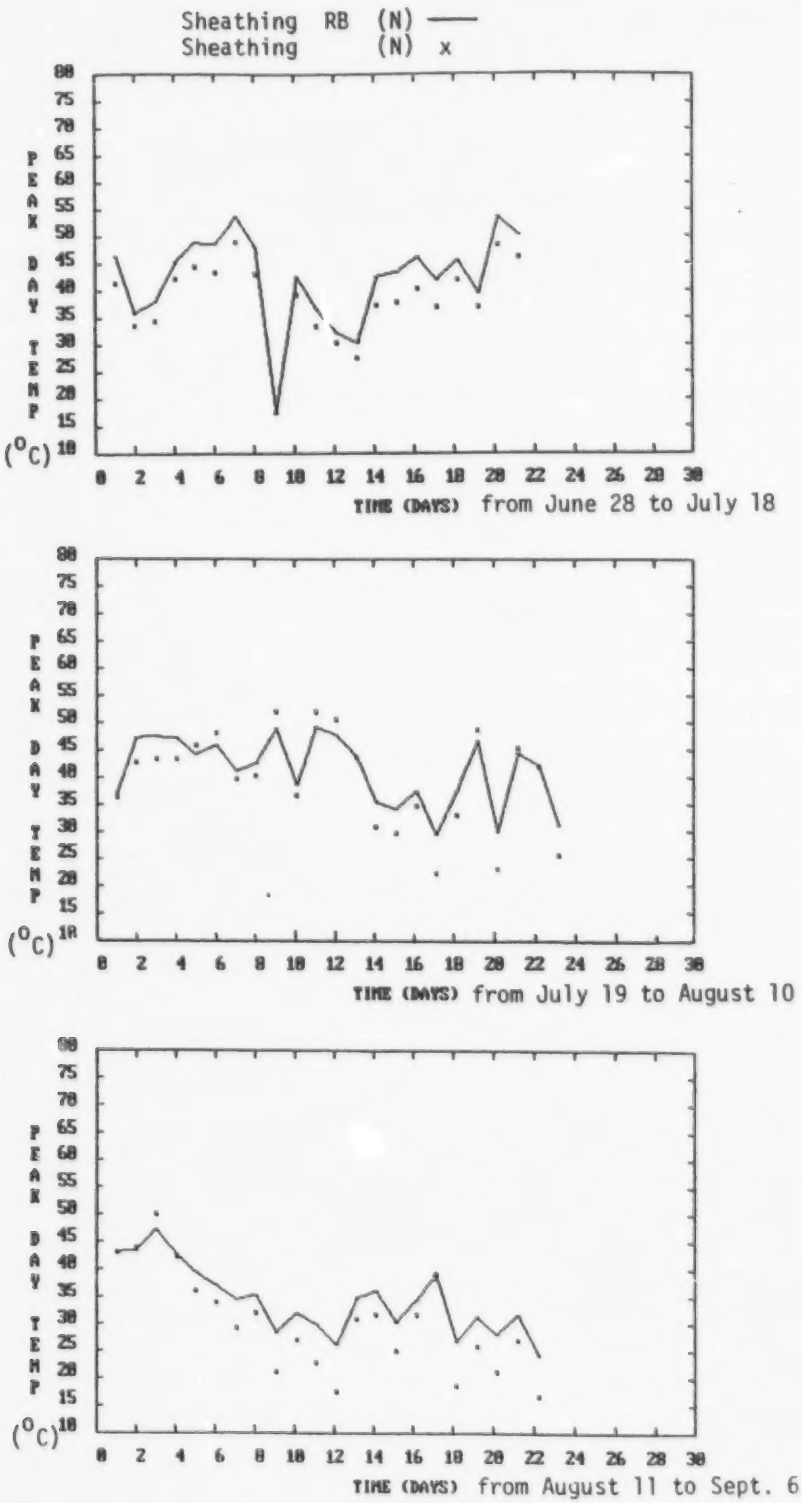
Sheathing RB (N)
Sheathing (N) x
PEAK DAY TEMP (°C)
TIME (DAYS) from June 28 to July 18
TIME (DAYS) from July 19 to August 10
TIME (DAYS) from August 11 to Sept. 6

Figure 35 Average daily peak temperature of sheathing on the north face of the roof versus time.

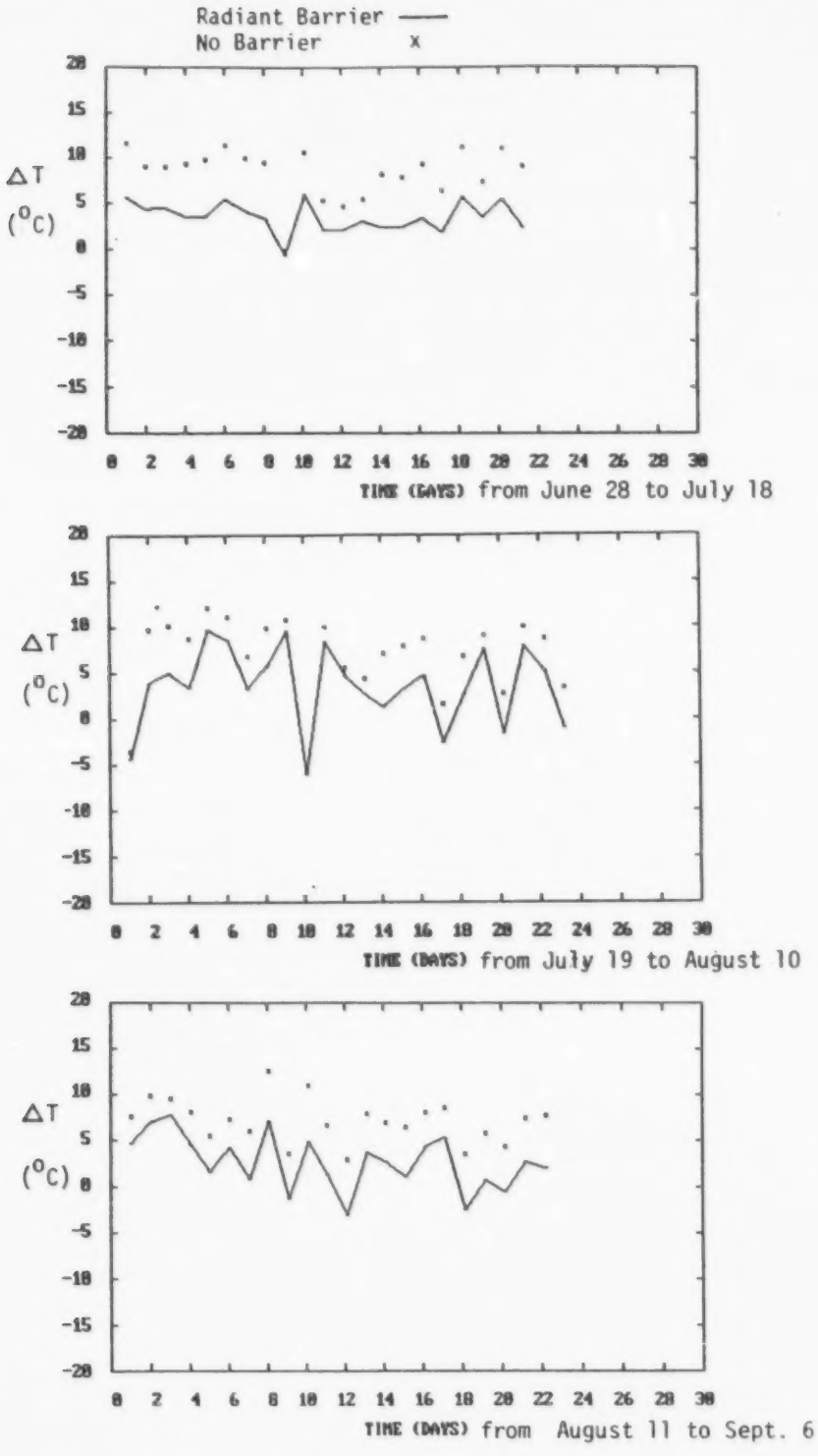
Radiant Barrier ——
No Barrier x
ΔT
(°C)
TIME (DAYS) from June 28 to July 18
TIME (DAYS) from July 19 to August 10
TIME (DAYS) from August 11 to Sept. 6

Figure 36 Difference between the average daily peak shingle and sheathing temperatures for the south face of the roof versus time.

transferred to the attic could dissipate to the environment by a corresponding increase in convection and radiation heat loss. It should be noted that one of the first applications of the radiant barrier concept was to attic spaces in southern U.S. houses during summer periods to reduce the heat gain through the ceiling and thus reduce air conditioning loads. The results in Fig. 36 show that, for this application, the radiant barrier does reduce the attic heat gain.

5.0 CONCLUSIONS

5.1 Thermal Performance and Cost Effectiveness

Results of laboratory and field testing on the cold weather thermal performance of attic radiant barriers point to a number of specific conclusions:

1. Both laboratory and field test results indicate that the thermal performance of ceiling insulation depends on the roof sheathing temperature relative to the attic air temperature. For a given indoor/attic temperature difference, the thermal resistance of ceiling insulation decreases when the roof sheathing is colder than the attic air. The decrease in thermal resistance is due to radiant heat loss from the attic floor to the sheathing. Conversely, when the roof sheathing is warmer than the attic air, the ceiling thermal resistance increases because the net ceiling heat loss is reduced by the radiant heat exchange from the sheathing to the attic floor.

2. The presence of a low emissivity radiant barrier affects the radiant heat exchange between the sheathing and the attic floor. When the sheathing is colder than the attic air, radiant barriers reduce the radiant heat loss from the attic floor to the sheathing, resulting in an increase in ceiling resistance by a maximum of 15% over that of uncovered insulation. This increase in ceiling resistance results in a reduction in heat loss from the interior to the attic space. Conversely, when the sheathing is warmer than the attic air, radiant barriers reduce the beneficial heat gain (via radiant transfer) from the sheathing to the attic floor. The ceiling resistance decreases by a maximum of 43%, resulting in increased heat loss from the interior to the attic space. The 15% increase and 43% reduction in ceiling resistance are for a nominal insulation level of RSI 2.1 (R12). For higher levels of ceiling insulation, the percentage changes in ceiling thermal resistance due to radiant barriers will be less than the measured values.

3. From the results of the field tests, the net seasonally averaged energy savings attributable to the use of attic radiant barriers during cold weather periods is estimated to be 5%. With ceiling heat losses accounting for only 15% of the total building heat loss (including air infiltration), the overall energy savings amount to less than 1%, a negligible amount.

4. Overall savings will vary from house to house, but it is concluded that radiant barriers are not a cost-effective energy saving product for cold weather applications in residential attics.

5.2 Moisture Performance

Laboratory and field tests were carried out on the moisture performance of attic radiant barriers. Tests were conducted with a radiant barrier directly over the ceiling insulation. A number of specific conclusions were reached:

1. The principal mechanism for moisture transport to the radiant barrier is by movement of air from indoors (warm and humid) to the attic space. Water vapour diffusion from indoors to the attic accounts for much smaller volumes. During prolonged cold periods, this air leakage can be predominantly into the attic resulting in a large amount of moisture being transported to the radiant barrier. Ceiling imperfections such as cracks, vent pipe penetrations, and recessed light fixtures should be sealed to prevent air leakage.
2. Under sub-freezing temperatures, most of the moisture accumulates as frost at the interface between the insulation and the radiant barrier. The amount of moisture accumulation in the insulation is much less than at the interface and is comparable to the amount of moisture that would accumulate if no radiant barrier were present. Thus, at sub-freezing temperatures, a radiant barrier over insulation increases the amount of frost deposition.
3. Noticeable moisture reduction on the radiant barrier only occurred when the frost melted. The moisture reduction was due to evaporation and gravity drainage of the water, although it was difficult to quantify these two effects.
4. With prolonged periods of sub-freezing temperatures, enough frost can accumulate on the radiant barrier that, when melting occurs, water can drain to the ceiling drywall which may cause problems.
5. For cold weather applications, it is recommended that radiant barriers not be placed directly over the insulation due to potential moisture

accumulation problems. This provides confirmation to the cautionary note affixed to the Alberta Labour Standata on radiant barriers [5].

5.3 Roof Overheating

Field tests on roof shingles and sheathing overheating were carried out during the summer months. A radiant barrier was stapled to the underside of the top chord of the roof trusses, according to Alberta Labour STANDATA 85 PL156. The radiant barrier increased the roof sheathing temperature by a maximum of 18% over that of the uncovered roof section. The increase in shingle temperature was a maximum of only 5% over that of the uncovered section. These maximum increases occurred at the largest observed temperatures of 60°C and 75°C for the sheathing and shingles, respectively. A 5% increase in shingle temperature should not pose a serious problem since asphalt shingles are designed to withstand temperatures on the order of 80 to 90°C.

BIBLIOGRAPHY

[1] Ozisik, M.N., Heat Transfer: A Basic Approach, McGraw-Hill, New York, 1985, pg. 593.

[2] Energy Design Update, "Residential Insulation: Research and Product Update", Section 7 Radiant Barriers, Cutter Information Corp., Arlington, MA, March 1986.

[3] Levins, W.P. and Karnitz, M.A., "Heating Energy Measurements of Unoccupied Single-Family Houses with Attics Containing Radiant Barriers", Oak Ridge National Laboratory, Report ORNL/CON-213, August, 1988.

[4] Levins, W.P., Karnitz, M.A., and Hall, J.A., "Moisture Measurements in Single-Family Houses with Attics Containing Radiant Barriers", ASHRAE Transactions, Vol. 95, Pt. 2, pp. 235-244, 1989.

[5] STANDATA 85 PL156, "Radiant Barrier", Building Standards Branch, Alberta Labour, Sept. 1988.

[6] Bankvall, G.C., "Heat Transfer in Fibrous Materials", National Swedish Institute for Building Research, Document D4, 1972.

[7] Private communication with Reflective Insulation Manufacturers Association, Pomona CA.

[8] Anderson, B., Solar Energy: Fundamentals in Building Design, McGraw-Hill, New York, 1977, pg. 306.

[9] Gilpin, R.R., Dale, J.D., Forest T.W., and Ackerman, M.Y., "Construction of the Alberta Home Heating Research Facility and Results for the 1979-1980 Heating Season", Department of Mechanical Engineering, University of Alberta, Report #23, 1980.

[10] ASHRAE, Handbook, 1985 Fundamentals, pg. 22.14.